Electroweak precision and intermediate scales in warped extra dimensions

Barry Dillon

Thesis submitted for the degree of

Doctor of Philosophy

in the

School of Mathematical and Physical Sciences,

Theoretical Particle Physics Group,

University of Sussex

June 2016

University of Sussex

Barry Dillon

Theoretical Particle Physics

Electroweak precision and intermediate scales in warped extra dimensions

In this thesis we study several topics within the subject of extra dimensions and composite Higgs models. We first look at a scenario with a warped extra dimension known as the Randall-Sundrum (RS) model, and put all Standard Model fields in the bulk. We investigate various aspects of the model and argue that the presence of higher dimensional operators in the 5D bulk has a non-negligible effect on the electroweak precision observables, meaning that current electroweak constraints on non-custodial warped models could be weaker than previously thought.

Then, using holographic techniques, we study correlations between the top partner masses and the Higgs potential in composite Higgs models. It is known that a light Higgs ($\sim$ 125 GeV) generally requires light top partners at around 700-800 GeV. However in these calculations the 5D volume is always fixed such that the 5D cutoff is around $\sim M_{Pl}$. The effect of lowering this 5D cutoff has been studied previously in bulk RS models as a way of reducing constraints from some flavour and electroweak precision observables, these models were dubbed "Little Randall-Sundrum models". Here we consider a similar setup in the context of holographic composite Higgs models and show that reducing the 5D cutoff leads to a lighter Higgs without a lowering of the top partner masses or an increase in fine-tuning. We find that the model is perfectly consistent with a 125 GeV Higgs and top partners above 1 TeV. This reduced 5D cutoff implies an intermediate scale between the electroweak scale and the Planck scale.

Lastly we consider a similar warped model with a low 5D cutoff, except this time our goal is to study diphoton signals from Kaluza-Klein gravitons in a warped extra dimension. With a KK graviton of mass 750 GeV and spin-1 states at $\sim$ 2.5 TeV, we show that having a low 5D cutoff increases the diphoton signal and the decay to gluons. With this model we show that we can explain the recently observed diphoton excess in terms of a Kaluza-Klein graviton from a holographic composite Higgs model, while keeping other decay channels within the relevant experimental bounds.

I hereby declare that this thesis has not been and will not be, submitted in whole or in part to another University for the award of any other degree.

The work in this thesis is based on research projects conducted with collaborators here at the University of Sussex, in which I took a leading role. This research has resulted in three publications:

- *'Non-custodial warped extra dimensions at the LHC?'*
  Barry M. Dillon and Stephan J. Huber
  hep-ph/1410.7345
  JHEP 1506 (2015) 066

- *'Exploring holographic composite Higgs models'*
  Djuna Croon, Barry M. Dillon, Stephan J. Huber and Veronica Sanz
  hep-ph/1510.08482
  Submitted to JHEP

- *'A little KK graviton at* 750 *GeV'*
  Barry M. Dillon and Veronica Sanz
  hep-ph/1603.09550
  Submitted to PLB

Signature:

Acknowledgements

I would like to thank all my colleagues here in the TPP group at Sussex, it wouldn't have been possible for me to complete this thesis without your help and guidance, in particular that of Veronica Sanz and my supervisor Stephan Huber. I would also like to thank my collaborators at other institutions; their expertise has been invaluable to my professional development and research.

A huge thank you goes to my girlfriend Laura Kelly, who has put up with 'physics talk' on a regular basis for over three years now. Even from the moment I decided to apply for PhD positions she has been a constant source of encouragement and motivation. And lastly, I am most indebted to my Mum and Dad, as without their support and advice throughout the years I would certainly not have had the opportunity to pursue this PhD, never mind complete it.

Contents

Chapter 1

Introduction

1.1 Overview

In 2015 the Large Hadron Collider (LHC) began its second run, colliding protons with centre of mass energies of 13 TeV, the highest energy collisions performed in a particle collider to date. On it's first run in 2010 the LHC was colliding protons with centre of mass energies of 7 TeV, and after a short shut down, began again in 2012 reaching centre of mass energies of 8 TeV. The first run culminated in 2012 with the discovery of the long sought after Higgs boson [1, 2] at a mass of 125 GeV, the smoking gun signature for a mechanism of electroweak symmetry breaking (EWSB) called the Higgs mechanism. For the theoretical work done in developing the Higgs mechanism the 2013 Nobel prize was awarded to François Englert and Peter Higgs.

This discovery opens up many questions as to the origin of the Higgs mechanism. In the Standard Model (SM) of particle physics, the Higgs mechanism is responsible for electroweak gauge bosons acquiring mass without violating gauge invariance. However it is possible that there is other new physics present which also plays a role in EWSB. If this is true, then it would lead to deviations in some of the measured properties of the Higgs and other particles of the SM. The discovery of other new physics may shed light on the origin of the Higgs mechanism and a more fundamental theory of nature. Thus far no significant deviations in these properties have been measured, however the presence of new physics is far from excluded. In fact, new physics at the energy scales probed by the LHC is very well motivated.

The SM is an immensely successful model, explaining the plethora of data collected at particle colliders over the last century. However the validity of the SM only extends over three of the four known fundamental forces, as it fails to provide a quantum description

of gravity. Effects of this quantum description of gravity could lay at scales far above the Higgs mass at $\sim 10^{18}$ GeV. This fact implies that the SM, our most advanced understanding of nature, is incomplete. Another issue is the so-called hierarchy problem. According to our current understanding, the natural mass scale of the discovered Higgs boson should be orders of magnitude larger than what was measured. This is due to the sensitivity of its mass to higher scales in the model, which must exist to explain how gravity is incorporated into our understanding of nature. Other issues include the origin of neutrino masses, the baryon asymmetry in the universe, the fact that the SM contains no dark matter candidates, and many more.

Many extensions to the SM have been proposed, and most only solve a few of the outstanding issues. However some Beyond the Standard Model (BSM) extensions provide a framework from which one can address many of the issues in the SM. Two of these BSM scenarios that we will focus on in this thesis are warped extra dimensional models and composite Higgs models. Neither of these models by themselves provide an explanation as to how gravity is incorporated into the SM, however they both provide explanations for why the Higgs mass is not be sensitive to higher scales. Thus they both provide solutions to the hierarchy problem, however this is only part of the story. Once we have a model which solves this problem, we must then check if it agrees with the stringent experimental tests that have been performed at particle colliders in the past, most notably at the Large Electron-Positron (LEP) collider and at the LHC. In general any model which adequately solves the hierarchy problem requires new physics laying at the TeV scale, and this new physics generally induces corrections to observables measured at LEP and at the LHC, causing tension with experimental results.

There are two ways in which this new physics may show up. One is by direct detection, by which the collisions at the LHC produce a new physics particle on-shell and its decay products are detected. And another is indirectly, in this way the new physics particle may either mix with the SM particles causing deviations in their couplings, or corrections to observables may arise from higher order radiative effects involving the new physics particle. Thus far the LHC has made no observations which are consistent with new physics beyond the SM. These experimental bounds narrow down the spectrum of BSM scenarios that are likely to exist beyond the electroweak scale.

This thesis is divided into five chapters, the first being the introduction, the last being the conclusions, and the others each corresponding to a self-contained sub-project:

2. Non-custodial warped extra dimensions at the LHC [3]

3. Exploring holographic composite Higgs models [4]

4. A Little KK graviton at 750 GeV [5].

In the first few sections of chapter 2 we present the background material required for that chapter. Chapters 3 and 4 also make use of this however these chapters will also require additional background material which is presented later. We then move on to discuss the idea of warped extra dimensions as a solution to the hierarchy problem. New physics in these models comes in the form of towers of resonances called Kaluza-Klein (KK) modes which are expected to have masses of the order $\sim$ TeV. We study indirect effects of these KK modes on the Electroweak Precision Observables (EWPOs). These observables were accurately measured at LEP and are still some of the most stringent constraints we have on BSM models. We end the chapter by studying corrections to the top quark Yukawa coupling of the SM induced indirectly via mixings between the Higgs boson, top quark, and KK top quarks.

We start chapter 3 by giving an overview of strongly coupled models in particle physics, starting with QCD and technicolor and moving on to composite Higgs models. In composite Higgs models the Higgs boson is not a fundamental particle, but is rather a bound state of some strongly coupled new physics. This new physics is expected to become visible in our particle colliders at energies around the TeV scale. The smoking gun signature for these composite Higgs models would be the detection of a so-called top-partner. In order to adequately solve the hierarchy problem these new particles are required to be somewhat lighter than other new physics particles in the model, expected to lay $\lesssim$ TeV. The 5D techniques introduced in the previous chapter can also be used to study composite Higgs models, where the methods used go under the name of *holographic techniques*. After developing some of these techniques further we move on to the main part of the chapter, which is a study of the Higgs potential and the top-partner masses when we have intermediate scales in the model. Thus far we have mentioned three scales, the Higgs mass (125 GeV), the scale of new physics required to adequately solve the hierarchy problem ($\sim$ TeV), and the scale of gravity ($\sim 10^{18}$ GeV). In chapter 3 we introduce an intermediate scale by lowering the UV scale of the holographic composite Higgs model to lay somewhere between the TeV scale and 10^{18} GeV. After presenting the results of this analysis we then study corrections to the top quark Yukawa coupling in the holographic composite Higgs model.

In the last sub-project we study the possibility that a spin-2 KK mode of a warped extra dimension with an intermediate scale can describe a once significant deviation at a

mass of 750 GeV in experimental data analysed by the ATLAS and CMS collaborations in December 2015 [6,7]. With the collection of more data this deviation has revealed itself to only be a statistical fluctuation [8], however the results of this chapter demonstrate how intermediate scales in warped extra dimensions open up interesting possibilities for new physics at low masses. We begin by reviewing the background material for spin-2 KK modes (KK gravitons) and relevant phenomenological quantities in terms of the 5D parameters. We then present a study of the phenomenology of these KK gravitons and show that with intermediate scales of the order 10^3 TeV we can adequately describe the deviation in the experimental data.

In the second part of this introduction we will provide an overview of the SM, focusing on parts relevant to this thesis such as the Higgs mechanism and the hierarchy problem. We will then move on the three sub-projects mentioned above, and will conclude the thesis in chapter 5.

1.2 The Standard Model of particle physics

All data collected from high energy particle physics experiments thus far can be described very well by a Lorentz invariant, renormalizable quantum field theory known as the *Standard Model (SM)*. This field theory has a local gauge symmetry, $G_{SM} = SU(3)_c \times SU(2)_L \times U(1)_Y$, under which the matter content of the model is charged. The physics of the $SU(3)_c$ gauge symmetry is known as *Quantum Chromodynamics (QCD)* and the eight spin-1 generators of this non-abelian group are responsible for the mediation of the *strong* force between fermion fields that we call quarks. Fermions not charged under this strong force are called leptons, and we call the generators of the local gauge symmetries *gauge fields*. A peculiar property of the $SU(2)_L$ symmetry in the SM is that the gauge fields of this symmetry, of which there are three, only interact with left-handed quarks and leptons. The force mediated by these gauge bosons is called the *weak* force. Lastly, the $U(1)_Y$ local symmetry, which has only one gauge boson, interacts with all quarks and leptons in the SM. This symmetry is known as *hypercharge*, and together we call the product $SU(2)_L \times U(1)_Y$ (and the fields charged under it) the *electroweak (EW) sector*.

The gauge symmetry of the EW sector is spontaneously broken by the vacuum to the subgroup $U(1)_Q$. This gauge group is responsible for *electromagnetism (EM)*, the force whose gauge boson is the *photon*. What we mean by spontaneously broken is that although the action is invariant under the full EW group, the vacuum is not.

Field	$\mathbf{SU(3)_c}$	$\mathbf{SU(2)_L}$	$\mathbf{U(1)_Y}$	$\mathbf{U(1)_Q}$	Generation notation
$L_{iL} = \begin{pmatrix} \nu_i \\ l_i \end{pmatrix}$	**1**	**2**	$-\frac{1}{2}$	0 -1	$\begin{pmatrix} \nu_e \\ e_L \end{pmatrix}, \begin{pmatrix} \nu_\mu \\ \mu_L \end{pmatrix}, \begin{pmatrix} \nu_\tau \\ \tau_L \end{pmatrix}$
e_{iR}	**1**	**1**	-1	-1	$e_R,\ \mu_R,\ ,\tau_R$
$Q_{iL} = \begin{pmatrix} u_i \\ d_i \end{pmatrix}$	**3**	**2**	$\frac{1}{6}$	$+2/3$ $-1/3$	$\begin{pmatrix} u \\ d \end{pmatrix}, \begin{pmatrix} c \\ s \end{pmatrix}, \begin{pmatrix} t \\ b \end{pmatrix}$
u_{iR}	**3**	**1**	$\frac{2}{3}$	$+\frac{2}{3}$	$u_R,\ c_R,\ ,t_R$
d_{iR}	**3**	**1**	$-\frac{1}{3}$	$-\frac{1}{3}$	$d_R,\ s_R,\ ,b_R$

Table 1.1: In this table we present the charge assignments of the SM quarks and leptons and the notation used to denote the three generations.

1.2.1 The quarks and leptons

Quarks and leptons are fermion fields, i.e. they transform in the spin-1/2 representation of the Lorentz group. An interesting and yet unexplained feature of the SM is that it consists of three *generations* each of quarks and leptons. The charges of these fields under the SM gauge symmetries are given in table 1.1. The EM charge is related to those of the weak and hypercharge via $Q = T_L^3 + Y$, where Y is the hypercharge generator and T_L^3 is the diagonal generator of $SU(2)_L$. The **2** tells us that the left-handed quarks transform as doublets of $SU(2)_L$, which is the fundamental representation. The upper and lower fields have either $T_L^3 = \pm 1/2$, respectively, hence the difference in EM charges. The quarks transform as colour triplets of the strong force, which again is the fundamental representation. This is in contrast to the gauge bosons of the SM which transform in the adjoint representations of the local symmetries. Note that the adjoint representation of an $SU(N)$ group has $N^2 - 1$ degrees of freedom.

The Lagrangian of the SM quarks, leptons and gauge fields can be compactly written in the form

$$\mathcal{L} = -\frac{1}{4}\mathrm{Tr}(G^{\mu\nu,a}G^a_{\mu\nu}) - \frac{1}{4}\mathrm{Tr}(W^{\mu\nu,i}W^i_{\mu\nu}) - \frac{1}{4}B^{\mu\nu}B_{\mu\nu} + \sum_{generations}\Big(\bar{L}_L i\gamma^\mu D_\mu^{lL} L_L$$
$$\bar{e}_R i\gamma^\mu D_\mu^{lR} e_R + \bar{Q}_L i\gamma^\mu D_\mu^{qL} Q_L + \bar{u}_R i\gamma^\mu D_\mu^{uR} u_R + \bar{d}_R i\gamma^\mu D_\mu^{dR} d_R\Big) \tag{1.2.1}$$

where the covariant derivatives are

$$\begin{aligned}
D_\mu^{lL} =& \partial_\mu + \frac{i}{2} g T_L^b W_\mu^b + i g_Y \left(-\frac{1}{2}\right) B_\mu \\
D_\mu^{eR} =& \partial_\mu + i g_Y \left(-1\right) B_\mu \\
D_\mu^{qL} =& \partial_\mu + \frac{i}{2} g_s \lambda^a G_\mu^a + \frac{i}{2} g T_L^b W_\mu^b + i g_Y \left(+\frac{1}{6}\right) B_\mu \\
D_\mu^{uR} =& \partial_\mu + \frac{i}{2} g_s \lambda^a G_\mu^a + i g_Y \left(+\frac{2}{3}\right) B_\mu \\
D_\mu^{dR} =& \partial_\mu + \frac{i}{2} g_s \lambda^a G_\mu^a + i g_Y \left(-\frac{1}{3}\right) B_\mu
\end{aligned} \tag{1.2.2}$$

where $a = 1, .., 8$ and $b = 1, 2, 3$. These expressions can be derived from the charge associations laid out in table 1.1.

1.2.2 Masses for the SM fields?

Adding mass terms for the SM fields cannot be done without explicitly breaking some of the gauge symmetries. First of all, any mass term for a gauge field violates the local symmetry generated by that field. And the charges associated with the fermion fields mean that one cannot write down Lorentz invariant mass terms without violating a gauge symmetry. For example if we add a Lorentz invariant mass term $\sim \bar{u}_L u_R$, this will break the EW symmetries because the fields have different hypercharge and only u_L interacts with the weak force. We know very well that most of the SM fields do in fact have mass, therefore there must be a mechanism to describe these masses. This is the famous *Higgs mechanism* mentioned in the overview, and it is responsible for the spontaneous breaking of the EW gauge group to $U(1)_Q$, as well as giving the SM particles masses. Therefore the vacuum only respects the $SU(3)_C \times U(1)_Q$ symmetry. From table 1.1 we can see that we can indeed build fermion masses which respect these gauge symmetries. When the vacuum spontaneously breaks local gauge symmetries one also finds that masses for certain gauge fields of the gauge symmetry are introduced in a gauge invariant way.

1.2.3 The Higgs mechanism

To spontaneously break the EW symmetry in the SM one introduces an additional set of complex scalar fields transforming in the fundamental representation of the $SU(2)_L$ group with hypercharge $+1/2$. This set of scalars is known as the Higgs doublet field. The Lagrangian (up to dimension 4) for such a field can be written

$$\mathcal{L} = \frac{1}{2} \left(D_\mu \Phi\right)^2 - \frac{\mu^2}{2} \Phi^2 - \frac{\lambda}{4} \Phi^4 \tag{1.2.3}$$

where

$$D_\mu = \partial_\mu + \frac{i}{2} T_L^b W_\mu^b + i g_Y \left(+\frac{1}{2}\right) B_\mu. \tag{1.2.4}$$

When we minimise the potential for the Higgs field we find two cases,

- $\mu^2 > 0$ and $\lambda > 0$: The minimum of the potential is at $\langle \Phi \rangle^2 = 0$.
- $\mu^2 < 0$ and $\lambda > 0$: The minimum of the potential is at $\langle \Phi \rangle^2 = -\mu^2/\lambda$.

The second case implies that when $\mu^2 < 0$ the Higgs field acquires a vacuum expectation value (vev). In this case we can write the Higgs field as

$$\Phi(x) = \exp\left(\frac{i}{2v}\xi(x)^b T_L^b\right) \begin{pmatrix} 0 \\ \frac{v+h(x)}{\sqrt{2}} \end{pmatrix} \tag{1.2.5}$$

where $v^2 = -\mu^2/\lambda$. From this we can rotate via a gauge transformation to

$$\Phi(x) = \begin{pmatrix} 0 \\ \frac{v+h(x)}{\sqrt{2}} \end{pmatrix}. \tag{1.2.6}$$

Expanding the kinetic term of this Higgs field, including its vev, we find mass terms for certain linear combinations of the W_L^b and $U(1)_Y$ fields, where one linear combination is left massless. The massive linear combinations are the W-bosons $W^\pm = (W_\mu^1 \mp i W_\mu^2)$ with mass $m_W^2 = g^2 v^2/4$ and the Z-boson $Z_\mu = (g W_\mu^3 - g_Y B_\mu)/\sqrt{g^2 + g_Y^2}$ with mass $m_Z^2 = (g^2 + g_Y^2)v^2/4$. The massless linear combination is the photon $A_\mu = (g_Y W_\mu^3 + g B_\mu)/\sqrt{g^2 + g_Y^2}$ which generates the residual EM gauge symmetry in the vacuum. This mixing can be compactly described in terms of the Weinberg mixing angle $\sin^2\theta_W = g_Y^2/(g^2 + g_Y^2)$. Re-writing the potential in the presence of the vev results in a Higgs mass of $m_h^2 = -2\mu^2$.

Yukawa couplings and fermion masses

With the Higgs field in the spectrum we can write down some additional dimension 4, gauge invariant interaction terms. For one generation of leptons we can write $Y_l \bar{L}_L \Phi e_R + \text{h.c.}$, since both Φ and L_L carry weak charge and the total hypercharge of the fields in the interaction is zero this term is invariant under the local symmetries of the SM. When the Higgs has a vev this term is expanded to

$$\frac{Y_l}{\sqrt{2}} v \bar{l} e_R + \frac{Y_l}{\sqrt{2}} h \bar{l} e_R + \text{h.c.}. \tag{1.2.7}$$

The first term in this expression is a mass term for the leptons ($Y_l v/\sqrt{2}$) and the second is a coupling to the Higgs. Note that the neutrino fields (ν) do not get a mass here. This

can be understood by noting that without another fermion with zero EM charge, a mass term invariant under $U(1)_Q$ cannot be written.

Following the same logic we have the quark-Higgs interaction for one generation of quarks

$$Y_d \bar{Q}_L \Phi d_R + Y_u \epsilon_{ab} \bar{Q}_{La} \Phi_b^\dagger u_R + \text{h.c.}. \tag{1.2.8}$$

In the same manner as before, when the Higgs has a vev mass terms for the up and down quarks are generated where $m_{u,d} = Y_{u,d} v/\sqrt{2}$.

However, the SM has three generations and there is no reason why we cannot write down Yukawa interactions which mix different generations. Thus we promote $Y_{l,u,d} \to Y_{l,u,d}^{ij}$. If the Higgs has a vev one would then diagonalise these interactions and express them in the mass basis. The physics associated with the mixings between these different generations is a rich subject and goes by the name *flavour physics*. Note that due to the SM not containing a right-handed partner for the neutrino, the mixings between the lepton generations vanish.

1.2.4 The naturalness problem

In standard quantum field theories the one-loop corrections to the masses of scalar fields are quadratically sensitive to the cut-off scale of the model. One exception to this is *supersymmetry* in which the quadratic one-loop corrections are cancelled by contributions from loops of *super-partners*. However in the SM there is no supersymmetry and one would naively expect the Higgs mass to be close to the cut-off scale in the model. The problem is that estimates of this cut-off scale place it at $\Lambda_{Pl} \sim 10^{18}$ GeV (the Planck scale), and the Higgs mass is measured to be 125 GeV implying $\mu \simeq 88$ GeV. These estimates rely on the assumption that above the electroweak scale there is no new physics until the Planck scale, at which point one would expect a UV completion to unify the forces of the SM with gravity. This *naturalness* (or *fine-tuning*, or *hierarchy*) problem has been a strong motivation to search for new physics at scales $\sim TeV$, and has led to a conclusion accepted by most physicists that the SM is merely an *effective theory* of nature valid at scales well below that of the Planck scale. Current collider experiments are now probing scales at and above the TeV scale and have yet to make any concrete discoveries of new physics. Thus even if there is new physics at several TeV, we would have no natural explanation for why the Higgs mass is $\lesssim 10\%$ of the new physics scale. This additional problem is known as the *little-hierarchy* problem. Exploring and testing solutions to these hierarchy problems will be one of the main goals of this thesis.

Chapter 2

Non-custodial warped extra dimensions at the LHC

Due to their attractive model building features and rich phenomenology, warped extra dimensional models have been studied extensively for over fifteen years. The first proposal of such a model was by Randall and Sundrum (RS) in 1999 [9], and consisted of an AdS space mapped onto an S_1/Z_2 orbifold bounded by two 3-branes. The AdS geometry imposes an exponential hierarchy in energy scales between the two branes, thus, with all SM fields residing on the low energy (IR) brane and with a suitable choice of parameters, this model offers a simple and natural solution to the hierarchy problem. Studying perturbations to this metric reveals that the graviton zero mode is localised towards the high energy (UV) brane and hence the interaction of gravity with SM fields is naturally weak. In addition to this, it was shown that the size of the extra dimension can be stabilised without fine-tuning using a bulk scalar field [10].

Extending this model to have the SM fields propagating in the bulk provides a more interesting phenomenology, but also more stringent constraints on model parameters. The most striking feature of these models is the presence of KK modes in the 4D effective theory, of which the zero modes are identified with the SM particles. These arise due to the compactification of the bulk fields. The masses of scalar, gauge and fermion KK modes represent a scale of new physics in the effective model which is expected to be in the TeV range.

In addition to solving the hierarchy problem, these models are motivated by explaining the fermion mass hierarchy [11,12], new mechanisms for supersymmetry breaking [13–15], and by composite Higgs models where the AdS background is dual to a strongly coupled 4D theory through the AdS/CFT correspondence [16,17] (see ref. [18] for a recent review).

In this chapter we begin by providing an overview of field theory in 5D warped spaces in which the fifth dimension is compactified, we cover spin-0, 1 and 1/2 fields. We also discuss the Kaluza-Klein decomposition method which allows us to decompose compactified 5D fields into towers of 4D mass eigenstates. We then revisit the case of a bulk Higgs field. We first look at how the presence of the Higgs KK modes induces corrections to the masses of SM particles. For other analyses on bulk fields see [13, 19, 20], and specifically for a bulk Higgs see [21, 22]. It was first thought that models with a bulk Higgs field required a large fine-tuning (of the order of that required in the SM) to obtain an EW scale zero mode with TeV scale KK modes [23]. However, it was realised that if the bulk Higgs is localised towards the IR then one can naturally accommodate a light Higgs in the spectrum.

In sections 2.4.1 and 2.4.2 we look at the Higgs potential in 5D and study the effects of bulk and brane quartic terms. We find that with a bulk quartic term the KK Higgs modes are more decoupled from the zero mode than with a brane quartic term. The higher modes in the Higgs potential acquire vev's and give additional mass to the SM fields, we find the effect this has on the Higgs couplings and particle masses to be too small for detection until we have a sub percent experimental accuracy on the Higgs quartic coupling or couplings to gauge bosons and fermions. An interesting observation which we discuss is that these effective theories may be viewed as multiple Higgs doublet models.

Constraints on the EW sector of these models are studied via the Peskin-Takeuchi parameters S, T, and U [24]. In section 2.4.3 we calculate these parameters for our model. The largest experimental bound comes from the T parameter. We confirm that with a Higgs localised to the IR brane the lower bound on KK gauge boson masses is about 15 TeV, and with a Higgs localised in the 5D bulk this is reduced to around 8 TeV. We refer to these cases as brane and bulk Higgs cases, respectively. One way of reducing these stringent constraints is to extend the bulk gauge symmetry such that the KK gauge bosons in the effective theory preserve the SM custodial symmetry after EWSB [25–27]. Another way is to introduce a scalar field which back-reacts on the metric causing a departure from AdS in the IR [28–32]. These mechanisms typically result in a lower bound of about 3 TeV. Similar results can be obtained by introducing large brane kinetic terms for the gauge bosons [33] or by extending the space-time to include more than 5 dimensions [34, 35]. Having more than 5 dimensions may allow for a reduction in constraints via volume suppression in the IR of the extra dimension. We do not consider these extensions here, but do include the extended bulk gauge symmetry in later chapters. In the SM there is a set of dimension-6 operators contributing to the EW parameters. In section 2.4.4 we promote these to 5D

operators and study their effects. The only one with a sizeable contribution is the 5D dimension-8 operator contributing to the T parameter. Assuming a mild cancellation, we find that this effect could provide considerable reductions in the M_{KK} bound, allowing KK resonances around 5 TeV, i.e. within the range of LHC.

An exciting aspect of future collider experiments is the increased precision on top quark measurements. Being the heaviest particle in the standard model, corrections to its properties from KK modes will generally be large. The top quark mass is already well measured with the error being sub-percent. However, measurements of the top Yukawa coupling still leave a lot of room for new physics, and the proposed future colliders could dramatically close this gap. The precision forecasts from ILC [36–38], CLIC [39, 40] and TLEP [41] state that they could achieve a precision $< 5\%$ on the bottom and tau Yukawa couplings, and precision forecasts for the high luminosity LHC [42, 43] indicate that they could achieve the same precision for the top quark. In light of this, section 2.5 focuses on the misalignment of the fermion Yukawa couplings due to mixing with KK fermions. The largest of these effects is by far with the top quark, for which we find deviations from the SM could be as large as $\sim 10\%$ for a bulk Higgs. Similar calculations were done in [44] for a brane Higgs. We find some differences between the bulk and brane Higgs cases here. One important difference is the reduced bound on the KK fermion scale, and another is the introduction of a new coupling not present in brane Higgs scenarios. Together, we find that these result in a larger Yukawa corrections for a bulk Higgs. While these are sizeable deviations from the SM, they currently do not lead to additional bounds beyond that from electroweak observables. KK resonances may therefore be observable at LHC in the bulk Higgs setup.

2.1 Physics in a warped extra dimension

Throughout this thesis we focus on models with one extra dimension compactified on an S_1/Z_2 orbifold, which we describe as an interval with the line element,

$$ds^2 = e^{-2A(y)}\eta_{\mu\nu}dx^\mu dx^\nu - dy^2, \tag{2.1.1}$$

where $A(y)$ describes the curvature of the extra dimension. Thus the metric is written as

$$g_{MN} = \text{diag}\left(e^{-2A(y)}, -e^{-2A(y)}, -e^{-2A(y)}, -e^{-2A(y)}, -1\right). \tag{2.1.2}$$

The end points of the element are denoted by 0 and L, i.e. y lies in $[0, L]$, and at these points we have 3-branes onto which we can add localised interactions for the 5D fields.

The S_1/Z_2 geometry implies that any action must be invariant under transformations of the form $y \to -y$ and $y \to y + L$. This is the most general line element we can write down assuming that we have 4D Lorentz invariance. Flat extra dimensions are described by $A(y) = 0$, whereas the Randall-Sundrum model is given by $A(y) = ky$. The curvature scale k in the RS model has mass dimension 1 and is naturally assumed to be of the order of the fundamental 5D mass scale. This is typically taken to be of the order 10^{18} GeV, in order to reproduce 4D Einstein gravity from the 5D picture. However later in our work, in chapters 3 and 4, we will consider smaller values of this scale (i.e. intermediate scales) and discuss how one can still obtain Einstein gravity in the 4D picture. This specific background geometry can be derived from 5D Einstein equations with a suitable 5D action.

In some cases we will use the so-called 'conformal frame' where we make a co-ordinate transformation such that $r = \frac{1}{k}e^{ky}$. This results in a more compact expression for the line element,

$$ds^2 = \left(\frac{R}{r}\right)^2 \eta_{MN} dx^M dx^N \tag{2.1.3}$$

where $M, N = 0, 1, 2, 3, 4$ and $dx^4 = dr$. The UV and IR branes are located at $r = R = 1/k$ and $r = R'$, respectively.

2.1.1 Scalar fields in 5D

Let us consider the following 5D action for a real scalar field,

$$S = \int d^4x \int_0^L \sqrt{|g|} \left(\frac{1}{2} g^{MN} \partial_M \Phi \partial_N \Phi - V(\Phi)\right), \tag{2.1.4}$$

where $g = \det(g_{MN}) = e^{-4A(y)}$. Note that in 5D the scalar field has mass dimension 3/2. Varying with respect to the scalar field we find that the volume and surface terms, respectively, are,

$$\begin{aligned}
\delta S_V &= -\int d^4x \int_0^L \sqrt{|g|} \left(\frac{1}{\sqrt{|g|}} \partial_M \left(\sqrt{|g|} g^{MN} \partial_N \Phi\right) + \frac{\partial V}{\partial \Phi}\right) \delta\Phi \\
\delta S_S &= \int d^4x \sqrt{|g|} g^{5N} \partial_N \Phi \delta\Phi|_{y=0}^{y=L} + \int dy \sqrt{|g|} g^{\mu N} \partial_N \Phi \delta\Phi|_{x=-\infty}^{x=+\infty} \\
&= \int d^4x \sqrt{|g|} g^{55} \partial_y \Phi \delta\Phi|_{y=0}^{y=L} + \int dy \sqrt{|g|} g^{\mu\nu} \partial_\nu \Phi \delta\Phi|_{x=-\infty}^{x=+\infty}.
\end{aligned} \tag{2.1.5}$$

The variational principle, $\delta S = 0$, allows us to derive equations of motion for Φ, for example the volume term gives rise to the following bulk equation of motion,

$$\frac{1}{\sqrt{|g|}} \partial_M \left(\sqrt{|g|} g^{MN} \partial_N \Phi\right) + \frac{\partial V}{\partial \Phi} = e^{2A} \partial^\mu \partial_\mu \Phi - e^{4A} \partial_y \left(e^{-4A} \partial_y \Phi\right) + \frac{\partial V}{\partial \Phi} = 0. \tag{2.1.6}$$

But we need to specify boundary conditions; for the 4D co-ordinates we simply assume $\Phi \to 0$ as $x^\mu \to \pm\infty$, however for the 5D boundary conditions there are two options which ensure $\delta S = 0$ on either brane,

$$\begin{aligned} \partial_y \Phi = 0 &\to \text{Neumann, } (+) \\ \Phi = 0 &\to \text{Dirichlet, } (-). \end{aligned} \tag{2.1.7}$$

Throughout this thesis we will make use of the following notation for boundary conditions,

$$(\pm, \pm) \quad \text{or} \quad (\pm, \mp),$$

where the ordering is assumed to be (UV, IR). However, these are not the only type of boundary conditions we can obtain. Adding mass terms or interaction terms on the branes can alter the outcome. Take, for example,

$$S \supset -\int d^4x \int_0^L dy\, \delta(y-L)\sqrt{|g|}\frac{1}{2}\frac{m^2}{M_5}\Phi^2, \tag{2.1.8}$$

where M_5 is a mass term put in place due to the scalar field having mass dimension $3/2$, while the mass dimension of the integral on the boundary is -4. In order for the surface term to vanish in this case, we require that,

$$\partial_y \Phi|_{y=L} = \frac{m^2}{M_5}\Phi|_{y=L}. \tag{2.1.9}$$

This is what we will refer to as a 'mixed' boundary condition.

2.1.2 Gauge fields in 5D

In 5D we can write a general action for an abelian gauge field, which will have mass dimension $3/2$, as

$$S = \int d^4x \int_0^L dy \sqrt{|g|}\left(-\frac{1}{4}g^{MN}g^{KL}F_{MK}F_{NL}\right) + S_{GF} \tag{2.1.10}$$

where S_{GF} contains some gauge fixing terms. Expanding this action in the background, neglecting gauge fixing for now, we find

$$S = \int d^4x \int_0^L dy \left(-\frac{1}{4}F^{\mu\nu}F_{\mu\nu} + \frac{1}{2}e^{-2A}\partial^\mu A_5 \partial_\mu A_5 - e^{-2A}\partial_\mu A_5 \partial_y A^\mu + \frac{1}{2}e^{-2A}\partial_y A_\mu \partial_y A^\mu\right). \tag{2.1.11}$$

We will use the gauge-fixing term to get rid of the derivative coupling between the A_5 and A_μ mode. First, we will perform a partial integration on the term with respect to both μ and y,

$$e^{-2A}\partial_\mu A_5 \partial_y A^\mu = -\partial_y\left(e^{-2A}A_5\right)\partial_\mu A^\mu + e^{-2A}A_5\partial_\mu A^\mu|_{y=0}^{y=L}. \tag{2.1.12}$$

Then it is clear that the gauge-fixing term needed is

$$\int d^4x \int_0^L dy \frac{1}{2\xi} \left(\partial_\mu A^\mu - \xi \partial_y \left(e^{-2A} A_5\right)\right)^2 \tag{2.1.13}$$

where ξ is the gauge-fixing parameter. As in the 4D R_ξ gauges, this term alone does not completely fix the gauge. A residual gauge freedom allows for unphysical forward and backward polarisations of massless gauge fields to contribute to amplitudes, however these can be removed by applying Ward identities. In studying non-abelian gauge symmetries one must include the interactions of the Faddeev-Popov ghosts in the action. We study non-abelian gauge symmetries in section 3.2.2, where we follow a gauge-fixing procedure laid out in [45] in which the ghosts do not contribute to the one-loop Higgs potential. In abelian gauge theories which are spontaneously broken, the Faddeev-Popov ghosts still do not couple to the gauge fields, however they will couple to the Higgs-like degrees of freedom that triggered the spontaneous breaking.

Choosing different values of ξ here corresponds to different gauge choices, the most popular being the Landau gauge ($\xi \to 0$) and the Feynman-'t Hooft gauge ($\xi = 1$). With this term, the action is now

$$\begin{aligned} S = \int d^4x \int_0^L dy \Big(& -\frac{1}{4} F^{\mu\nu} F_{\mu\nu} + \frac{1}{2} e^{-2A} \partial^\mu A_5 \partial_\mu A_5 + \frac{1}{2} e^{-2A} \partial_y A_\mu \partial_y A^\mu \\ & + \frac{1}{2\xi} \left(\partial^\mu A_\mu\right)^2 + \frac{1}{2} \xi \left(\partial_y \left(e^{-2A} A_5\right)\right)^2 \Big) \\ & + \int d^4x \; e^{-2A} A_5 \partial_\mu A^\mu |_{y=0}^{y=L}. \end{aligned} \tag{2.1.14}$$

Varying this action with respect to the A_μ field gives rise to the following volume and surface terms,

$$\begin{aligned} \delta S_V &= \int d^4x \int_0^L dy \; \delta A_\mu \left(\left(\eta^{\mu\nu} \eta^{\alpha\beta} \partial_\alpha \partial_\beta - \left(1 - \frac{1}{\xi}\right) \partial^\mu \partial^\nu \right) - \eta^{\mu\nu} \partial_y e^{-2A} \partial_y \right) A_\nu \\ \delta S_S &= \int d^4x^{-2A} \delta A_\mu \left(\partial_y A^\mu - \partial^\mu A_5\right) |_{y=0}^{y=L}, \end{aligned} \tag{2.1.15}$$

and varying with respect to A_5 results in,

$$\begin{aligned} \delta S_V &= \int d^4x \int_0^L dy \; e^{-2A} \delta A_5 \left(-\eta^{\mu\nu} \partial_\mu \partial_\nu + \xi \partial_y^2 e^{-2A}\right) A_5 \\ \delta S_S &= \int d^4x \; e^{-2A} \delta A_5 \left(\xi \partial_y \left(e^{-2A} A_5\right) + \partial^\mu A_\mu\right), \end{aligned} \tag{2.1.16}$$

implying the following bulk equations of motion,

$$\begin{aligned} \left(\left(\eta^{\mu\nu} \eta^{\alpha\beta} \partial_\alpha \partial_\beta - \left(1 - \frac{1}{\xi}\right) \partial^\mu \partial^\nu \right) - \eta^{\mu\nu} \partial_y e^{-2A} \partial_y \right) A_\nu = 0 \\ \left(\eta^{\mu\nu} \partial_\mu \partial_\nu - \xi \partial_y^2 e^{-2A}\right) A_5 = 0. \end{aligned} \tag{2.1.17}$$

When studying spontaneous symmetry breaking in 4D models with an R_ξ gauge-fixing procedure, one finds that Goldstone bosons of the spontaneous symmetry breaking have ξ-dependent masses. This means that the fields mass is gauge dependent and implies that the field is unphysical. In these 5D models, the 4D masses of the KK modes are related to 5D momentum, and from the above equation we see that these terms are ξ-dependent for the A_5 field. This leads to the A_5 KK modes having ξ-dependent masses, also implying that they are unphysical. In analogy with the 4D spontaneous symmetry breaking models, we can say that the A_5 modes are eaten to form the longitudinal components of the massive A_μ KK modes. We will return to this discussion briefly in section 2.2.2 when we discuss the KK decomposition for the 5D gauge fields.

For the boundary conditions there are two clear options;

$$\begin{aligned} A_5 = 0 \quad &\Rightarrow \quad \partial_y A_\mu = 0 \\ A_\mu = 0 \quad &\Rightarrow \quad \partial_y \left(e^{-2A} A_5 \right) = 0, \end{aligned} \tag{2.1.18}$$

where we will use the following short hand notation,

$$\begin{aligned} A_5 = 0 \quad &\rightarrow \quad {}'+' \\ A_\mu = 0 \quad &\rightarrow \quad {}'-' . \end{aligned} \tag{2.1.19}$$

Just as in the scalar field case we will present the boundary conditions in the form $(\pm, \pm)$ or $(\pm, \mp)$, where the ordering is assumed to be (UV,IR).

A mixed boundary condition is defined as the boundary condition which arises when we have a mass term for a field on a brane. If one adds a mass term to the UV brane in the 5D gauge field action, the UV mixed boundary condition for A_μ is modified to $\partial_y A_\mu = m A_\mu$. One can think of a Dirichlet boundary condition as a mixed boundary condition, with the brane mass taken to infinity. Note that if we have some bulk gauge symmetry, we cannot have mixed boundary conditions without breaking (explicitly or spontaneously) the gauge symmetry on the brane. However one can add kinetic terms to the branes without breaking the bulk gauge symmetry.

2.1.3 Fermion fields in 5D

The spinorial representation of the Lorentz algebra in 5D consists of five anti-commuting Dirac matrices. We can take these to be

$$\Gamma^A = \left(\gamma^\mu, -i\gamma^5 \right), \tag{2.1.20}$$

which can be written in the Weyl representation as

$$\gamma^\mu = \begin{pmatrix} 0 & \sigma^\mu \\ \bar{\sigma}^\mu & 0 \end{pmatrix}$$
$$\gamma^5 = \begin{pmatrix} -\mathbb{1}_{2\times 2} & 0 \\ 0 & \mathbb{1}_{2\times 2} \end{pmatrix}. \tag{2.1.21}$$

The σ^μ tensors above are defined by

$$\sigma^\mu = \left(\mathbb{1}_{2\times 2}, \sigma^i\right)$$
$$\bar{\sigma}^\mu = \left(\mathbb{1}_{2\times 2}, -\sigma^i\right), \tag{2.1.22}$$

where the σ matrices here are simply the Pauli matrices. From these definitions it is clear that $\{\Gamma^A, \Gamma^B\} = 2\eta^{AB}$, as is required.

One important consequence of having fermions in 5D, is that the 4D chirality operator is now part of the spinorial representation of the Lorentz group. Thus Dirac spinors in 5D are not reducible, and since 5D Lorentz transformations will mix left and right handed Weyl spinors, we do not have a chiral theory. This issue can be resolved by suitable choices of boundary conditions, which we will see soon.

Since the 5D background is, in general, not flat, we need a few additional tools to describe fermions. The first is the fünfbein e^A_M, which is defined by

$$g_{MN} = e^A_M e^B_N \eta_{AB}$$
$$e^M_A e^B_M = \delta^B_A. \tag{2.1.23}$$

In the background of eq. (2.1.2), we have

$$e^\mu_\alpha = e^A \delta^\mu_\alpha$$
$$e^y_5 = 1. \tag{2.1.24}$$

And secondly we need to define the covariant derivative so that it accounts for both general co-ordinate invariance and local Lorentz invariance. The spin connection, ω^{AB}_M, is defined such that

$$D_M = \partial_M + \omega_{MAB}\left[\Gamma^A, \Gamma^B\right]. \tag{2.1.25}$$

This requires that

$$\omega^{AB}_M = e^A_N\left(\partial_M e^{NB} + e^{SB}\Gamma^N_{SM}\right), \tag{2.1.26}$$

where Γ^N_{SM} are the Christoffel symbols. The only non-zero components are,

$$\omega^{\nu 5}_\mu = -\omega^{5\nu}_\mu = \partial_y\left(e^{-A}\right)\delta^\nu_\mu, \tag{2.1.27}$$

meaning that we can write the covariant derivative as

$$D_\mu = \partial_\mu - \frac{i}{2}e^{-A}A'\gamma_\mu\gamma_5$$
$$D_5 = \partial_y. \tag{2.1.28}$$

Now that we have made these definitions we can proceed to look at the 5D fermion action, in which the fermion has mass dimension 2, and derive the bulk equations of motion. We can write the 5D action for a fermion field as

$$\begin{aligned} S &= \int d^4x \int_0^L dy \sqrt{|g|}\left(\frac{i}{2}\bar{\Psi}e_A^M\Gamma^A D_M\Psi - \frac{i}{2}\left(D_M\Psi\right)^\dagger\Gamma^0 e_A^M\Gamma^A\Psi - m_\Psi\bar{\Psi}\Psi\right) \\ &= \int d^4x \int_0^L dy\ e^{-3A}\left(i\bar{\Psi}\gamma^\mu\partial_\mu\Psi + \frac{1}{2}e^{-A}\left(\bar{\Psi}\gamma_5\partial_y\Psi - \left(\partial_y\bar{\Psi}\right)\gamma_5\Psi\right) - e^{-A}m_\Psi\bar{\Psi}\Psi\right) \end{aligned} \tag{2.1.29}$$

where we assumed that the field vanishes at $x^\mu \to \pm\infty$. Varying with respect to $\bar{\Psi}$ we find the following volume and surface terms,

$$\begin{aligned} \delta S_V &= \int d^4x \int_0^L dy\ e^{-3A}\delta\bar{\Psi}\left(i\gamma^\mu\partial_\mu\Psi + e^{-A}\gamma_5\partial_y\Psi - 2A'e^{-A}\gamma_5\Psi - e^{-A}m_\Psi\Psi\right) \\ \delta S_S &= -\int d^4x\ e^{-4A}\delta\bar{\Psi}\gamma_5\Psi|_{y=0}^{y=L}. \end{aligned} \tag{2.1.30}$$

Assuming that the boundary terms vanish, we arrive at the following bulk equation of motion,

$$\left(ie^A\gamma^\mu\partial_\mu + \left(\partial_y - 2A'\right)\gamma_5 - m_\Psi\right)\Psi = 0. \tag{2.1.31}$$

Decomposing into left and right components, the requirement that the surface term vanishes can be written as

$$\delta\bar{\Psi}_L\Psi_R - \delta\bar{\Psi}_R\Psi_L|_{y=0}^{y=L} = 0, \tag{2.1.32}$$

hence if we have a Dirichlet $(-)$ boundary condition for either field on each brane, the surface term vanishes. Note that fixing the boundary condition for one chirality automatically fixes the boundary condition for the other. To see this, we re-write the bulk equation of motion, eq. (2.1.31), in terms of left and right-handed fields,

$$\begin{aligned} ie^A\gamma^\mu\partial_\mu\Psi_L + \left(\left(\partial_y - 2A'\right) - m_\Psi\right)\Psi_R = 0 \\ ie^A\gamma^\mu\partial_\mu\Psi_R + \left(-\left(\partial_y - 2A'\right) - m_\Psi\right)\Psi_L = 0. \end{aligned} \tag{2.1.33}$$

Now it is clear that there are two possibilities for boundary conditions at each brane,

$$\begin{aligned} \Psi_L = 0 \quad &\Rightarrow \quad \partial_y\Psi_R = \left(2A' + m_\Psi\right)\Psi_R \\ \Psi_R = 0 \quad &\Rightarrow \quad \partial_y\Psi_L = \left(2A' - m_\Psi\right)\Psi_L. \end{aligned} \tag{2.1.34}$$

We will use the following short hand notation for the boundary conditions,

$$\begin{aligned} \Psi_R = 0 \quad &\rightarrow \quad '+' \\ \Psi_L = 0 \quad &\rightarrow \quad '-' \end{aligned} \tag{2.1.35}$$

where again we write them in the form $(\pm, \pm)$ or $(\pm, \mp)$ in the order (UV,IR). One could also add localised mass terms on the branes to obtain mixed boundary conditions, just as in the scalar case.

2.2 Kaluza-Klein expansions

When considering fields in a compact extra dimension it can be useful to perform a Fourier decomposition on the 5D field in order to express the action in terms of 4D mass eigenstates with 5D 'wave functions'. This similar to what is done when studying the 'particle in a box' solution in 1D quantum mechanics. The procedure is very similar regardless of the field. The masses of these KK particles are related to the 5D momentum along the direction of the extra dimension, thus in relation to the previous section we will see that they are a direct consequence of the ∂_y terms.

2.2.1 Scalar KK decomposition

The first step is to re-write the field as

$$\Phi(x^\mu, y) = \frac{1}{\sqrt{L}} \sum_{n=0}^{n=\infty} f_n(y)\phi_n(x^\mu) \tag{2.2.1}$$

such that we isolate the y-dependence of the field in the 'wave-function' $f_n(y)$ which we are free to choose. As a matter of convenience, we will choose these functions such that the effective theory describes, at the quadratic level, towers of non-interacting states. The factor of $\frac{1}{\sqrt{L}}$ is inserted to make the wave-function dimensionless, since $[\Phi] = 3/2$ and $[\phi_n] = 1$.

Inserting this expansion into the bulk equation of motion eq. (2.1.6), with $V(\Phi) = \frac{1}{2}M^2\Phi^2$, we find

$$e^{2A} f_n \partial^\mu \partial_\mu \phi_n - \left(e^{4A}\partial_y \left(e^{-4A}\partial_y f_n\right) - M^2 f_n\right)\phi_n = 0. \tag{2.2.2}$$

We want this equation of motion to have the following form,

$$\partial^\mu \partial_\mu \phi_n + m_n^2 \phi_n = 0, \tag{2.2.3}$$

where m_n is referred to as the Kaluza-Klein mass of the nth mode. Thus, the wave-functions must be chosen to satisfy,

$$f_n'' - 4A' f_n' - M^2 f_n + e^{2A} m_n^2 = 0. \tag{2.2.4}$$

We can see that the 4D KK masses arise from momentum along the direction of the extra dimension, and even when the 5D mass M is zero, the 4D KK modes still have masses. This feature is obviously independent of the spin of the particle under consideration, but we will see it explicitly for spin-1 and spin-1/2 particles later in this section, and for spin-2 particles later in the thesis. The equation of motion for the scalar field is self-adjoint and thus it is guaranteed that the wave-functions will form a complete set of solutions and that they will be orthogonal to each other, i.e.,

$$\left(m_n^2 - m_m^2\right) \int_0^L dy\ e^{-2A} f_n f_m = 0. \tag{2.2.5}$$

With the bulk equation of motion and the boundary conditions, one can solve to find the KK masses (m_n^2) and the wave-functions ($f_n(y)$). Once this is done we insert them back into the action, integrate over the y co-ordinate and treat the resulting 4D action as we usually would. Without specifying what $A(y)$ is we cannot write down analytic expressions for the KK masses and wave-functions, however in the coming sections this will be done for the case when the bulk geometry is AdS. The normalisation constant is usually chosen such that upon substituting this expansion into the action the kinetic term for the field is canonical,

$$\frac{1}{L} \int_0^L dy\ e^{-2A} f_n f_m = \delta_{mn}. \tag{2.2.6}$$

Note that the KK procedure does not solve for $f_n(y)$ via some variational procedure, it is simply a re-definition of the fields done in such a way that once we integrate over y the quadratic part of the action describes towers of non-interacting fields. Also, when we apply boundary conditions, we simply use the boundary conditions for the entire 5D field eq. (2.1.7) or eq. (2.1.9), but apply them on a mode by mode basis, i.e. to each wave function.

In the RS case, where $A(y) = ky$, we find that the 5D wave functions for scalar fields are given by

$$f_n = \frac{e^{2ky}}{N_n} \left(J_\alpha \left(\frac{m_n}{k} e^{ky} \right) + \beta(m_n) Y_\alpha \left(\frac{m_n}{k} e^{ky} \right) \right), \tag{2.2.7}$$

where m_n is the mass of the nth mode, α is a constant related to the bulk and brane masses, and N_n is determined by the normalisation condition [13]. The constants $\beta(m_n)$ and the KK masses m_n are determined by the boundary conditions. The J_α and Y_α

functions in this expression are Bessel functions. In the limit $kL \gg 1$ the KK masses can be approximated as

$$m_n \simeq \left(n + \frac{\alpha}{2} - \frac{3}{4}\right) \pi k e^{-kL} \tag{2.2.8}$$

when we have Neumann boundary conditions on the UV and IR branes. There is also a massless mode solution, however we will leave this discussion for section 2.3.

2.2.2 Gauge KK decomposition

We expand the A_μ and A_5 fields in their 4D and 5D components,

$$\begin{aligned} A_\mu(x^\mu, y) &= \frac{1}{\sqrt{L}} \sum_{n=0}^{n=\infty} f_n^A(y) A_\mu^{(n)} \\ A_5(x^\mu, y) &= \frac{1}{\sqrt{L}} \sum_{n=0}^{n=\infty} f_n^5(y) A_5^{(n)}(x^\mu). \end{aligned} \tag{2.2.9}$$

Plugging these expansions into the bulk equations of motion for these fields, eq. (2.1.17), we find that in order to obtain mass eigenstates it is required that,

$$\begin{aligned} \partial_y \left(e^{-2A} \partial_y f_n^A\right) + m_n^2 f_n^A &= 0 \\ \partial_y^2 \left(e^{-2A} f_n^5\right) + m_n^2 f_n^5 &= 0. \end{aligned} \tag{2.2.10}$$

From eq. (2.2.10) one can see that,

$$m_n \neq 0 \quad \Rightarrow \quad f_n^5 = \frac{1}{m_n} \partial_y f_n^A, \tag{2.2.11}$$

where the $1/m_n$ factor arises from normalisation of the A_5 kinetic term. This can be verified by plugging eq. (2.2.11) into eq. (2.2.10) and integrating once with respect to y. For the same reasons as in the scalar case, the wave-functions of the gauge modes are also orthogonal and form a complete solution to the eigenvalue problem. Once we insert these expansions into the action we require the following normalisations to ensure the kinetic terms are canonical,

$$\frac{1}{L} \int_0^L dy f_m^{A,5} f_n^{A,5} = \delta_{nm}. \tag{2.2.12}$$

Gauge invariance requires that there are no mass terms for the gauge field on the branes or in the bulk, assuming we do not want to break the gauge symmetry. Note also that the boundary conditions for the whole 5D field, eq. (2.1.18), are simply applied to each of the 5D wave functions separately. Regardless of the background geometry, there are several features we can discuss at this point:

- If the A_μ components have $(+,+)$ boundary conditions, i.e. no mass terms on the branes, there will be a massless zero mode present in the spectrum with a flat wave function, $f_0^A = 1$. And there will be no zero mode for the A_5 field.

- If the A_μ field has $(-,-)$ boundary conditions on the branes, there will be no massless mode for the vector field. However the A_5 field will have a massless mode, with a profile exponentially localised in the IR, $f_0^5 \sim e^{2A(y)}$.

- If the fields have mixed boundary conditions, $(\pm,\mp)$, there will be no massless modes from either the vector or the scalar components.

- Lastly, we know that 4D gauge fields require an extra longitudinal degree of freedom when they become massive. From the KK picture it is clear that these degrees of freedom are provided by the tower of A_5 KK modes, which are eaten by the A_μ tower. In this case the A_5 modes can be removed by a gauge transformation. However when the A_μ field has $(-,-)$ boundary conditions, the A_5 zero mode remains uneaten.

This information can be summarised in figure 2.1.

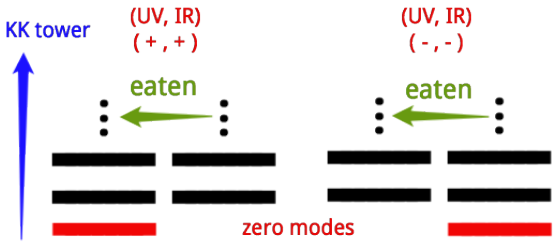

Figure 2.1: A diagrammatic representation of the 5D gauge fields in the effective theory

The gauge fixing procedure derived in section 2.1.2 along with eq. (2.2.10) shows that the A_5 modes eaten by the massive A_μ modes have a ξ-dependent mass, implying that they are unphysical particles. In unitary gauge, where $\xi \to \infty$, we decouple these A_5 modes from the other particles in the model by taking their masses to infinity. However if we have a massless A_5 mode in the spectrum, as is the case in the diagram on the right hand side of fig. 2.1, that mode is physical and is not eaten by a vector field. This can be seen by noting that even in unitary gauge the particle does not decouple as its mass has no gauge dependence.

In addition to the discussion above, it is useful to point out that if a gauge field has anything other than a Neumann boundary condition on both branes, the gauge symmetry is broken. The gauge symmetry in the 4D effective theory will only consist of the generators of the bulk gauge symmetry which have the Neumann boundary conditions. Whereas KK modes will exist for all generators thus the KK spectrum will respect the global bulk symmetry.

In this thesis we will mostly work with the Randall-Sundrum background, $A(y) = ky$, in which the solutions for the 5D wave functions of the KK gauge modes are found to be,

$$f_n^A = \frac{e^{ky}}{N_n}\left(J_1\left(\frac{m_n}{k}e^{ky}\right) + \beta(m_n)Y_1\left(\frac{m_n}{k}e^{ky}\right)\right) \tag{2.2.13}$$

where J_k and $Y_{k]}$ are Bessel functions and the normalisation constant N_n is fixed using the normalisation condition. The integration constants $\beta(m_n)$ and the KK masses m_n are fixed by the boundary conditions for the field on the two branes. In fact, in the $kL \gg 1$ limit the KK gauge masses are approximately found to be,

$$m_n \simeq \left(n - \frac{1}{4}\right)\pi k e^{-kL}. \tag{2.2.14}$$

The mass scale of the KK resonances is fixed by $ke^{-kL} \sim$ TeV. Through the relation in 2.2.11 these expressions also give us the 5D wave functions of the A_5 scalars.

Since the zero mode gauge field is flat, one can simply calculate the relation between the 5D gauge coupling and the effective 4D coupling. By inspecting the interactions among the zero mode gauge fields one can see that we must have $g_5 = g_4\sqrt{L}$, which makes sense considering that the 5D gauge coupling has mass dimension $-1/2$. This relation can be modified by the inclusion of brane kinetic terms for the gauge field, however we will not consider these here. Due to the localisation of their profiles, the interactions of the KK gauge fields are a lot different than those of the zero modes, and since g_5 is fixed in terms of g_4 and L, the strength of the interactions can be controlled by L. If we wanted to keep the mass of the KK modes constant and vary L, this would require a variation in k such that ke^{-kL} is kept constant.

2.2.3 Fermion KK decomposition

For the last demonstration of the KK method we turn our attention to fermions. We write the field expansion as before,

$$\Psi_{L,R}(x^\mu, y) = \frac{1}{\sqrt{L}}\sum_{n=0}^{n=\infty} f_n^{L,R}(y)\psi_n^{L,R}(x^\mu). \tag{2.2.15}$$

Again, in order to obtain a tower of non-interacting fermion states at quadratic level in the effective theory we require that

$$\begin{aligned}\left(\partial_y - m_\Psi - 2A'\right) f_n^R &= -m_n e^A f_n^L \\ \left(\partial_y + m_\Psi - 2A'\right) f_n^L &= m_n e^A f_n^R,\end{aligned} \tag{2.2.16}$$

where m_n is the mass of the left and right-handed vector-like modes. Just as in the scalar and gauge cases, these wave functions form a complete basis for the solution to the

eigenvalue equation, and are orthonormal. We fix the overall normalisation constant by requiring that the kinetic term be canonical,

$$\frac{1}{L}\int_0^L dy\; e^{-3A} f_m^{L,R} f_n^{L,R} = \delta_{m,n}, \tag{2.2.17}$$

where the e^{-3A} term comes from the $\sqrt{|g|}\; e^A$ terms from the metric component and the fünfbein.

From the equations of motion we can clearly see a zero mode solution, $m_n = 0$,

$$f_0^{L,R} \sim e^{(2A \mp m_\Psi y)}. \tag{2.2.18}$$

Applying the boundary conditions, eq. (2.1.34), to this mode reveals an important feature of this scenario,

$$\begin{aligned} {}'+' \quad &\rightarrow \quad \Psi_R = 0 \quad \Rightarrow \quad \textbf{No RH zero mode} \\ {}'-' \quad &\rightarrow \quad \Psi_L = 0 \quad \Rightarrow \quad \textbf{No LH zero mode}, \end{aligned} \tag{2.2.19}$$

thus despite having a vector-like theory in 5D, in the 4D theory the zero modes are chiral and only the KK modes are vector-like. These boundary conditions ensure that the surface terms vanish, and fixing the boundary condition of one chirality automatically fixes the boundary condition for the other,

$$\begin{aligned} {}'+' \quad &\rightarrow \quad \left(\partial_y + m_\Psi - 2A'\right) f_n^L = 0 \\ {}'-' \quad &\rightarrow \quad \left(\partial_y - m_\Psi - 2A'\right) f_n^R = 0. \end{aligned} \tag{2.2.20}$$

In the case that we have a bulk Higgs acquiring a vev, the bulk fermions will get a y-dependent mass. In our work we will have a bulk Higgs, but will assume that the Higgs vev term is small enough to be treated as a perturbation, so that m_Ψ is always treated as a constant.

In the Randall-Sundrum case ($A(y) = ky$), we can solve for the fermion KK modes exactly. In some works the authors like to re-scale the fermion profiles to modify the normalisation condition, so here we will first find general solutions where the profiles have been rescaled such that $f_{m,n}^{L,R} \rightarrow e^{rky} f_{m,n}^{L,R}$. In this case the normalisation condition is

$$\frac{1}{L}\int_0^L dy\; e^{(2r-3)ky} f_m^{L,R} f_n^{L,R} = \delta_{mn} \tag{2.2.21}$$

where some people refer to $r = 3/2$ as a physical normalisation. With this rescaling we can write the zero and excited mode wave functions as

$$\begin{aligned} f_0^{L,R}(m_0 = 0) &= \frac{1}{\sqrt{N_0}} e^{(2-r\pm c)ky} \\ f_n^{L,R}(m_n \neq 0) &= \frac{1}{\sqrt{N_n}} e^{\left(\frac{5}{2}-r\right)ky} \left(J_{|c\pm 1/2|} + \beta(m_n) Y_{|c\pm 1/2|}\right) \end{aligned} \tag{2.2.22}$$

where we write $m_\Psi = ck$, and the normalisation constant N_n is fixed by the normalisation condition. Again, the integration constants $\beta(m_n)$ and the KK masses m_n are fixed by the boundary conditions of the field on the two branes.

2.3 Natural hierarchies for bulk scalars

It is well known that the Randall-Sundrum model can naturally give rise to mass hierarchies for scalar fields when they are localised on the IR brane, or when they are allowed to leak slightly into the bulk. In this section we investigate this idea thoroughly and look at the fine-tuning involved if one wishes to obtain a scalar mode with a mass well below the KK scale.

We write the action for the 5D scalar field as

$$S_\Phi = \int d^4x \int_0^L dy \, \frac{1}{2}\sqrt{|g|}\left((\partial_M \Phi)^2 - m_\Phi^2 \Phi^2\right), \tag{2.3.1}$$

where $M = \mu, y$ and $\sqrt{|g|} = e^{-4ky}$. The 5D mass term consists of both bulk and brane terms such that

$$m_\Phi^2 = (b^2 + \delta b^2)k^2 - \delta(y)a^2 k + \delta(y-L)(a^2 + \delta a^2)k. \tag{2.3.2}$$

We could also have a mass perturbation on the UV brane but that parameter is negligible due to the requirement that scalars with light modes be IR localised. Note that these bulk and brane masses are of the order M_{Pl}, it is the warping of the bulk geometry that gives the exponentially suppressed KK masses. Next we perform a Kaluza-Klein expansion on the scalar field,

$$\Phi(x,y) = \frac{1}{\sqrt{L}} \sum_n \Phi_n(x) f_n(y). \tag{2.3.3}$$

When δb^2 and δa^2 are zero and the remaining bulk and brane mass terms are related by [46, 47]

$$b^2 = a^2(a^2 + 4), \tag{2.3.4}$$

the 4D spectrum contains a massless mode. In figure 2.2 we see that the minimum value of the bulk mass (b^2) which permits a massless solution is -4, this is known as the Breitenlohner-Freedman bound [48]. By normalising the kinetic term and imposing the boundary conditions,

$$\begin{aligned} f_n'(L) &= -a^2 k f_n(L) \\ f_n'(0) &= -a^2 k f_n(0), \end{aligned} \tag{2.3.5}$$

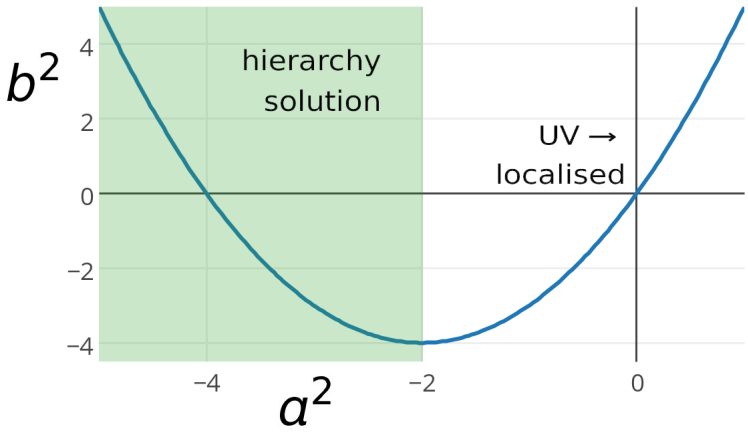

Figure 2.2: The solid line shows the relationship between the bulk and brane mass terms required to have a massless scalar mode of eq. (2.3.4). The shaded region shows the parameter space for which the Higgs profile is sufficiently IR localised such that the hierarchy problem is resolved.

we find the zero mode profile to be,

$$f_0(y) = \sqrt{\frac{2(1+a^2)kL}{1-e^{-2(1+a^2)kL}}} e^{-a^2 ky}. \tag{2.3.6}$$

The parameter a^2 defines the localisation of the field in 5D and $a^2 < 0$ implies IR localisation. Along with this zero mode one obtains a tower of KK scalar fields with the following 5D profiles

$$f_n = \frac{e^{2ky}}{N_n}\left(J_\alpha\left(\frac{m_n}{k}e^{ky}\right) + \beta(m_n)Y_\alpha\left(\frac{m_n}{k}e^{ky}\right)\right), \tag{2.3.7}$$

where m_n is the mass of the nth mode, $\alpha = \sqrt{4+b^2}$, and N_n is determined by the normalisation condition [13]. The constants $\beta(m_n)$ and the KK masses m_n are determined by the boundary conditions and in the limit $kL \gg 1$ the KK masses can be approximated as

$$m_n \simeq \left(n + \frac{\alpha}{2} - \frac{3}{4}\right)\pi k e^{-kL}. \tag{2.3.8}$$

Note that to obtain TeV-scale resonances we require that $kL \sim 35$.

Switching on the mass perturbations δb^2 and δa^2 introduces a mixing between the KK modes of eq. (2.3.3). The effective action for the scalar can be written as

$$S = \int d^4x \sum_{mn} \frac{1}{2}\left((\partial_\mu \Phi_n)^2 - m_n^2 \Phi_n^2 - \delta m_{mn}^2 \Phi_m \Phi_n\right), \tag{2.3.9}$$

where Φ_n are the 4D fields with wave functions $f_n(y)$ respecting the boundary conditions of eq. (2.3.5). The resulting contributions to the mass matrix are given by

$$\delta m_{mn}^2 = \frac{\delta b^2 k^2}{L}\int_0^L dy\, e^{-4ky} f_m f_n + \frac{\delta a^2 k}{L} e^{-4kL} f_m(L) f_n(L). \tag{2.3.10}$$

Once we turn on the mass perturbations δb^2 and δa^2 we turn on the mass mixings in the 4D effective theory. This requires us to diagonalize the mass matrix and in turn the zero mode becomes massive. The effect on the masses of the higher modes is negligible. With a slight tuning we can obtain a zero mode much lighter than the KK scale if the Higgs field is localised in the IR [21, 22]. Going to the mass eigenbasis we find that the zero mode mass is

$$m_0^2 \simeq \delta m_{00}^2 - \sum_{n=1}^{\infty} \frac{(\delta m_{0n}^2)^2}{m_n^2}. \tag{2.3.11}$$

To adequately suppress the mass perturbations from δb^2 and δa^2 we will see that we need $a^2 \leq -2$. The mass scale for the zero mode is set by δm_{00}^2. Setting $a^2 = -2 - x$ we find that

$$\delta m_{00}^2 = \frac{2(1+x)k^2}{e^{2(1+x)kL} - 1} \left(\frac{\delta b^2}{2x} \left(e^{2xkL} - 1 \right) + \delta a^2 e^{2xkL} \right). \tag{2.3.12}$$

Taking the limit $a^2 \to -2$, this is found to be

$$\delta m_{00}^2 \simeq 2(\delta b^2 kL + \delta a^2) k^2 e^{-2kL}, \tag{2.3.13}$$

and for $e^{2xkL} \gg 1$, i.e. $x \gtrsim 1/(kL)$

$$\delta m_{00}^2 \simeq 2(1+x) \left(\frac{\delta b^2}{2x} + \delta a^2 \right) k^2 e^{-2kL}. \tag{2.3.14}$$

We see that, for $a^2 = -2$, the bulk mass correction needs to be more tuned due to the kL factor. However, as the field becomes localised further towards the IR brane this enhancement of the bulk term quickly diminishes. In all, we find that in order to have a zero mode at the electroweak scale we only require a percent level fine-tuning. If $a^2 > -2$, the mass corrections do not get the required suppression and thus there cannot be a light mode in the spectrum without a tuning of the bulk and brane mass parameters.

This is the solution to the hierarchy problem that we require. If the Higgs boson is localised on or near ($a^2 \leq -2$) the IR brane then the Higgs mass is not sensitive to large scales in the model. In other words, radiative corrections to its mass will be cut-off at the scale associated with the IR brane. In [9] they show that the graviton in this scenario is localised near the UV brane, which means that the mass scale associated with gravity is that of the UV brane, i.e. the fundamental mass scale M_5[1]. If we have $M_5 \sim k \simeq M_{Pl} = 10^{18}$ GeV and $ke^{-kL} = 1$ TeV, then we require $kL = 34.5$. Therefore with an $\mathcal{O}(10)$ hierarchy in the model parameters, we can naturally generate the exponential hierarchy between the Planck and electroweak scales.

[1] We also discuss this in section 3.2.4.

2.4 EWSB in non-custodial RS models

The non-custodial model simply has the SM in the bulk, with no additional symmetries. Additional particle content only arises from KK modes of the 5D SM fields. We will start here by looking at the Higgs potential, thus we have an $SU(2)$ Higgs doublet Φ consisting of complex scalars,

$$S = \int d^4x \int_0^L dy\, e^{-4ky} \left((D^M \Phi)^\dagger (D_M \Phi) - m_\Phi^2 \Phi^\dagger \Phi - \lambda_5 (\Phi^\dagger \Phi)^2 \right) \tag{2.4.1}$$

and

$$\Phi(x^\mu, y) = \begin{pmatrix} \phi^+(x^\mu, y) \\ \phi^0(x^\mu, y) \end{pmatrix}, \tag{2.4.2}$$

where ϕ^+ and ϕ^0 are complex scalar fields. The mass term, defined in eq. (2.3.2), and quartic coupling in this model can have localised brane contributions and in principle can be y-dependent in the bulk (however we assume them to be constant). The quartic coupling then is of the form

$$\lambda_5 = \lambda_B + \frac{1}{k}\lambda_{IR}\delta(y - L) + \frac{1}{k}\lambda_{UV}\delta(y). \tag{2.4.3}$$

The λ_{UV} term is irrelevant for an IR scalar, here thus we will only consider the IR contribution. In this section we will study models in which we have a quartic term on the brane and/or in the bulk. In both cases we go to the 4D theory before we treat the breaking of SU(2).

2.4.1 Brane EWSB

To reach the 4D effective theory we follow a method exactly like that in section 2.3.3 and find the same scalar profiles. The only difference is an extra term in the effective action corresponding to the brane quartic coupling

$$S = \int d^4x \frac{1}{2} \left(\sum_n |\partial_\mu \Phi_n|^2 - m_n^2 \Phi_n^\dagger \Phi_n - \sum_{m,n} \delta m_{mn}^2 \Phi_m^\dagger \Phi_n - \lambda_{lmnp} \sum_{lmnp} \Phi_l^\dagger \Phi_m \Phi_n^\dagger \Phi_p \right), \tag{2.4.4}$$

where

$$\lambda_{lmnp} = \frac{\lambda_5}{L} e^{-4kL} f_l(L) f_m(L) f_n(L) f_p(L) \tag{2.4.5}$$

and δm_{mn}^2 is defined in eq. (2.3.10). The standard model Higgs will be identified with the lightest mass eigenstate, being predominately composed of Φ_0. Taking the approximation with just the zero mode plus first N KK states, we have $(N + 1)$ Higgs doublets in the effective theory. From here we can minimise the potential and find expressions for the

vacuum expectation values of these fields, $\langle \Phi_m \rangle = v_m$. The largest correction to the standard model Higgs potential will be of the form $\lambda_{1000}\Phi_0^3\Phi_1$, making λ_{1000} the most important BSM coupling in this sector.

2.4.2 Bulk EWSB

We write the scalar doublet so that we can see clearly the excitations around its minimum,

$$\Phi(x^\mu, y) = \frac{1}{\sqrt{2}} \begin{pmatrix} \phi^+(x^\mu, y) \\ v(y) + \phi^0(x^\mu, y) \end{pmatrix}. \tag{2.4.6}$$

With a quartic term in the bulk we can write the total energy functional of the 5D system in the ground state as

$$E[v(y)] = \int dx^3 \int_0^L dy \frac{1}{2}\sqrt{|g|}\left((\partial_y v)^2 + m_\Phi^2 v^2 + \lambda_5 v^4\right). \tag{2.4.7}$$

Minimising this, we find that in the ground state the field must obey the following EOM

$$-\frac{1}{\sqrt{|g|}}\partial_y(\sqrt{|g|}\partial_y v) + b^2k^2v + \lambda_B v^3 = 0. \tag{2.4.8}$$

Boundary terms in the scalar mass will induce non-trivial boundary condition, similar to the discussion in section 2.3.3. We choose a gauge in which we can write the doublet as

$$\Phi(x^\mu, y) = \frac{1}{\sqrt{2}} \begin{pmatrix} 0 \\ v(y) + \eta(x^\mu, y) \end{pmatrix}, \tag{2.4.9}$$

where $\eta = \mathrm{Re}(\phi^0)$. We can now write the action for the physical field η as

$$\begin{aligned} S = \int d^4x \int_0^L dy \frac{1}{2}\sqrt{|g|}\Bigg(e^{2A}\frac{1}{2}\partial^\mu\eta\partial_\mu\eta - \frac{1}{2}\left(-\frac{1}{\sqrt{|g|}}\partial_y(\sqrt{|g|}\partial_y\eta) + b^2k^2\eta + \lambda_B v^2\eta\right)\eta \\ -\frac{\lambda_B}{4}\eta^4 - \lambda_B v\eta^3 + \lambda_B v^4\Bigg), \end{aligned} \tag{2.4.10}$$

where $A(y) = k|y|$ denotes the warp factor. Expanding η into KK modes to diagonalize the fields in the mass eigenbasis, the equation of motion for the 5D profiles reads

$$-\frac{1}{\sqrt{|g|}}\partial_y(\sqrt{|g|}\partial_y f_n) + b^2k^2 f_n + \lambda_B v^2 f_n = \sqrt{|g|}e^{2A}m_n^2 f_n. \tag{2.4.11}$$

Again nontrivial boundary conditions are induced by the brane masses. Here m_n^2 is the mass of the nth KK mode. Thus m_0^2 and f_0 refer to the physical Higgs mode. This shows us that the Higgs fluctuation and the vacuum expectation value have different 5D profiles, thus their interaction with the fermion and gauge fields will differ from the standard model. This difference is determined by the Higgs mass and the KK scale [49].

	λ_{0000}	λ_{1000}	λ_{1100}	λ_{1110}	λ_{1111}
Brane Quartic	1.00	-1.00	1.00	-1.00	1.00
Bulk Quartic	1.00	-0.54	0.66	-0.34	0.70

Table 2.1: This shows the values of the quartic couplings for brane and bulk EWSB with $a^2 = -2$ and $\lambda_B = 1$ or $\lambda_{IR} = 1/4$, chosen such that $\lambda_{0000} = 1$ in both cases.

Ideally we would like to solve these non-linear differential equations and have the correct 5D profiles for the mass eigenbasis at our disposal. However, it is difficult to obtain reliable numerical solutions. Instead we will not diagonalize the fields in the mass eigenbasis, but will expand them in the basis (2.3.9) we used in section 2.3.3. Hence we use the same 5D profile for the zero mode and the vacuum expectation value. This will result in an effective theory similar to that in the brane EWSB case, except now the effective quartic term is given by

$$\lambda_{lmnp} = \frac{\lambda_5}{L^2} \int_0^L dy \sqrt{|g|} f_l f_m f_n f_p. \tag{2.4.12}$$

The only difference we have is that the relationship between the different quartic couplings changes. In table 2.1 we show the values of these bulk and brane quartics for $a^2 = -2$ and take the two cases $\lambda_B = 1$ and $\lambda_{IR} = 1/4$. The effects of KK modes in the Higgs sector are usually proportional to the quartic couplings, the largest effect is $\sim \lambda_{1000} v_1$ and hence the most relevant coupling is λ_{1000}. From table 2.1 we see that having bulk EWSB terms reduces the higher mode quartic terms with respect to λ_{0000} and will therefore reduce the KK effects in general.

The SM particles receive small mass corrections from the vev of KK Higgs fields, which induces a misalignment of Higgs couplings and particle masses. We find that KK vev's are approximately

$$v_n \simeq -\frac{\lambda_{n000}}{\lambda_{0000}} \frac{m_H^2}{m_n^2} v_0. \tag{2.4.13}$$

From table 2.1 we see that the ratio for a brane quartic coupling is $\lambda_{1000}/\lambda_{0000} = -1$, and for a bulk quartic $\simeq -0.5$. If we were to fully account for the mixing effects arising from the λ_{1000} terms in calculating the Higgs vev we would expect $\mathcal{O}(m_H^2/M_{KK}^2)$ corrections to the Higgs vev and mass. However the only way of seeing these effects would be through a precise sub-percent level measurement of the Higgs quartic coupling, which will not be possible with current particle colliders.

In the next section we will see that electroweak constraints force KK resonances into the multi-TeV range, thus leading to v_n/v_0 in the sub per-mille range. The resulting

impact on couplings between the Higgs and gauge bosons is then also in the sub per-mille range, and too small to make an impact even at TLEP [21]. (A different and potentially observable source of modifications of the gauge Higgs coulings we will discuss in the the next section.) Also modifications of the Higgs cubic self coupling are at similar level and thus too small to be observed. The other important factor is the coupling of SM particles to the Higgs KK modes. Gauge zero modes have flat profiles, hence the normalisation of the Higgs field ensures that they couple equally to all Higgs KK modes. For the fermion fields we also find that the fermion zero modes couple to Higgs zero and KK modes almost identically, as the Higgs is IR localised.

Multiple Higgs doublet models

Since the tower of Higgs doublets in the effective theory all couple to the up and down type quarks, this could be viewed as a theory of multiple Higgs doublets with vev's given by eq. (2.4.13) and couplings given by eq. (2.4.12). If we include one additional mode for simplicity, we have a type III 2HDM which is well studied phenomenologically. The experimental constraints for these models are summarised in [50]. They express the constraints in terms of $\tan(\beta) = v_1/v_0$ and $\cos(\beta - \alpha)$, the ratio of the Higgs KK mode and zero mode couplings to the SM gauge bosons. In this model both these observables are $\sim \frac{v^2}{M_{KK}^2}$, i.e. per-mille, and well within the experimental constraints. For these bounds to be relevant we would need $M_{KK} \lesssim 1$ TeV.

2.4.3 Electroweak precision observables

We have a non-custodial $SU(2)_L \times U(1)_Y$ bulk gauge sector with bulk fermions and a bulk Higgs. Calculating the Peskin-Takeuchi parameters [24] is straightforward assuming universal UV fermion localisations for the light fermions. Corrections to the SM can arise from the zero mode fields mixing with KK modes, and from the exchange of KK particles in a physical process. For our purposes the latter is only a small effect and will be ignored. For a detailed analysis of the case of a brane Higgs, see e.g. [51]. The low energy 4D effective theory can be written in the form [52]

$$\begin{aligned}\mathcal{L} = &-\frac{1}{4}F^{\mu\nu}F_{\mu\nu} - \frac{1}{2}W^{\mu\nu}W_{\mu\nu} - \frac{1}{4}Z^{\mu\nu}Z_{\mu\nu} - \frac{1}{2}(1+\delta z)m_Z^2 Z^\mu Z_\mu - (1+\delta w)m_W^2 W^\mu W_\mu \\ &-e(1+\delta a^\psi)\sum_i \bar{\psi}_i\gamma^\mu Q_i\psi_i A_\mu - \frac{e}{s_W\sqrt{2}}(1+\delta w^\psi)\sum_{ij}(V_{ij}\bar{\psi}_i\gamma^\mu P_L\psi_j W_\mu^+ + c.c.) \\ &-\frac{e}{s_W c_W}(1+\delta z^\psi)\sum_i \bar{\psi}_i\gamma^\mu\left(T_{3i}P_L - Q_i s_W^2 + Q_i s_W c_W \lambda_{ZA}\right)\psi_i Z_\mu,\end{aligned} \tag{2.4.14}$$

where V_{ij} is the CKM matrix and δz, δw, δa^ψ, δw^ψ and δz^ψ are flavour independent new physics contributions to the Lagrangian. Note that the above action only parameterises the oblique electroweak corrections, i.e. those in which the vertex corrections are independent of the fermion species. This is a good approximation in our case, since the processes contributing to the EWPOs only involve light fermions which can all be approximated to have the same 5D wave function localised near the UV brane. Differences in the 5D profiles for light fermions would lead to non-oblique corrections to the above action, however these are expected to be small and we neglect their effects here. From this Lagrangian we can identify the S, T and U parameters with

$$\begin{aligned} \alpha S &= 4s_W^2 c_W^2(-2\delta a^\psi + 2\delta z^\psi) \\ \alpha T &= (\delta w - \delta z) - 2(\delta w^\psi - \delta z^\psi) \\ \alpha U &= 8s_W^2(-\delta a^\psi s_W^2 + \delta w^\psi - c_W^2 \delta z^\psi). \end{aligned} \tag{2.4.15}$$

We decompose the 5D $SU(2)_L$ and $U(1)_Y$ gauge fields as

$$\begin{aligned} W^{M3} &= \frac{1}{\sqrt{L}} \sum_n f_n^3(y) W_n^{\mu 3}(x^\mu), \\ W^{M\pm} &= \frac{1}{\sqrt{L}} \sum_n f_n^\pm(y) W_n^{\mu\pm}(x^\mu), \\ B^M &= \frac{1}{\sqrt{L}} \sum_n f_n^B(y) B_n^\mu(x^\mu). \end{aligned} \tag{2.4.16}$$

Note that since we are treating EWSB as a perturbation, we have $f_n^3 = f_n^\pm = f_n^B = f_n^A$ where f_n^A are the wave functions defined in eq. (2.2.13). In unitary gauge the Higgs can be written in the following form

$$\Phi(x^\mu, y) = \frac{1}{\sqrt{2L}} f_0(y) \begin{pmatrix} 0 \\ v_0 + h(x^\mu) \end{pmatrix}, \tag{2.4.17}$$

where f_0 is given from eq. (2.3.6) and we ignore KK Higgs modes. When we go to the 4D effective theory, we can write the mass matrices for the gauge fields as

$$M_W^2 = \frac{g^2}{4} \begin{pmatrix} M_{00}^2 & M_{01}^2 & \dots \\ M_{01}^2 & \frac{4}{g^2} m_1^2 + M_{11}^2 & \dots \\ \vdots & \vdots & \ddots \end{pmatrix} \tag{2.4.18}$$

$$M_Z^2 = \frac{g^2 + g'^2}{4} \begin{pmatrix} M_{00}^2 & M_{01}^2 & \dots \\ M_{01}^2 & \frac{4}{g^2+g'^2} m_1^2 + M_{11}^2 & \dots \\ \vdots & \vdots & \ddots \end{pmatrix} \tag{2.4.19}$$

$$M_\gamma^2 = \begin{pmatrix} 0 & 0 & \dots \\ 0 & m_1^2 & \dots \\ \vdots & \vdots & \ddots \end{pmatrix}, \tag{2.4.20}$$

where

$$M_{mn}^2 = \frac{v_0^2}{L}\int_0^L dy\, e^{-2ky} f_m^A f_n^A f_0^2 \tag{2.4.21}$$

and m_n^2 are the gauge KK masses. The normalisation of the Higgs field means that $M_{00}^2 = v_0^2$. We can approximately diagonalize these mass matrices assuming that $M_{00}^2, M_{0n}^2 \ll m_n^2$, and find lowest mass eigenvalues to be

$$\begin{aligned} \left(M_W^2\right)_0 &\simeq \frac{g^2 v_0^2}{4}\left(1 - \frac{g^2 v_0^2}{4}\sum_n \frac{R_n^2}{m_n^2}\right) \\ \left(M_Z^2\right)_0 &\simeq \frac{(g^2+g'^2)v_0^2}{4}\left(1 - \frac{(g^2+g'^2)v_0^2}{4}\sum_n \frac{R_n^2}{m_n^2}\right), \end{aligned} \tag{2.4.22}$$

where $R_n = M_{0n}^2/v_0^2$ and parametrizes the coupling between the Higgs and gauge excitations. The photon remains massless. In moving to the mass eigenbasis the fermion and Higgs couplings to the W and Z bosons get shifted. We are only interested in the shift in the fermion-gauge coupling since, at tree-level, the gauge-Higgs couplings do not alter the electroweak precision analysis. We write the unshifted vertex term between a fermion and the W boson as

$$\sum_n \frac{g_{0n}}{\sqrt{2}s_W}\sum_i (V_{i0}\bar{\psi}_{i0}\gamma^\mu P_L \psi_{j0} W_{\mu n}^+ + c.c.), \tag{2.4.23}$$

where g_{mn} is the effective coupling,

$$g_{mn} = \frac{g_5}{L^{\frac{3}{2}}}\int_0^L dy\, e^{-3ky}(f_m^L)^2 f_n^A \tag{2.4.24}$$

with $r = 0$ and f_m^L defined in eq. (2.2.22). When we go to the mass eigenbasis, the interaction of the fermion with the zero mode gauge field is of the form

$$\frac{g_{00}}{\sqrt{2}s_W}\left(1 - \frac{g^2}{4}\sum_n \frac{M_{0n}^2}{m_n^2}\frac{g_{0n}}{g_{00}}\right)\sum_i (V_{ij}\bar{\psi}_{i0}\gamma^\mu P_L \psi_{j0} W_{\mu 0}^+ + c.c.). \tag{2.4.25}$$

For the Z coupling we have an analogous expression proportional to $g^2 + g'^2$. Since the photon remains massless the photon vertices do not get extra contributions. With this information we can express the electroweak parameters as

$$\begin{aligned} S &\simeq \left(\frac{-9\pi}{2}\sum_n \frac{R_n}{(n-\frac{1}{4})^2}\frac{g_{0n}}{g_{00}}\right)\frac{v_0^2}{M_{KK}^2} \\ T &\simeq \left(\frac{9\pi}{16 c_W^2}\sum_n \frac{R_n}{(n-\frac{1}{4})^2}\left(R_n + 2\frac{g_{0n}}{g_{00}}\right)\right)\frac{v_0^2}{M_{KK}^2} \end{aligned} \tag{2.4.26}$$

	R_1	R_2	R_3	R_4
Brane Higgs	8.4	-8.3	8.1	-8.2
Bulk Higgs ($a^2 = -2$)	5.6	-0.9	0.5	-0.3

Table 2.2: Here we show how the couplings between the zero mode Higgs and the gauge KK tower differ for a brane and bulk Higgs.

whereas $U \sim \left(g^2 - (g^2 + g'^2)c_W^2\right) = 0$. In the above calculation we used the expressions for the gauge KK masses in section 2.2.2 and have taken $M_{KK} = m_1 \simeq (3\pi/4)ke^{-kL}$, i.e. the mass of the first gauge boson excitation[2]. From the expressions in eq. (2.4.26), neglecting contributions from higher KK modes, we find a correlation between the S and T parameters which can be expressed as

$$T \simeq \frac{1}{8c_W^2}\left(2 - \frac{g_{00}}{g_{01}}R_1\right)S. \tag{2.4.27}$$

Depending on T/S, the model can live in more or less experimentally favoured regions of the parameter space, possibly resulting in reductions to the M_{KK} constraint.

To a good approximation R_n and g_{0n}/g_{00} do not vary with L, meaning that the only L dependence in S and T comes from M_{KK}. R_n varies with the Higgs localisation, and becomes smaller as the Higgs leaks to the bulk. Table 2.2 shows that the bulk Higgs couples less to gauge KK modes than the brane Higgs. As a result, not only will the T parameter be smaller for a bulk Higgs, but we find that a two mode approximation is accurate for a bulk Higgs, but not sufficient for a brane Higgs.

Light fermions must be localised in the UV so that their overlap with the Higgs is small, this corresponds to $c_L > 0.5$ [46,53,54]. From figure 2.3 we can see that this implies a small coupling with the KK gauge modes and therefore small vertex contributions to the electroweak parameters. For all fermion localisations we find that the coupling decreases for heavier KK modes.

Current bounds on S and T with $U = 0$ are given in [55] (see figure 2.5). Taking the 95% CL bound, we find the following bounds for a brane and bulk Higgs:

- Brane Higgs: Due to the large values of R_n the KK gauge modes have large contributions to the T parameter. If we approximate $R_n^2 \simeq 8.4^2$ for all n, we can sum the full tower contributions by taking the sum $\sum_{n=1}^{\infty}(n - 1/4)^{-2} \simeq 2.54$. We then find

[2] In the first part of this thesis we define M_{KK} as the lightest KK gauge mass in the model, however in the second and third parts we define it as $M_{KK} = ke^{-kL}$.

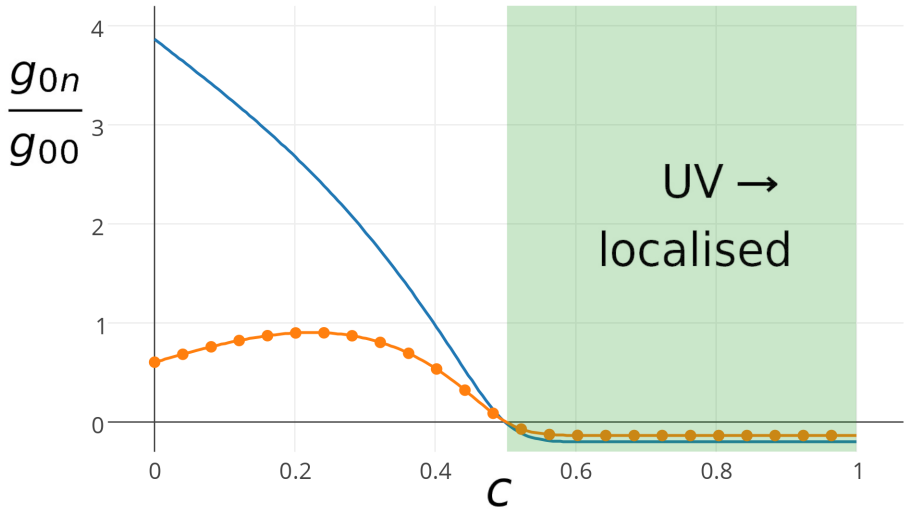

Figure 2.3: This plot shows g_{0n}/g_{00} over a range of fermion localisations for $n = 1$ (solid) and $n = 2$ (dotted). The shaded region shows the parameter space for which the fermions are UV localised.

that the electroweak constraints require $M_{KK} \gtrsim 15$ TeV.

- Bulk Higgs ($a^2 = -2$): Since the R_n values are small for $n > 1$ we find that the first mode makes the only sizeable contribution to the electroweak parameters. With just the first excited mode we find the bounds to be $M_{KK} \gtrsim 8$ TeV. Including the first 10 modes only corrects the 8 TeV bound by 0.3%, and the second excited mode contributes 0.26% of this correction. We find similar effects for the S parameter.

These results are in agreement with the bounds found elsewhere in the literature [30,56,57].

Another thing one should consider is the misalignment in the gauge boson masses and their coupling to the Higgs zero mode. The couplings between the Higgs zero mode and the gauge modes can be written as a matrix similar to eq. (2.4.18) but without the large contributions from the KK masses. The absence of the KK masses here is what causes the misalignment when we go to the mass eigenbasis. We find that the HHZ and the HHZZ interactions receive identical corrections $\sim R_1^2\, m_Z^2/M_{KK}^2$, and similarly for the W boson. With the lightest gauge boson mass at 8 TeV we find a 0.4% misalignment for the Z boson and a 0.3% misalignment for the W boson. This would be visible at the ILC [36, 37] or TLEP [41]. The only way to reduce this misalignment is to either increase M_{KK} or to reduce the coupling of the Higgs zero mode to the gauge KK modes, which can be achieved by modifying the background geometry in the bulk [28–32].

2.4.4 Higher dimensional operator contributions to S, T and U

In the previous section we demonstrated how to estimate the size of the calculable contributions to the electroweak parameters in the 4D effective theory. There will also be incalculable contributions from the UV theory which we will parameterise using higher dimensional operators in the 5D theory. The three leading operators contributing to the oblique parameters are

$$\begin{aligned} S: &\quad \frac{\rho}{M_5^3}(\Phi^\dagger T^a \Phi) W^a_{MN} B_{MN} \\ T: &\quad \frac{\lambda}{M_5^3}|\Phi^\dagger D^M \Phi|^2 \\ U: &\quad \frac{\theta}{M_5^6}|\Phi^\dagger W^{MN} \Phi|^2, \end{aligned} \tag{2.4.28}$$

where ρ, λ and θ are unknown $\mathcal{O}(1)$ dimensionless parameters. By taking these to be $\mathcal{O}(1)$ we are implying that the relevant mass scale for these operators in 5D is $\sim M_5$. However we will see that, due to the warping of the extra dimension and the IR localisation of the KK gauge mode wave functions, this mass scale gets warped down to $\mathcal{O}(M_{KK})$ after integrating over the extra dimension. This is implies that the effective cut-off for the effective theory obtained after integrating over the extra dimension is also of this scale.

These higher dimensional operators could be present both on the branes or in the bulk, i.e. $\rho = \rho_B + \rho_{IR} M_5^{-1} \delta(y - \pi R)$. In the brane case there is an extra mass scale suppression. There is also a possible contribution from the UV brane, which is negligible for an IR localised Higgs. The S and T operators both have effective coefficients $\sim v_0^2/M_{KK}^2$, but due to the higher dimension of the U operator it is of the order $\sim \left(v_0^2/M_{KK}^2\right)^2$. Thus only S and T will receive sizeable corrections from these operators, while S also has an additional suppression $\sim \frac{1}{kL}$ with the respect to the T coefficient. Once we do the integrations over the extra dimension, taking $M_5 \sim \mathcal{O}(k)$, we see that all three operators show similar dependence on the Higgs localisation. The effective coefficients grow exponentially as a^2 decreases until, at $a^2 = -1$, the exponential growth stops, which is due to the normalisation of the Higgs field. At $a^2 < -1$, operators on the IR brane increase linearly with a^2 while operators in the bulk remain mostly constant. At $a^2 = -2$ the operator coefficients from the IR brane contributions are

$$\begin{aligned} \rho_{IR} \to \alpha\delta S &= \rho_{IR}(kL)^{-1}\kappa^4 \left(\frac{v_0}{ke^{-kL}}\right)^2 \\ \lambda_{IR} \to \alpha\delta T &= -4\lambda_{IR}\kappa^4 \left(\frac{v_0}{ke^{-kL}}\right)^2 \\ \theta_{IR} \to \alpha\delta U &= -4\theta_{IR}(kL)^{-1}\kappa^7 \left(\frac{v_0}{ke^{-kL}}\right)^4 \end{aligned} \tag{2.4.29}$$

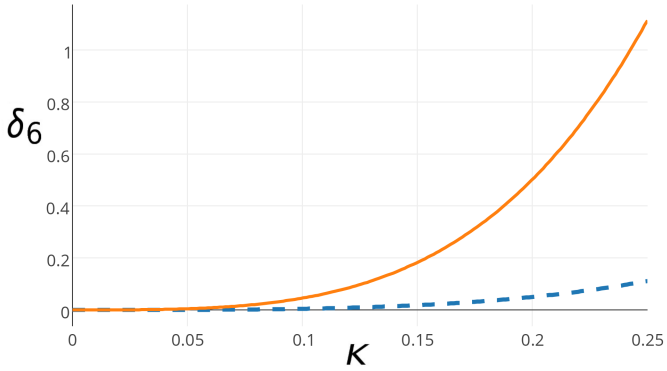

Figure 2.4: Here we show how δ_6 varies with κ for $\lambda_B = \lambda_{IR} = 1$ (dashed) and $\lambda_B = \lambda_{IR} = 10$ (solid).

and in the bulk are

$$\begin{aligned}
\rho_B \to \alpha\delta S &= \rho_B (2kL)^{-1}\kappa^3 \left(\frac{v_0}{ke^{-kL}}\right)^2 \\
\lambda_B \to \alpha\delta T &= -\frac{2}{3}\lambda_B \kappa^3 \left(\frac{v_0}{ke^{-kL}}\right)^2 \\
\theta_B \to \alpha\delta U &= -\theta_B (2kL)^{-1}\kappa^6 \left(\frac{v_0}{ke^{-kL}}\right)^4 ,
\end{aligned} \tag{2.4.30}$$

where the B and IR subscripts refer to the bulk and brane parameters, respectively, and $\kappa = k/M_5$. With $\mathcal{O}(1)$ values for the operator coefficients we would only expect a sizeable contribution from the operator contributing to the T parameter. With respect to this operator, the operator contributing to the U parameter is suppressed by two additional powers of mass, and the operator contributing to the S parameter has an additional volume suppression. This behaviour in the U parameter has been noted in [58] also. We see that from an EFT perspective the relevant scale of these operators depends on the 5D localisation of the Higgs wave function. If the wave function is localised towards the UV, the relevant scale will be of the order M_{Pl}, whereas if it is localised near the IR the relevant scale will be of the order M_{KK}.

If we ignore the vertex corrections, and include the effects of these operators in the T parameter expression from eq. (2.4.26), we find total T parameter

$$T_6 \simeq \left(\frac{3\pi}{4}\right)^2 \left(\frac{1}{\pi c_W^2}\sum_n \frac{R_n^2}{(n-0.25)^2} + \frac{2}{3}\frac{\kappa^3}{\alpha}\lambda_B + 4\frac{\kappa^4}{\alpha}\lambda_{IR}\right)\frac{v_0^2}{M_{KK}^2} = T\left(1+\delta_6\right), \tag{2.4.31}$$

where we again took $M_{KK} = m_1 \simeq (3\pi/4)ke^{-kL}$. Here δ_6 parameterises the contribution from higher dimensional operators,

$$\delta_6 = \left(\frac{1}{\pi c_W^2}\sum_n \frac{R_n^2}{(n-0.25)^2}\right)^{-1}\left(\frac{2}{3}\frac{\kappa^3}{\alpha}\lambda_B + 4\frac{\kappa^4}{\alpha}\lambda_{IR}\right). \tag{2.4.32}$$

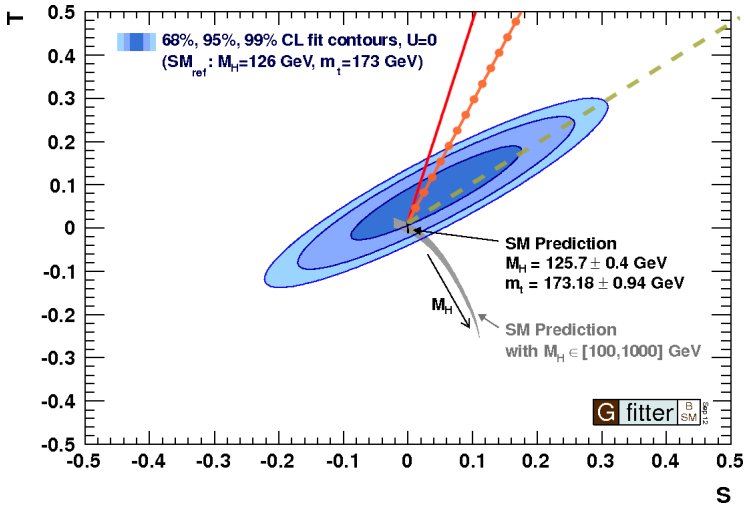

Figure 2.5: Here we have overlaid the bounds from [55] with the S and T correlations for $\delta_6 = 0$ (solid), $\delta_6 = -0.4$ (dots) and $\delta_6 = -0.8$ (dashed).

From figure 2.4 we see it may be reasonable to argue that these contributions could be large enough to provide a reduction in the T parameter calculated in eq. (2.4.26). This also modifies eq. (2.4.27) such that the correlation is expressed as

$$T_6 \simeq \frac{1}{8c_W^2}\left(2 - \frac{g_{00}}{g_{01}}R_1\right)(1+\delta_6)\,S. \tag{2.4.33}$$

From figure 2.5 we see that as well as directly reducing the T parameter, $\delta_6 \neq 0$ can take us to a more favourable region of the parameter space, depending on the relative sign, thus allowing for a further reduction on the M_{KK} bound. If we take the 95% CL bound from figure 4, we find that the lower bound on M_{KK} is approximately 6 TeV and 2.7 TeV for $\delta_6 = -0.4$ and -0.8, respectively. So it is plausible to assume that incalculable contributions to the T parameter lead to a partial cancellation and so relax the bound on the KK scale. It therefore seems premature to exclude discovery of such a scenario at the forthcoming LHC run.

2.4.5 Custodial models, Little-Randall Sundrum models, and EWPOs

The standard model electroweak sector has an accidental global symmetry in the limit of zero hypercharge coupling, $g' \to 0$. This global symmetry is $SU(2)_L \times SU(2)_R$, and when the Higgs gets a vev it is broken to a subgroup denoted $SU(2)_V$. In the limit of zero hypercharge, this $SU(2)_V$ symmetry is called the custodial symmetry, and it ensures $M_W = M_Z$. When hypercharge is turned on, we find that $M_W = \cos(\theta_W)M_Z$ holds at tree-level and, due to the approximate custodial symmetry, only receives corrections at loop level. These corrections, as we have seen, are represented by the T parameter

observable. The problem in this warped extra dimension scenario is that these corrections are induced at tree-level, and thus have the potential to be much larger. This essentially happens because the gauge KK modes have mass before EWSB. The tree-level T parameter corrections coming from mixing with KK gauge modes are proportional to g'^2, which comes from $\alpha T \supset \delta w - \delta z$, where $\delta w \sim m_W^2$ and $\delta z \sim m_Z^2$. Thus in the zero hypercharge limit these tree-level corrections would vanish and the warped extra dimensional scenario would also enjoy an accidental custodial symmetry.

An elegant way to suppress these tree-level corrections is to introduce a local $SU(2)_L \times SU(2)_R \times U(1)_X$ gauge symmetry in the bulk, where hypercharge is embedded as $Y = T_R^3 + X$ [25]. This leads to additional contributions to the T parameter which exactly cancel the g' terms we found in the previous section. However, it also leads to additional massless gauge fields. These can be eliminated by giving these fields Dirichlet boundary conditions on the UV brane. This is an explicit breaking of the custodial symmetry, however since all the KK modes are IR localised, it is only important that we keep the custodial symmetry on the IR brane. Thus ensuring that the interactions between SM fields and the KK modes respect this global symmetry.

With the additional bulk gauge fields the 5D covariant derivative is now of the form,

$$\begin{aligned} D_\mu &= \partial_\mu - ig_5 L_\mu^a T_L^a - ig_5 R_\mu^a T_R^a - ig_{5X} A_\mu X \\ &\supset -i\left(g_5 R_\mu^3 T_R^3 + g_{5X} A_\mu X\right). \end{aligned} \tag{2.4.34}$$

We assume that there exists some dynamics on the UV brane which mixes these R_μ^3 and A_μ fields such that, in the mass eigenbasis, we are left with a massless mode corresponding to the hypercharge generator, and a massive mode. Note that this mixing essentially gives a Dirichlet boundary condition to one linear combination of R_μ^3 and A_μ, and a Neumann boundary condition to the other. This requires a rotation of the form,

$$\begin{pmatrix} R_\mu^3 \\ A_\mu \end{pmatrix} = \begin{pmatrix} \cos(\theta_C) & \sin(\theta_C) \\ -\sin(\theta_C) & \cos(\theta_C) \end{pmatrix} \begin{pmatrix} Z'_\mu \\ B_\mu \end{pmatrix} \tag{2.4.35}$$

where,

$$\begin{aligned} \sin(\theta_C) &= \frac{g_{5X}}{\sqrt{g_5^2 + g_{5X}^2}} \\ \cos(\theta_C) &= \frac{g_5}{\sqrt{g_5^2 + g_{5X}^2}}. \end{aligned} \tag{2.4.36}$$

After this rotation the B_μ and Z'_μ enter the covariant derivative as

$$D_\mu \supset -i\Big(\tilde{g}_5(T_R^3 + X)B_\mu + \tilde{g}_{5Z}(T_R^3 - s_{\theta_C}^2(T_R^3 + X))Z'_\mu\Big), \tag{2.4.37}$$

where $s_{\theta_C} = \sin(\theta_C)$, and the couplings are,

$$\tilde{g}_5 = \frac{g_5 g_{5X}}{\sqrt{g_5^2 + g_{5X}^2}}, \quad \tilde{g}_{5Z} = \sqrt{g_5^2 + g_{5X}^2} \tag{2.4.38}$$

and $\tilde{g}_5$ is to be interpreted as the hypercharge coupling. With this mechanism in place it can been shown that the contributions of the R_μ^a fields to the T parameter cancel the tree-level contributions from L_μ^a. In this case one should take into account the one loop contributions of the KK top and bottom fields; since the KK masses of t_L and b_L will not be equal, sizeable corrections to the T parameter occur in much the same way as the SM quark contribution. One can also consider a scenario where the bulk custodial symmetry is broken. In this case the KK modes of L_μ^a and R_μ^a do no have the same mass thus the exact cancellation of the tree-level corrections does not occur.

Another way to reduce contributions to the T parameter (and some flavour observables) is to reduce the 5D volume, kL. In the work in this chapter we have always kept the fundamental 5D mass scale ($\sim k$) near M_{Pl}, such that the model connects the electroweak scale and the scale at which quantum corrections to gravity are expected to become important. However, as mentioned in the introduction, it is entirely plausible that there may be an intermediate scale laying between the electroweak scale and M_{Pl}, in which case the RS models we consider need not address the hierarchy between m_W and M_{Pl}. In such a scenario we can replace the 5D mass scale by a lower scale, which has an important effect on some observables calculated from the model. These models were first studied in [59] and dubbed 'Little Randall-Sundrum' (LRS) models. These authors show that the T parameter and some flavour observables depend strongly on the 5D mass scale, and that the corrections to the SM values for these observables are decreased when this scale is lowered. Thus with an intermediate scale corrections to the T parameter are naturally smaller, and helps to avoid the stringent bounds set by measurements at LEP. These LRS models will play an important role later in this thesis, hence why we have briefly mentioned them here.

2.5 Yukawa coupling corrections with a bulk Higgs

The aim of this section is to investigate possible bounds on the bulk Higgs scenario from corrections to SM Yukawa couplings. Consider an SU(2) singlet fermion t and doublet $Q = (T, B)$ in the 5D theory. The action for such a system, omitting terms in B, can be

written as [46, 53]

$$S = \int d^4x \int_0^L dy\, \sqrt{|g|} \left(\frac{1}{2} \left(\bar{t}\gamma^M D_M t - D_M \bar{t}\gamma^M t \right) - m_t \bar{t}t \right.$$
$$\left. + \frac{1}{2} \left(\bar{T}\gamma^M D_M T - D_M \bar{T}\gamma^M T \right) - m_T \bar{T}T + \lambda_t^{(5)} \sqrt{L} \phi^0 \bar{T}t + \text{h.c.} \right), \tag{2.5.1}$$

including a Yukawa interaction term with dimensionless coupling $\lambda_t^{(5)}$. The index "t" represents the fermion species considered. The most interesting case will be the one of the top quark. We choose boundary conditions such that t and T have only right and left handed zero modes, respectively. After electroweak symmetry breaking, as well as giving the zero modes mass, the Yukawa interaction induces a mixing between the different modes. The resulting mass matrix for one flavour is of the form

$$\begin{pmatrix} \bar{T}_L^0 & \bar{T}_L^1 & \bar{t}_L^1 & \bar{T}_L^2 & \bar{t}_L^2 & \dots \end{pmatrix} \begin{pmatrix} m_{t,0}^{T,0} & 0 & m_{t,1}^{T,0} & 0 & m_{t,2}^{T,0} & \dots \\ m_{t,0}^{T,1} & M_{T,1} & m_{t,1}^{T,1} & 0 & m_{t,2}^{T,1} & \dots \\ 0 & m_{T,1}^{t,1} & M_{t,1} & m_{T,2}^{t,1} & 0 & \dots \\ m_{t,0}^{T,2} & 0 & m_{t,1}^{T,2} & M_{T,2} & m_{t,2}^{T,2} & \\ 0 & m_{T,1}^{t,2} & 0 & m_{T,2}^{t,2} & M_{t,2} & \dots \\ \vdots & \vdots & \vdots & \vdots & \ddots & \end{pmatrix} \begin{pmatrix} t_R^0 \\ T_R^1 \\ t_R^1 \\ T_R^2 \\ t_R^2 \\ \vdots \end{pmatrix}, \tag{2.5.2}$$

where $M_{T,1}$ and $M_{t,1}$ are the KK masses of the doublet and singlet fields and the mixing terms are of the form

$$m_{\phi,n}^{\psi,m} = \frac{1}{\sqrt{2}} \lambda_{\phi,n}^{\psi,m} v_0 = \frac{\lambda_t^{(5)} v_0}{\sqrt{2}L} \int_0^L dy\, \sqrt{|g|} f_m^{\psi L} f_n^{\phi R} f_0. \tag{2.5.3}$$

In the case of a brane Higgs, the boundary conditions imply that $m_{T,n}^{t,m} = 0$ $(m, n > 0)$ since odd fields are zero at the IR brane.[3] With a bulk Higgs however these terms are non-zero and additional corrections arise upon diagonalization. The mass entries $m_{T,n}^{t,m}$ vary significantly in magnitude depending on whether or not zero modes are involved, i.e. whether $m, n = 0$, and on the localisations of these zero modes. The smallest entry is $m_{T,0}^{t,0}$, which includes potential suppressions from both left and right handed zero modes. A suppression by either a left or right handed zero mode occurs for $m_{T,0}^{t,m}$ and $m_{T,n}^{t,0}$, respectively. All other entries $m_{T,n}^{t,m}$ do not suffer a suppression and therefore are of similar magnitude.

[3] In ref. [49] the presence of such a term was argued for even in the case of a brane Higgs, once the IR brane was smeared out by regularising the delta function defining the brane and then performing an appropriate brane limit.

Neglecting CP violation, the mass matrix (2.5.2) can be partially diagonalized using orthogonal transformations of the left and right handed KK modes,

$$O_L^T M O_R = \begin{pmatrix} 1-\frac{\theta_{L2}^2}{2} & \theta_{L1} & \theta_{L2} \\ -\theta_{L1} & 1 & 0 \\ -\theta_{L2} & 0 & 1-\frac{\theta_{L2}^2}{2} \end{pmatrix} \begin{pmatrix} m_{t,0}^{T,0} & 0 & m_{t,1}^{T,0} \\ m_{t,0}^{T,1} & M_{T,1} & m_{t,1}^{T,1} \\ 0 & m_{T,1}^{t,1} & M_{t,1} \end{pmatrix} \begin{pmatrix} 1-\frac{\theta_{R1}^2}{2} & -\theta_{R1} & -\theta_{R2} \\ \theta_{R1} & 1-\frac{\theta_{R1}^2}{2} & 0 \\ \theta_{R2} & 0 & 1 \end{pmatrix}, \tag{2.5.4}$$

where we assume a small angle approximation and consider contributions from the first KK modes only. This transformation will isolate the "zero mode" from the KK excitations. Below we will find that θ_{L1} and θ_{R2} are higher order in powers of v_0/M_{KK}, which explains the form of the orthogonal matrices used. To find the Yukawa coupling of the physical zero mode fermion, we need to know the mixing angles in the O_L and O_R matrices. Expanding to second order in powers of v_0/M_{KK}, we find

$$\begin{aligned} \theta_{L1} &\simeq -\frac{m_{t,0}^{T,0} m_{t,0}^{T,1}}{M_{T,1}^2} + \frac{m_{t,1}^{T,0} m_{T,1}^{t,1}}{M_{T,1} M_{t,1}} \;\; ; \;\; \theta_{L2} \simeq -\frac{m_{t,1}^{T,0}}{M_{t,1}} \\ \theta_{R2} &\simeq -\frac{m_{t,0}^{T,0} m_{t,1}^{T,0}}{M_{t,1}^2} + \frac{m_{t,0}^{T,1} m_{T,1}^{t,1}}{M_{T,1} M_{t,1}} \;\; ; \;\; \theta_{R1} \simeq -\frac{m_{t,0}^{T,1}}{M_{T,1}}. \end{aligned} \tag{2.5.5}$$

We can see that the second terms in θ_{L1} and θ_{R2} vanish in the brane Higgs limit. For the mass of the lowest lying mode ("zero mode") we then find

$$m_t^{(4)} = m_{t,0}^{T,0} \left(1 - \frac{(m_{t,1}^{T,0})^2}{2M_{t,1}^2} - \frac{(m_{t,0}^{T,1})^2}{2M_{T,1}^2} + \left(\frac{m_{T,1}^{t,1}}{m_{t,0}^{T,0}} \right) \frac{m_{t,1}^{T,0} m_{t,0}^{T,1}}{M_{T,1} M_{t,1}} + \mathcal{O}\left(\frac{m^3}{M_{KK}^3} \right) \right). \tag{2.5.6}$$

A matrix analogous to eq. (2.5.2) encodes the Yukawa interactions of the fermion KK modes with the Higgs. In this matrix, diagonal terms corresponding to $M_{T,n}$ and $M_{t,n}$ are missing. This results in a relative shift between the Yukawa coupling and mass of the "zero mode" compared to the standard model. With the transformation defined in eq. (2.5.4), we find that the "zero mode" Yukawa coupling can be written as

$$\lambda_t^{(4)} = \lambda_{t,0}^{T,0} \left(1 - \frac{3}{2} \frac{(\lambda_{t,0}^{T,1} v_0)^2}{M_{T,1}^2} - \frac{3}{2} \frac{(\lambda_{t,1}^{T,0} v_0)^2}{M_{t,1}^2} + 3 \left(\frac{\lambda_{T,1}^{t,1}}{\lambda_{t,0}^{T,0}} \right) \frac{\lambda_{t,1}^{T,0} \lambda_{t,0}^{T,1} v_0^2}{M_{T,1} M_{t,1}} + \mathcal{O}\left(\frac{\lambda^3 v_0^3}{M_{KK}^3} \right) \right). \tag{2.5.7}$$

We can now quantify the misalignment in the fermion "zero mode" mass and Yukawa coupling as

$$r_t^{(4)} = \frac{\sqrt{2}\, m_t^{(4)}}{\lambda_t^{(4)} v} - 1 = \frac{(\lambda_{t,0}^{T,1} v_0)^2}{M_{T,1}^2} + \frac{(\lambda_{t,1}^{T,0} v_0)^2}{M_{t,1}^2} - 2 \left(\frac{\lambda_{T,1}^{t,1}}{\lambda_{t,0}^{T,0}} \right) \frac{\lambda_{t,1}^{T,0} \lambda_{t,0}^{T,1} v_0^2}{M_{T,1} M_{t,1}} + \frac{\delta w}{2} + \mathcal{O}\left(\frac{\lambda^3 v_0^3}{M_{KK}^3} \right). \tag{2.5.8}$$

Note that because $\lambda_{t,1}^{T,0}$ is negative there is no cancellation in the contributions to $r_t^{(4)}$. The δw term is related to the gauge boson mass correction from section 2.4.3, eqs. (2.4.14), (2.4.22). We use it here because the measured vev, v, includes the mass correction to the W boson. We only include this factor for completeness since from the electroweak precision tests we know that it does only result in a negative per-mille correction.

Before we look at numerical evaluations of $r_t^{(4)}$, a few general statements can be made. Irrespectively of the fermion locations, $r_t^{(4)}$ scales with the 5D Yukawa couplings as $(\lambda_t^{(5)})^2$ and with the KK scale as $1/M_{KK}^2$. The third term in eq. (2.5.8) is never weak in comparison to the first two terms, except for the case of a brane Higgs, where we take this term to be absent. Further statements on $r_t^{(4)}$ depend on the fermion locations. In the left-right symmetric case $c_L = -c_R$, the first and second terms in $r_t^{(4)}$ scale as $m_t^{(4)} v/M_{KK}^2$, while the third term scales as v^2/M_{KK}^2. So for small fermion masses the third term completely dominates. For other fermion locations these simple relations will be modified.

Our numerical evaluations of $r_t^{(4)}$ are summarised in table 2.3. For the case of a bulk Higgs we use a KK scale of $M_{KK} = 5.9$ TeV. As discussed in the previous section, a small contribution from higher dimensional operators is required in this case to reduce electroweak constraints to meet experimental bounds. For a KK scale of 8 TeV, the Yukawa deviations from the table will be reduced by a factor of $(5.9/8)^2 = 0.54$, while for a KK scale of 5 TeV they will increase by a factor of 1.4. We give separate results for the three individual contributions and the total result from eq. (2.5.8), $r_t^{(4)}$, denoted by (a), (b), (c) and Total, respectively. As anticipated, the third term (c) is always very important, and completely dominates for smaller fermion masses. Note that the scaling in 5D Yukawa couplings is somewhat distorted by changes in the fermion locations needed to keep the fermion mass constant. For the top quark these modifications can easily be larger than the anticipated 4% accuracy from HL-LHC [42,43]. Also for the bottom quark the correction in the Yukawa coupling could be larger than the 2.4% or 0.4% accuracies aimed for at ILC and TLEP, respectively [41]. For the tau Yukawa coupling it seems questionable whether a deviation could be seen at ILC (predicted accuracy 2.9%), while a detection at TLEP (predicted accuracy 0.5%) seems promising [41].

The comparison to the case of a brane Higgs is not unique, as one has to decide which parameters should be kept constant in this procedure. In our opinion the most meaningful comparison is done by keeping the crucial off-diagonal elements $m_{t,1}^{T,0}$ and $m_{t,0}^{T,1}$ constant, in addition the to resulting 4D fermion mass. This can always be achieved by choosing a suitable brane Yukawa coupling and values for the fermion location parameters c_L and c_R.

$m_t^{(4)}$ [GeV]	$\lambda_t^{(5)}$	c_L	c_R	M_{T1} [TeV]	M_{t1} [TeV]	(a) [%]	(b) [%]	(c) [%]	Total [%]
173.48	4	0.550	-0.26	6.52	7.12	12.97	0.05	19.72	32.7
173.73	2	0.530	-0.07	6.05	7.64	5.93	0.01	3.35	9.29
173.07	1	0.488	-0.20	5.98	7.12	1.29	0.03	1.31	2.62
4.17	4	0.526	-0.6320	6.04	6.46	$\sim 10^{-3}$	0.02	6.76	6.78
4.17	2	0.510	-0.6190	5.97	6.41	$\sim 10^{-3}$	0.02	2.48	2.50
4.17	1	0.500	-0.6004	5.93	6.33	$\sim 10^{-3}$	0.02	0.98	1.00
1.79	4	0.542	-0.650	6.10	6.53	$\sim 10^{-3}$	$\sim 10^{-3}$	3.86	3.87
1.79	2	0.508	0.650	5.97	6.53	$\sim 10^{-4}$	$\sim 10^{-3}$	1.07	1.08
1.79	1	0.516	-0.621	6.00	6.41	$\sim 10^{-4}$	$\sim 10^{-3}$	0.58	0.58

Table 2.3: Relative shifts in the 4D Yukawa coupling, $r_t^{(4)}$, from eq. (2.5.8). The columns denoted by (a), (b), (c) and Total give the first, second, third contribution and the total result in percent. M_{KK} is taken to be 5.9 TeV.

The resulting value for $r_t^{(4)}$ can be derived from table 2.3 by setting the contribution from column (c) to zero. The contributions from (a) and (b) will receive small changes due to the modified fermion locations. A large effect will be that for a brane Higgs we have to use a larger value of M_{KK} =15 TeV. So the brane Higgs cases related to the parameter sets in table 2.3 will have values for $r_t^{(4)}$ roughly given by the sum of contributions (a) and (b) divided by a factor of four. E.g. the brane Higgs case related to the top quark with bulk Higgs of the first row ($r_t^{(4)} = 32.7\%$) will have $r_t^{(4)} \approx (12.97\% + 0.05\%)/4 \approx 3.3\%$. So only if the 5D Yukawa couplings is somewhat large a detection at HL-LHC seems plausible. For lighter fermions these modifications of the Yukawa couplings will be completely undetectable in the foreseeable future.

We have numerically verified that the expressions (2.5.5) to (2.5.8), which are derived from considering a single KK level, receive only small corrections of $\lesssim 10\%$ when we include more fermion KK modes.

Finally we would like to remark that in variants of the warped geometry, where the KK scale is lowered to a few TeV [25–27, 29–35], the modifications of Yukawa couplings presented in table 2.3 have to be upscaled accordingly. In the case of a KK scalar of

3 TeV, the corrections from in table 2.3 will increase by a factor of 3.9. Then 5D top Yukawa couplings $\lambda_t^{(5)} \gtrsim 1.5$ will then already be disfavoured by present observations of Higgs production via gluon fusion at the LHC.

Yukawa coupling misalignment also has impact on flavour violation mediated by Higgs exchange, as e.g. discussed in [49, 60, 61]. Also Higgs corrections to the muon anomalous magnetic moment were found to depend on the Higgs localisation [62]. Analysing the resulting constraints for the scenario investigated here, however, is beyond the scope of the present work. For generic $\mathcal{O}(1)$ 5D Yukawa couplings Higgs induced flavour violation will be large, certainly pushing the bound on the KK scale beyond the bounds we derived from electroweak precision constraints in section 2.4.3. However, flavour violation can be significantly reduced if fermion localizations are generation independent (at least for the first and second generation). In such a case the dominant bounds on the KK scale are those we derived in section 2.4.3. Here we conclude that unavoidable Yukawa misalignment does not lead to additional bounds on the KK scale.

Chapter 3

Exploring holographic composite Higgs models

In composite Higgs models the Higgs field is composed of some new particles interacting via a strongly interacting gauge theory which confines at the TeV scale. In this scenario the hierarchy between the TeV scale and the Planck scale is solved by the confinement of the strongly coupled gauge theory. Because the Higgs is now a bound state, the effective cut-off for this state is of the order of the confinement scale, i.e. $\sim$ TeV. A "little hierarchy" between the electroweak scale and the TeV scale can then arise naturally if the Higgs bound state is a pseudo-Goldstone boson of this new strongly interacting sector.

Despite difficulties in extracting predictions from strongly coupled gauge theories, several methods have been developed. The most basic of these makes use of large N approximations in $SU(N)$ gauge theories, and of the global symmetry structure in the low energy effective theory [63–70]. These methods, although useful, can be rather limited. It is possible to make progress beyond this using computational tools such as lattice simulations, and while determining baryon states is still challenging, some studies in non-minimal composite Higgs models have been done regarding the structure of the meson states [71–73]. In this paper we adopt another popular method, namely holography, which has been proven useful to describe another strongly coupled theory, QCD at low energies [74–78] as well as a way to develop new, non-QCD like, models of Technicolor [79–82]. In the context of composite Higgses, the pioneer papers of Contino et al. [16, 18], followed an intense exploration of the Higgs as a holographic pseudo-Goldstone boson in warped extra-dimensions, see e.g. [83].

Holography is a method based on the conjectured duality between strongly interacting gauge theories in 4D and weakly coupled gravitational theories on a 5D AdS space like

those studied in the previous chapter. Since the dual theory is weakly coupled, we are able to extract precise predictions for the form factors and all masses and couplings in the model. Here the word *precision* comes from the determination of 4D observables in terms of the 5D model parameters after dimensional reduction, yet the relation with the target strongly coupled 4D theory is still a conjecture and hence bound to an inherent uncertainty.

The physics of 5D AdS spaces [9, 11, 12, 20] was studied independently of its application to composite Higgs models, and many of the results and constraints are the same in both cases. As mentioned in the previous chapter, the most important of these are the constraints imposed by the EWPOs. In the absence of additional symmetries, large corrections to the T parameter imply a lower bound on the spin-1 resonances of ~ 8 TeV [3,30]. In most realistic composite Higgs models the global symmetry structure of the strong sector is enlarged such that tree-level corrections to the T-parameter are avoided. As discussed in section 2.4.5, in the 5D realisations this corresponds to an enlargement of the bulk gauge symmetry.

The space of composite Higgs models is parametrised by the global symmetry structure of the low energy effective theory, and the embedding of the quarks and leptons into this global symmetry. A large literature exists on the simplest composite Higgs models. We will focus on what is known as the Minimal Composite Higgs Model (MCHM) [16,18] with the quarks and leptons embedded in fundamental representations of the global symmetry (MCHM_5) [84,85]. This model has a global $SO(5)$ symmetry broken to $SO(4)$ at the TeV scale, thus employing the custodial protection of the T parameter. A detailed discussion of this model is reserved for section 3.1.3. For further details on the model-building approaches in composite Higgs models see [86–96].

Using the holographic approach it has been shown that it is possible to reproduce the correct top mass, Higgs vev and Higgs mass quite naturally. However it is found that this usually requires light top partners [84, 85]. Typically top partners below about 700 GeV are required, and this is already in tension with bounds on vector-like quarks at the LHC [97, 98] which, for single channel final states, already reach 900 GeV. For specific information on top partner phenomenology we refer the reader to [99–111] and for general LHC phenomenology of the MCHM to [112–123].

There have been some attempts to alleviate the need for the light top partners in holographic models. It has been shown that by embedding the leptons in larger representations, their contributions to the Higgs potential can help alleviate the need for light

top partners [124]. Also using the holographic realisations (although with a flat non-AdS background), authors in [125] use larger representations for the third generation to reduce the fine-tuning in the Higgs potential and allow for heavier top-partners. More recently, models of composite Higgs with more than one breaking scale have been studied in a 4D realisation, and it was found that this also allows for heavier top partners [126].

In general, tension from light top partners is not as much of a problem in the 4D explicit realisations as it is in the holographic models. In [64, 127] it has been demonstrated that one can achieve heavy top partners while having a light Higgs and keeping the fine-tuning at acceptable values. The correspondence between the 4D and 5D models can be described in terms of a dictionary from which one can relate the 4D and 5D parameters. One entry in this relates the number of "colours" in the strongly coupled 4D gauge theory to the UV scale in the 5D AdS theory, more details of this will be discussed in section 3.2.4. In this work we investigate how the top partner spectrum changes as we vary this parameter. The effects of lowering this UV cutoff has been studied previously in 5D AdS scenarios in which the Higgs is not a pseudo-Goldstone boson, these models are referred to as "Little Randall-Sundrum" (LRS) models [59, 128]. It has been shown that these models reduce bounds on some flavour and electroweak observables. In these LRS models we have a UV scale which lies below the Planck scale (10^{18} GeV), and this is what we refer to as the intermediate scale. However this intermediate scale introduces a problem. When implementing it we find that the graviton now couples too strongly to matter such that we no longer correctly reproduce 4D gravity. The natural solution here is to introduce brane kinetic terms (BKTs) for gravity on the UV brane in order to suppress the coupling of the graviton to matter [129].

In models of gauge-Higgs unification, lowering the UV scale allows for smaller corrections to the Higgs couplings while keeping the KK scale constant. In doing this we find in section 3.5.1 that, while keeping the KK scale and the Higgs and top quark masses at the observed values, we can increase the mass of the lightest top resonance. This is easily understood in the KK picture, where lowering the UV scale modifies the couplings of the KK modes. Quantifying the fine-tuning in the Higgs potential using the Barbieri-Guidici parameterisation, we also show that some areas of parameter space with larger top partner masses are actually less fine-tuned than those with smaller top partner masses, which is a direct consequence of lowering this UV scale.

Having constructed an MCHM without light top partners, in section 3.5.2 we investigate deviations in the top Yukawa coupling, motivated by the ongoing experimental effort

at LHC to put bounds on deviations from the SM prediction. In composite Higgs models the top Yukawa is generally suppressed compared to the SM. If this effect is too large, it could lead to a potential conflict with current or future data. We study the top Yukawa coupling in the 5D realisation and find that in some regions of parameter space the deviations to the SM can be suppressed relative to what is expected from pure (4D) symmetry arguments. This will be very relevant once the experimental precision on the top Yukawa increases.

Overall, we find that our 5D holographic realisation of the MCHM_5 with a smaller UV cutoff is not in tension with current experimental data (both on the top partner spectrum and the top Yukawa coupling). In fact, we find that having a lower 5D cut-off allows for a better comparison between the holographic and 4D explicit realisations, and we find good agreement between the results. The mechanisms we study that allow for heavier top partners and suppressed Yukawa deviations are very general, and in particular do not rely on any specific coset or fermion embedding. Therefore, we expect that these results will generalise to non-minimal versions of composite Higgs, and it will be interesting and fruitful to study this in detail in the future.

Before presenting these results we will take a few sections to cover the relevant background material. In the next section we will begin with an overview of some strongly coupled models in particle physics, that is low energy QCD, technicolor, and then composite Higgs. We will also present an overview of the MCHM_5 which we use in this work. Then in section 3.2 we will extend our discussion of particle physics in 5D to cover holographic techniques for scalar fields and gauge fields. We will describe how gauge-Higgs unification works and show how the mass spectrums and holographic profiles for fields can be calculated. We will then give an overview of the relationship between the UV scale of these 5D models and the number of colours in the dual strongly coupled 4D gauge theory. In section 3.3 we then describe the relevant holographic calculations we need to study the fermionic sectors of these models.

3.1 Strongly coupled models

Strongly coupled extensions to the Standard Model provide a natural explanation for many of the phenomena we see in experiments probing the electroweak scale today. In particular they provide a solution to the hierarchy problem via a mechanism which is very similar to the physics we see in low energy QCD. In this section we will introduce strongly coupled models with a very brief overview of a simplified QCD-like model and a discussion of

technicolor. We will then define what we mean by a composite Higgs model and introduce the minimal model that we focus on in the following chapters.

3.1.1 QCD and technicolour

The model of chiral symmetry breaking described here in the QCD case was originally proposed in [130–132], for a review see [133]. Consider a QCD-like model with only two massless Dirac fermions, u and d, with the same quantum numbers as the SM u and d quarks. Ignoring electroweak interactions for now, we can write the action as

$$\mathcal{L} = \bar{q}_L i\not{D} q_L + \bar{q}_R i\not{D} q_R, \quad q_{L,R} = \begin{pmatrix} u_{L,R} \\ d_{L,R} \end{pmatrix}. \tag{3.1.1}$$

This action has a global $U(2)_L \times U(2)_R$ symmetry which can be decomposed into $SU(2)_L \times SU(2)_R$ and two $U(1)$ symmetries associated with Baryon number and isospin transformations. At large energies far above 200 MeV ($= \Lambda_{QCD}$), the QCD coupling is perturbative and the quarks behave almost like free particles. At lower energies however, $p^2 \lesssim \Lambda^2_{QCD}$, the QCD coupling becomes strong and the quarks form into quark-anti-quark bound states such that,

$$\langle 0|\bar{q}q|0\rangle = \langle 0|\bar{q}_L q_R + \bar{q}_R q_L|0\rangle \neq 0. \tag{3.1.2}$$

The above vacuum state is no longer invariant under the full $SU(2)_L \times SU(2)_R$ symmetry, but only under a subgroup of this in which the rotation parameters of the left and right handed transformations are equal, $\alpha_L = \alpha_R$. This subgroup is known as the diagonal, or vectorial, subgroup, $SU(2)_V$. Thus the vacuum state below Λ_{QCD} is in a spontaneously broken phase, where we expect to have three Goldstone bosons in the spectrum. The dynamics of this system at $p^2 \ll \Lambda^2_{QCD}$ are described by the chiral Lagrangian,

$$\begin{aligned} \mathcal{L} =& \frac{f_\pi^2}{4} \mathrm{Tr}\left(\partial_\mu \Sigma^\dagger \partial^\mu \Sigma\right) + \alpha_1 \left[\mathrm{Tr}\left(\partial_\mu \Sigma^\dagger \partial^\mu \Sigma\right)\right]^2 \\ &+ \alpha_2 \mathrm{Tr}\left(\partial_\mu \Sigma^\dagger \partial_\nu \Sigma\right) \mathrm{Tr}\left(\partial^\mu \Sigma^\dagger \partial^\nu \Sigma\right) \end{aligned} \tag{3.1.3}$$

where the Σ field encodes the Goldstone modes from the spontaneous symmetry breaking,

$$\Sigma = e^{i\frac{\vec{\pi}\cdot\vec{\sigma}}{\sqrt{2}f_\pi}}. \tag{3.1.4}$$

In QCD these fields are known as pions, and although this is a simplified example, it still provides a good qualitative description of pions in QCD. If we were to compute the amplitude for pion-pion scattering from this action we would see that it grows with energy $\sim E^2$, indicating a break down of theory at some scale which we will call m_ρ. At this

scale some new interactions must appear to unitarize the scattering amplitude. This new physics comes in the form of additional bound states of the u and d quarks, known as mesons. In fact, in any strongly coupled model we expect to see towers of heavier states which interact with the low energy degrees of freedom. The m_ρ is simply the mass scale of these meson resonances and is expected to be $\sim \Lambda_{QCD}$.

At this point we will look at what happens to the electroweak symmetry (in the absence of a Higgs sector) when we are in the QCD vacuum. The electroweak symmetry, $SU(2)_L \times U(1)_Y$, is actually a subgroup of the $U(2)_L \times U(2)_R$ symmetry where the $SU(2)_L$ fields are obtained by gauging the global $SU(2)_L$ and the hypercharge field is obtained by gauging a linear combination of the global symmetry generators, $Y = T_R^3 + B/2$, where B is the generator associated with the $U(1)$ baryon symmetry. It is obvious that when we break the global symmetry from $SU(2)_L \times SU(2)_R$, we also break the electroweak symmetry. What is nice is that the surviving subgroup is precisely electromagnetism, $Q = T_L^3 + T_R^3 + B/2 = T_L^3 + Y$. The spontaneous symmetry breaking gives masses to the W and Z bosons $\sim f_\pi$, and the three Goldstone bosons (pions) are eaten to form the longitudinal components of the gauge fields.

This model does not suffer from a hierarchy problem, since it only depends on the scale Λ_{QCD}, which is defined by the scale at which the gauge symmetry becomes strongly coupled. It is natural to ask whether or not the Standard Model could be a low energy description of a strongly coupled model, in which the scale Λ_{QCD} is replaced by $\Lambda_{TeV} \sim$ TeV. The first such proposal was that of Technicolor [134], for a review see [135–137].

Technicolor is directly based on a scaled up version of the model described above. The gauge structure of the theory is

$$SU(N_{TC}) \times SU(3) \times SU(2)_L \times U(1)_Y \tag{3.1.5}$$

where the new gauge group becomes strongly coupled at Λ_{TC}. In addition to this there will be new techni-fermions transforming in the fundamental of $SU(N_{TC})$ and charged under the electroweak group.

Going into the details of the different Technicolor models is beyond the scope of this thesis, however there are some tensions between these models and recent experimental data which are worth noting. The first stringent constraints on these models came from S parameter measurements at LEP. Results from large-N field theory [138, 139] calculations indicate that Technicolor models invoke corrections to this electroweak observable which can be estimated by,

$$S \simeq 0.25 N_D \frac{N_{TC}}{3}, \tag{3.1.6}$$

where N_D is the number of techni-doublets, i.e. $SU(2)_L$ doublets of techni-fermions. Assuming optimal T parameter contributions, the upper bound on S is ~ 0.3, $\Rightarrow N_{TC} \leq 3$ if we want to have $N_D \neq 0$. A lot of work has been done on S-parameter bounds in these Technicolor models, see [140–143]. Additional mechanisms need to be introduced to generate fermion masses (extended Technicolor [144, 145], walking Technicolor [146–151], ...) and these generally result in large 4-fermion operators which give rise to flavour changing processes not observed by current experiments. Lastly, an obvious issue is that we do not appear to have a Higgs boson in the model. It has been proposed that the Higgs boson observed at the LHC could in fact be a dilaton state which one would expect due to the spontaneous breaking of a scale symmetry. However, measurements from the LHC disfavour this scenario and indicate that the Higgs couplings are closer to what is expected from the Standard Model.

Thankfully, there are other strongly coupled extensions of the Standard Model, i.e. composite Higgs, which do not suffer such large disagreements with experiment. The crucial difference between Technicolor models and these composite Higgs models is that the bound states which break the global symmetry actually preserve the electroweak symmetry, and the Goldstones of this global breaking give rise to a Higgs doublet. We will learn more about these models in the next chapter.

3.1.2 Composite Higgs

Just as in QCD and Technicolor, we suppose that at high energies (above the TeV scale) there is an additional gauge symmetry with a small coupling which grows strong at $p^2 \sim \Lambda_{TeV}^2$ causing bound states to form. Unlike in Technicolor models here we do not assume anything about the UV theory. Nor do we assume that the global symmetry at high energies is the same as the left-right symmetry we seen in the previous chapter. We only assume that there is some global symmetry $\mathcal{G}$ at high energies that is spontaneously broken by the condensation of a strong force to a subgroup $\mathcal{H}$ at $p^2 \sim \Lambda_{TeV}^2$. We are free to choose $\mathcal{G}$ and $\mathcal{H}$ so long as the SM electroweak group is a subgroup of $\mathcal{H}$ and the number of Goldstones, $\#G - \#H$, is ≥ 4 and give rise to at least one Higgs doublet, i.e. we require four Goldstones transforming as a complex doublet of $SU(2)_L$ with hypercharge $\pm 1/2$. A minimal model is defined as a model in which the only Goldstones are those which form the Higgs doublet, whereas non-minimal models have more Goldstone modes.

Since the SM gauge group ($\mathcal{G}_{SM}$) is a subgroup of $\mathcal{G}$, the SM fields only partially fill representations of $\mathcal{G}$. The embedding of the gauge fields in the global symmetry is

trivial, however with fermions there is more choice, and one can choose among different ways to couple the SM fermions to the bound states. The important feature here is that having massless SM fields that only partially fill representations of $\mathcal{G}$ constitutes an explicit breaking of $\mathcal{G}$, which induces a potential for the Higgs from loops of SM fields. This is of course welcome, since without it the Higgs degrees of freedom would be exact Goldstone bosons and have no potential at any order in perturbation theory.

3.1.3 The minimal composite Higgs model

In this thesis we focus on the custodial minimal composite Higgs model with the fermions in fundamentals of $\mathcal{G}$, this is known as the MCHM$_5$ [16, 84]. For reviews covering the material described in this section see [18, 87]. In relation to the previous section we have,

$$\mathcal{G} = SO(5) \times U(1)_X, \quad \text{and} \quad \mathcal{H} = SO(4) \times U(1)_X \tag{3.1.7}$$

where $SO(4) \sim SU(2)_L \times SU(2)_R$ contains the SM $SU(2)_L$ gauge group as a subgroup. The hypercharge generator is related to those of the $SO(4) \times U(1)_X$ generators via $Y = T^3_R + X$. One can see that we have exactly four Goldstone bosons as a result of this breaking, and once we look at the group algebra we shall see that these do indeed have the correct quantum numbers to play the role of the SM Higgs.

We can express the $SO(5)$ generators as

$$\begin{aligned}
\left(T^a_{L,R}\right)_{i,j} &= -\frac{i}{2}\left(\frac{1}{2}\epsilon^{abc}\left(\delta^b_i\delta^c_j - \delta^b_j\delta^c_i\right) + \left(\delta^a_i\delta^4_j \mp \delta^a_j\delta^4_i\right)\right) \\
\left(T^{\hat{a}}\right)_{i,j} &= -\frac{i}{\sqrt{2}}\left(\delta^{\hat{a}}_i\delta^5_j - \delta^{\hat{a}}_j\delta^5_i\right)
\end{aligned} \tag{3.1.8}$$

where $a = 1, 2, 3$, $\hat{a} = 1, 2, 3, 4$ and $\text{Tr}\left(T^A T^B\right) = \delta^{AB}$. Clearly, $\hat{a}$ represents the generators broken at low energy, and a represents those which remain unbroken. With these one can work out the commutation relations,

$$\begin{aligned}
&[T^a_L, T^b_L] = i\epsilon^{abc}T^c_L, \quad [T^a_R, T^b_R] = i\epsilon^{abc}T^c_R, \quad [T^a_L, T^b_R] = 0 \\
&[T^{\hat{a}}, T^{\hat{b}}] = i\epsilon^{\hat{a}\hat{b}c}\left(T^c_L + T^c_R\right), \quad [T^{\hat{a}}, T^4] = \frac{i}{2}\left(T^{\hat{a}}_L - T^{\hat{a}}_R\right), \\
&[T^a_{L,R}, T^{\hat{b}}] = \frac{i}{2}\left(\epsilon^{ab\hat{c}}T^{\hat{c}} \pm \delta^{a\hat{b}}T^4\right), \quad [T^a_{L,R}, T^4] = \mp\frac{i}{2}T^{\hat{a}}.
\end{aligned} \tag{3.1.9}$$

Just as for the chiral Lagrangian, we will choose to describe the effective action for our Goldstones using a non-linear sigma model, where the Goldstones are parameterised by,

$$\Sigma = \Sigma_0 U = \Sigma_0 \exp\left(-\frac{i}{\sqrt{2}}T^{\hat{a}}h^{\hat{a}}\right) \tag{3.1.10}$$

where $\Sigma_0 = (0,0,0,0,1)$ is the $SO(4)$ preserving vacuum state. This can be derived by assuming we have some vector of $SO(5)$, say Φ, with an $SO(5)$ invariant potential. Now let us suppose Φ has a vev along its fifth component, spontaneously breaking the $SO(5)$ global symmetry to $SO(4)$. Exponentiating the degrees of freedom transforming under the broken generators we can write this field as

$$\Phi = \exp\left(-\frac{i}{\sqrt{2}}T^{\hat{a}}h^{\hat{a}}\right)\begin{pmatrix}\vec{0}\\ v_\Phi + \phi(x)\end{pmatrix} \tag{3.1.11}$$

where $\vec{0}$ is an $SO(4)$ vector filled with zeros. At energies $\ll v_\Phi$ we can integrate out the $\phi(x)$ field leaving only the Goldstone degrees of freedom in the action, which we can write in the form of eq. (3.1.10). We can manipulate eq. (3.1.10) into the form

$$\Sigma = \frac{\sin\left(h/f_\pi\right)}{h}\left(h_1, h_2, h_3, h_4, h\cot\left(h/f_\pi\right)\right) \tag{3.1.12}$$

where $h = \sqrt{h^{\hat{a}}h_{\hat{a}}}$. In the model we will have massive vector resonances transforming in the adjoint of $SO(5)\times U(1)_X$, and massless gauge fields gauging only the $SU(2)_L \times U(1)_Y$ subgroup. To derive the interactions of the Goldstone bosons with the massless gauge fields and the vector resonances we will first gauge the whole $SO(5)\times U(1)_X$ global symmetry. We do this by writing a covariant derivative for Φ under which all generators of the global symmetry are promoted to local gauge symmetries. Since we have integrated out the $\phi(x)$ field the effective action can be written as

$$\mathcal{L} = \frac{f_\pi^2}{2}\left(D_\mu\Sigma\right)^\dagger D^\mu\Sigma - \frac{1}{4}X^{\mu\nu}X_{\mu\nu} - \frac{1}{4}\mathrm{Tr}\left(F^{\mu\nu,A}F^A_{\mu\nu}\right) + \ldots \tag{3.1.13}$$

where $X^{\mu\nu}$ and $F^{\mu\nu}$ are the field strength tensors for the $U(1)_X$ and $SO(5)$ symmetries, respectively, and the covariant derivative is given by

$$D_\mu = \partial_\mu - i\frac{g}{2}T^A A^A_\mu - i\frac{g_X}{2}X_\mu. \tag{3.1.14}$$

The coupling g is that of the SM $SU(2)_L$ gauge group and in order to get the correct SM hypercharges we require

$$g_X^2 = \frac{g'^2 g^2}{g'^2 + g^2} \tag{3.1.15}$$

where g' is the SM hypercharge. The next step is to expand eq. (3.1.13) and go to momentum space. However we introduce form factors, $\Pi(p^2)$, that parameterise the effects of the strongly coupled sector in the low energy regime. These effects come in the form of resonances, or poles, in the form factors as seen in eq. (3.1.18). They are introduced by promoting the kinetic terms in momentum space to general functions of p^2. The action for the vector bosons in momentum space is then written as

$$\mathcal{L} \supset \frac{1}{2}\left(P_T\right)^{\mu\nu}\left(\Pi_0^X\left(p^2\right)X_\mu X_\nu + \Pi_0\left(p^2\right)\mathrm{Tr}\left(A_\mu A_\nu\right) + \Pi_1\left(p^2\right)\Sigma A_\mu A_\nu \Sigma^T\right), \tag{3.1.16}$$

where $(P_T)^{\mu\nu} = \eta^{\mu\nu} - \frac{p^\mu p^\nu}{p^2}$, X_μ are the $U(1)_X$ generators and $A_\mu = A_\mu^A T^A$ (with $A = 1, \ldots, 10 = (a, \hat{a})$), are the $SO(5)$ generators. To look at just the vector fields, we expand around Σ_0 and separate the broken and unbroken generators. It can easily be seen that the only terms surviving in the Goldstone-A_μ interaction are the terms $\Sigma_0 A_\mu^{\hat{a}} T^{\hat{a}} A_\nu^{\hat{b}} T^{\hat{b}} \Sigma_0^\dagger = \frac{1}{2} A_\mu^{\hat{a}} A_\nu^{\hat{a}}$. So, after expanding around Σ_0 we can write the action as

$$\mathcal{L} = \frac{1}{2} (P_T)^{\mu\nu} \left(\Pi_0^X(p^2) X_\mu X_\nu + \Pi_a(p^2) A_\mu^a A_\nu^a + \Pi_{\hat{a}}(p^2) A_\mu^{\hat{a}} A_\nu^{\hat{a}} \right) \tag{3.1.17}$$

where $\Pi_a = \Pi_0$ and $\Pi_{\hat{a}} = \Pi_0 + \frac{1}{2}\Pi_1$. We expect the unbroken generators to have a massless mode in the spectrum, whereas the broken generators should not. In the study of large N gauge theories with strong coupling in the IR leading to the spontaneous breaking of some global symmetry, the form factors can be calculated explicitly. These results imply that the form factors should be of the form

$$\begin{aligned} \Pi_a(p^2) &= \sum_n \frac{p^2 F_{\rho,n}^2}{p^2 - m_{\rho,n}^2} \\ \Pi_{\hat{a}}(p^2) &= \frac{f_\pi^2}{2} + \sum_n \frac{p^2 F_{a,n}^2}{p^2 - m_{a,n}^2} \end{aligned} \tag{3.1.18}$$

where $m_{\rho,n}$ and $m_{a,n}$ are the masses of spin-1 resonances associated with the unbroken and broken generators, respectively. The $F_{\rho,n}$ and $F_{a,n}$ terms are the decay constants for these resonances and f_π is the decay constant for the Goldstone modes. Comparing with the $\Pi_{0,1}$ relations we see that this implies,

$$\Pi_1(0) = f_\pi^2, \quad \Pi_0(0) = \Pi_0^X(0) = 0. \tag{3.1.19}$$

So far we have gauged the whole global symmetry and introduced massive vector resonances transforming under each generator of the global symmetry. To obtain the physical picture in which the only gauged symmetry is that of the SM EW model, we simply remove the massless degrees of freedom for the generators not comprising the $SU(2)_L \times U(1)_Y$ subgroup. This method of deriving the couplings of the Goldstone bosons to the gauge bosons and massive vector resonances is called the method of sources. To maintain the $SO(5) \times U(1)_X$ global symmetry of the strong sector, the masses of each of the vector fields in each multiplet must be the same.

The next step is to derive the couplings of the Higgs boson to the SM gauge fields. To do so we expand the momentum space action for the gauge fields only keeping the fields transforming with the $SU(2)_L \times U(1)_Y$ generators,

$$\mathcal{L} = (P_T)^{\mu\nu} \left(\left(\Pi_0^X + \Pi_0 + \frac{s_h^2}{4}\Pi_1 \right) B_\mu B_\nu + \left(\Pi_0 + \frac{s_h^2}{4}\Pi_1 \right) L_\mu^a L_\nu^a + 2 s_h^2 \Pi_1 \hat{H}^\dagger T_L^a Y \hat{H} L_\mu^a B_\nu \right), \tag{3.1.20}$$

where

$$\hat{H} = \frac{1}{h}H = \frac{1}{h}\begin{pmatrix} h_1 - ih_2 \\ h_3 - ih_4 \end{pmatrix} \tag{3.1.21}$$

and B_μ is the $U(1)_Y$ hypercharge generator. We have not yet looked at the Higgs potential, but let us assume that it does get a vacuum expectation value, denoted by $\hat{H} = (0, 0, 1, 0)$ and $s_{\langle h\rangle} = \sin(\langle h\rangle / f_\pi)$. Expanding around this vacuum expectation value, and expanding the form factors around $p^2 \simeq 0$, we find

$$\begin{aligned}\mathcal{L} = &(P_T)^{\mu\nu}\left(\frac{f_\pi^2 s_{\langle h\rangle}^2}{4}\right)\left(\frac{1}{2}\left(B_\mu B_\nu + L_\mu^3 L_\nu^3 - 2L_\mu^3 B_\nu\right) + L_\mu^+ L_\nu^-\right) + \\ &(P_T)^{\mu\nu}\, p^2\left(\Pi_0'(0) L_\mu^a L_\nu^a + \left(\Pi_0'(0) + \Pi_0^{X\prime}(0)\right) B_\mu B_\nu - \frac{s_{\langle h\rangle}^2}{2}\Pi_0'(0) L_\mu^3 B_\nu\right).\end{aligned} \tag{3.1.22}$$

First, let us normalise the kinetic terms. We recognise that,

$$\Pi_0'(0) = -\frac{1}{g^2}, \quad \Pi_0^{X\prime}(0) = -\frac{1}{g_X^2} = -\frac{g'^2 + g^2}{g'^2 g^2}, \tag{3.1.23}$$

such that $\Pi_0'(0) + \Pi_0^{X\prime}(0) = -1/g'^2$ where g and g' are the $SU(2)_L$ and hypercharge couplings, respectively. So when we absorb these into the fields we see that,

$$m_W^2 = \frac{g^2 f_\pi^2 \sin(\langle h\rangle / f_\pi)^2}{4}, \;\Rightarrow\; \sin(\langle h\rangle / f_\pi)^2 = \frac{v^2}{f_\pi^2}. \tag{3.1.24}$$

To derive the couplings to the Higgs boson we expand around this vev, $\sin(h/f_\pi) \to \sin((\langle h\rangle + h)/f_\pi)$, implying that,

$$f_\pi^2 s_h^2 \simeq v^2 + v\sqrt{1 - s_{\langle h\rangle}^2}\, h + \left(1 - 2s_{\langle h\rangle}^2\right) h^2 + \ldots, \tag{3.1.25}$$

which, by substituting into the action, gives the corrections to the SM couplings for the W and Z bosons,

$$g_{VVh} = g_{VVh}^{SM}\sqrt{1 - s_h^2}, \quad g_{VVhh} = g_{VVhh}^{SM}\left(1 - 2s_h^2\right), \tag{3.1.26}$$

where we simply use s_h to denote v/f_π, and will do so from now on in this thesis.

3.2 Holography for scalars and gauge fields

Now that we have covered what a composite Higgs model is and why it is an interesting avenue to explore as a BSM sector, we will now outline what the holographic method is and how it can be applied to different fields. We will also show how one can use this to build models which have effective theories exactly like those expected from composite Higgs models, where the symmetry breaking structure of the 4D model determines the particle content and boundary conditions of the fields in the 5D model.

3.2.1 A simple scalar example

As an introductory example we will study a real scalar field in a flat extra dimension ($k = 0$). Following the same steps outlined in section 2.1.1, we obtain the following 5D action,

$$S = -\frac{1}{2}\int_0^L dy\Phi\left(\Box - \partial_y^2\right)\Phi + \Phi\left(\partial_y - \frac{m_{UV,IR}^2}{M_5}\right)\Phi\Big|_0^L \tag{3.2.1}$$

where we have assumed that $\Phi \to 0$ as $x^\mu \to \pm\infty$. If we were to use the Kaluza-Klein method we would do a mode expansion and find an eigenvalue equation linking the 5D derivatives on Φ with the 4D Kaluza-Klein masses. Solving this we would find the 5D profiles of the KK modes and then apply boundary conditions to determine the mass spectrum. In the holographic procedure we do not do a mode expansion. Instead we solve the full bulk equation of motion,

$$\left(p^2 - \partial_y^2\right)\Phi = 0 \tag{3.2.2}$$

for which we find the solution,

$$\Phi(x^\mu, y) = A(p)\cos(py) + B(p)\sin(py). \tag{3.2.3}$$

How we apply the boundary conditions is also different than in the Kaluza-Klein case. In that case we had two integration constants and the mass eigenvalue to be fixed by two boundary conditions, leaving one integration constant to be fixed by the normalisation. In the holographic case we have no mass eigenvalue, hence we can only use the integration constants to fix one of the boundary conditions and the normalisation. It is convention here to fix the IR boundary condition and define a 'holographic' field on the UV brane, however the results will be independent of this choice. So we have,

$$\Phi(x^\mu, 0) = \hat{\Phi}(x^\mu), \quad \left(\partial_y - \frac{m_{IR}^2}{M_5}\right)\Phi(x^\mu, L) = 0 \tag{3.2.4}$$

where $m_{IR} \to \infty$ and $m_{IR} \to 0$ correspond to Dirichlet and Neumann boundary conditions respectively. The solution for the bulk holographic wave-function is

$$\Phi(x^\mu, y) = \frac{f_\Phi(p, y)}{f_\Phi(p, 0)}\hat{\Phi}(x^\mu) \tag{3.2.5}$$

where,

$$f_\Phi(p, y) = A(p)\cos(pL)\Big[\left(\frac{m_{IR}}{p} + \tan(pL)\right)\sin(py) + \left(1 - \tan(pL)\frac{m_{IR}}{p}\right)\cos(py)\Big]. \tag{3.2.6}$$

In the Neumann and Dirichlet limits, respectively, we have,

$$f_\Phi^N(y,p) = A(p)\Big[\tan(pL)\sin(py) + \cos(py)\Big]$$
$$f_\Phi^D(y,p) = A(p)\Big[\cot(pL)\sin(py) + \cos(py)\Big]. \tag{3.2.7}$$

Plugging these wave functions into the action the IR and bulk terms vanish, leaving us with the projection of these fields onto the UV brane,

$$S = -\frac{1}{2}\hat{\Phi}\,\Pi^{N,D}(p)\hat{\Phi} \tag{3.2.8}$$

where,

$$\Pi^N = \left(\partial_y - \frac{m_{UV}^2}{M_5}\right)\frac{f_\Phi^N(y,p)}{f_\Phi^N(0,p)}\Big|_{y=0} = \left(p\tan(pL) - \frac{m_{UV}^2}{M_5}\right)$$
$$\Pi^D = \left(\partial_y - \frac{m_{UV}^2}{M_5}\right)\frac{f_\Phi^D(y,p)}{f_\Phi^D(0,p)}\Big|_{y=0} = \left(p\cot(pL) - \frac{m_{UV}^2}{M_5}\right). \tag{3.2.9}$$

These form factors encode information on a whole tower of states, where the masses of these states correspond to the zeros of the form factors. Also, the propagators for the fields can easily be obtained by inverting the form factors.

One can easily see from eq. (3.2.9) that the UV boundary conditions are dynamically imposed by the 4D equations of motion on the UV brane. In the $m_{UV} = 0$ case, the zeros of $p\tan(pL)$ and $p\cot(pL)$ correspond to the mass spectrum obtained by the KK method with Neumann UV boundary conditions, it is also obvious that there is a zero at $p \to 0$ for the Neumann case.

When $m_{UV} \neq 0$ one can see that neither of the form factors contain a massless mode, and the masses of the KK modes shift. In the Dirichlet limit where $m_{UV} \to \infty$, these KK masses shift to the poles, rather than the zeros, of $\Pi^{N,D}$. Thus the mass spectrum for Neumann and Dirichlet UV boundary conditions, respectively, are given by,

$$m_\Phi = \text{zeros}\left(\Pi^{N,D}(p)\right)$$
$$m_\Phi = \text{poles}\left(\Pi^{N,D}(p)\right). \tag{3.2.10}$$

We have seen now that this holographic method results in the quadratic parts of the action being described entirely by the field values at the UV brane. This, however, is not the case for interaction terms. Taking as an example a quartic scalar interaction in the bulk, we find

$$S \supset \int_0^L dy \frac{\lambda_{5D}}{4}\Phi^4(x^\mu, y) = \frac{\lambda_{eff}}{4}\hat{\Phi}^4(x^\mu) \tag{3.2.11}$$

where,

$$\lambda_{eff} = \int_0^L dy \left(\frac{f_\Phi^N(y,p)}{f_\Phi^N(0,p)}\right)^4. \tag{3.2.12}$$

This simple example demonstrates some nice features of the holographic method, that it allows us to describe the effects of a whole tower of states with just one form factor, and that the mass spectrum and interactions of these states can be extracted quite easily from the model. There are other advantages of this approach which will become apparent when we study 5D gauge theories and symmetry breaking.

3.2.2 Gauge fields and symmetry breaking

In this section we will move on from the simple case presented before, and look at the holographic set-up for a gauge field in a warped extra dimension. From now on we will use the conformal frame for a warped extra dimension, that is

$$ds^2 = \left(\frac{R}{r}\right)^2 \eta_{MN} dx^M dx^N \tag{3.2.13}$$

where $M, N = 0..4$ and $dx^4 = dr$. The UV and IR branes are located at $r = R = 1/k$ and $r = R'$, respectively. The previous work on gauge and fermion fields still applies, however the formulae will be written slightly differently. The 5D action for an non-abelian gauge field can be written as

$$\begin{aligned} S &= \frac{1}{2g_5^2}\int d^5x \left(\frac{R}{r}\right)\left(-\frac{1}{2}F^{\mu\nu A}F^A_{\mu\nu} - F^{\mu 5A}F^A_{\mu 5}\right) \\ &= \frac{1}{2g_5^2}\int d^5x \left(\frac{R}{r}\right)\left(A^A_\mu \mathcal{P}^{\mu\nu}A^A_\nu + \frac{r}{R}A^A_\mu \partial_y\left(\frac{R}{r}\partial_y A^{\mu A}\right)\right) - \int d^4x \left(\frac{R}{r}A^A_\mu \partial_y A^{\mu A}\Big|^{R'}_R\right) \end{aligned} \tag{3.2.14}$$

where we have taken out a factor of $1/g_5^2$, 'A' superscripts label the generator, $\mathcal{P}^{\mu\nu} = \eta^{\mu\nu}\Box - \partial^\mu\partial^\nu$, and we have only kept the terms quadratic terms in A_μ. We have dropped the A_5 terms for now, however these are crucial to our work and will be discussed in the next subsection. As in the previous section we will choose the boundary conditions in the IR such that the boundary term vanishes, and in the UV we will define a source field,

$$A^A_\mu(x^\mu, R) = \hat{A}^A_\mu(x^\mu) \quad \text{and} \quad A^{\hat{a}}_\mu(x^\mu, R') = 0, \qquad \partial_y A^a_\mu(x^\mu, R') = 0. \tag{3.2.15}$$

where A=$\hat{a}, a$. The Dirichlet boundary condition in the IR breaks the gauge symmetry explicitly on the brane, whereas the Neumann boundary condition preserves the gauge symmetry. Here we have stuck to the convention that $\hat{a}$ labels broken generators and a labels unbroken generators. One should recall from section 2.1.2 that the IR boundary conditions on the A_5 modes will be opposite to the A_μ modes. To find the bulk equations of motion we again want to go to a mixed position-momentum basis, and it is useful to write the gauge fields in terms of their longitudinal and transverse components,

$$A^{\mu A} = \left(\eta^{\mu\nu} - \frac{p^\mu p^\nu}{p^2}\right)A^{tA}_\nu + \frac{p^\mu p^\nu}{p^2}A^{lA}_\nu. \tag{3.2.16}$$

The boundary conditions on the longitudinal and transverse components of each generator must be the same. Writing the action in terms of these components results in,

$$\begin{aligned} S =& \frac{1}{2g_5^2}\int d^5x \left(\frac{R}{r}A_\mu^{tA}\mathcal{P}^{\mu\nu}A_\nu^{tA} + A_\mu^{tA}\partial_y\left(\frac{R}{r}\partial_y A^{\mu tA}\right) + A_\mu^{lA}\partial_y\left(\frac{R}{r}\partial_y A^{\mu lA}\right)\right) \\ & - \frac{1}{2g_5^2}\int d^5x \left(A_\mu^{tA}\partial_y A^{\mu tA} + A_\mu^{lA}\partial_y A^{\mu lA}\right)\Big|_R. \end{aligned} \tag{3.2.17}$$

Going to unitary gauge via some gauge fixing terms, as demonstrated in section 2.1.2, we find the equations of motion for the fields to be,

$$\begin{aligned} \left(p^2 + \frac{r}{R}\partial_y\left(\frac{r}{R}\partial_y\right)\right)A_\mu^{tA} &= 0 \\ \partial_y\left(\frac{R}{r}\partial_y\right)A_\mu^{lA} &= 0. \end{aligned} \tag{3.2.18}$$

We write the solutions as a product of a 5D component and the holographic field,

$$\begin{aligned} A_\mu^{tA} &= G_\pm^{tA}(p,r)\hat{A}_\mu^{tA} \\ A_\mu^{lA} &= G_\pm^{lA}(p,r)\hat{A}_\mu^{lA} \end{aligned} \tag{3.2.19}$$

where the $\pm$ indicate the choice of IR boundary condition. The 5D components, which are normalised to satisfy the UV boundary condition, can be expressed as

$$\begin{aligned} G_+^{tA}(p,r) =& \frac{r}{R}\frac{Y_1(pR')J_1(pr) - J_1(pR')Y_1(pr)}{Y_1(pR')J_1(pR) - J_1(pR')Y_1(pR)} \\ G_-^{tA}(p,r) =& \frac{r}{R}\frac{Y_0(pR')J_1(pr) - J_0(pR')Y_1(pr)}{Y_0(pR')J_1(pR) - J_0(pR')Y_1(pR)} \\ G_+^{lA}(p,r) =& 1 \\ G_-^{lA}(p,r) =& \frac{\left(\left(\frac{r}{R'}\right)^2 - 1\right)}{\left(\left(\frac{R}{R'}\right)^2 - 1\right)} \simeq \left(1 - \left(\frac{r}{R'}\right)^2\right). \end{aligned} \tag{3.2.20}$$

By plugging these solutions back into the action we arrive at the holographic action for the gauge fields, where only the terms on the UV brane survive,

$$\begin{aligned} S_{hol} &= -\frac{1}{2g_5^2}\int d^5x \left(A_\mu^{tA}\partial_y A^{\mu tA}\right)\Big|_R \\ &= -\frac{1}{2g_5^2}\int d^4x \left(A_\mu^{ta}\Pi_+(p^2)A^{\mu ta} + A_\mu^{t\hat{a}}\Pi_-(p^2)A^{\mu t\hat{a}}\right) \end{aligned} \tag{3.2.21}$$

and,

$$\begin{aligned} \Pi_+ &= G_+^{tA}\partial_y G_+^{tA}\Big|_R \\ \Pi_- &= G_-^{tA}\partial_y G_-^{tA}\Big|_R. \end{aligned} \tag{3.2.22}$$

If we want a Dirichlet boundary condition on the UV brane we do the same thing that we did in the scalar case, that is, introduce a large mass for the appropriate generators thus

effectively making them non-dynamical at the brane. In the limit where the Goldstone modes do not get a vacuum expectation value, the masses of the KK resonances associated with the unbroken and broken generators are associated with the zeros and poles, respectively, of the above form factors. Upon inspection one can see that the unbroken generators will have a massless mode whereas the broken generators will not. However, as discussed in section 2.2.2, broken generators give rise to massless A_5 zero modes.

Goldstone A_5 modes

We know from section 2.1.2 that the $\hat{a}$ generators will have massless A_5 modes in the spectrum, whereas the a generators will not. And we have discussed how massive A_5 modes can be gauged away, or are 'eaten' by the massive A_μ modes. In this way they gain the extra degree of freedom they require to have mass. Massless A_5 modes are different, they are not eaten by any of the A_μ modes and thus remain in the spectrum. In using the holographic procedure we do not use the concept of KK modes, so we must re-express this idea in another way. In describing this gauge fixing procedure we follow the work of [45].

Again, the boundary conditions for the unbroken and broken generators are,

$$\begin{aligned} A^a_\mu(x^\mu, R) &= \hat{A}^a_\mu(x^\mu) \quad \text{and} \quad \partial_y A^a_\mu(x^\mu, R') = 0 \\ A^{\hat{a}}_\mu(x^\mu, R) &= \hat{A}^{\hat{a}}_\mu(x^\mu) \quad \text{and} \quad A^{\hat{a}}_\mu(x^\mu, R') = 0. \end{aligned} \tag{3.2.23}$$

One might suppose that the following field redefinition, along with an appropriate gauge transformation, might fix the A_5 modes to zero,

$$A_M(x^\mu, r) \to \Omega \left(\tilde{A}_M - i\partial_M \right) \Omega^\dagger, \quad \Omega_A = e^{i \int_R^{R'} dr' A_5^A T^A} \tag{3.2.24}$$

where T^A are the generators of the non-abelian group. If we were to perform this field transformation and then use the gauge freedom to absorb the A_5 fields into the A_μ fields such that they 'eat' the A_5 modes, we would have fixed to unitary gauge. The problem however, is that the full symmetry is not gauged on the IR brane, the $\hat{a}$ generators are broken. Therefore we can not use the gauge freedom to absorb all the A_5 modes into the A_μ modes on the IR brane. The solution proposed in [45] involves adding Goldstone degrees of freedom on the IR brane, to restore the full non-abelian symmetry, thus allowing us to fully gauge away all the A_5 modes. These Goldstone degrees of freedom should arise from the spontaneous breaking of the gauge symmetry on the IR brane. The inclusion of

these fields modifies the IR boundary conditions to,

$$\begin{aligned} UF^a_{\mu 5}U^\dagger\Big|_{R'} &= 0 \\ U\left(A^{\hat{a}}_\mu - i\partial_\mu\right)U^\dagger\Big|_{R'} &= 0, \end{aligned} \tag{3.2.25}$$

where

$$U = e^{\frac{i\pi^{\hat{a}}(x^\mu)}{f_\pi}T^{\hat{a}}}. \tag{3.2.26}$$

With these boundary conditions one can now go to unitary gauge consistently, setting $A_5 = 0$ everywhere in the action. Note that we have not added any additional degrees of freedom here. The massive A_5 degrees of freedom become the longitudinal components of the massive A_μ modes, and the massless A_5 degrees of freedom have been traded for the Goldstone degrees of freedom on the IR brane. By making another transformation, $C^A_\mu = U\left(A^A_\mu - i\partial_\mu\right)U^\dagger$, the IR boundary conditions revert back to Neumann or Dirichlet, and the interactions with the Goldstone fields shift to the UV boundary,

$$A^A_\mu(x^\mu, R) = \hat{A}^A_\mu(x^\mu) = U^\dagger\left(C^A_\mu - i\partial_\mu\right)U. \tag{3.2.27}$$

Thus we can see that this manipulation has projected the interactions between the Goldstones and the gauge fields (up to quadratic order) to the UV brane.

If one was to follow the KK method, and keep the A_5 zero mode in the bulk, the results would be the same. This method has been used by several authors [152]. One way to see the connection between the Σ and the A_5 modes is to perform the field redefinition in eq. (3.2.24) without the additional Goldstone fields on the IR brane. In the bulk and on the UV brane one is able to absorb this redefinition via a gauge transformation, i.e.,

$$A^A_\mu \equiv \Omega_A\left(A^A_\mu - i\partial_\mu\right)\Omega^\dagger_A. \tag{3.2.28}$$

But on the IR brane one can only absorb the unbroken generators, i.e.

$$A^a_\mu \equiv \Omega_a\left(A_\mu - i\partial_\mu\right)\Omega^\dagger_a, \tag{3.2.29}$$

leaving the IR boundary conditions as

$$\begin{aligned} \Omega_{\hat{a}}F^a_{\mu 5}\Omega^\dagger_{\hat{a}}\Big|_{R'} &= 0 \\ \Omega_{\hat{a}}\left(A^{\hat{a}}_\mu - i\partial_\mu\right)\Omega^\dagger_{\hat{a}}\Big|_{R'} &= 0. \end{aligned} \tag{3.2.30}$$

From this one can explicitly see the connection between the Goldstone and A_5 degrees of freedom, i.e. $U = \Omega_{\hat{a}}$. From this point forward we will use the U field to represent the A_5 Goldstone degrees of freedom. This U matrix is the same as we used in the

4D description of the global symmetry breaking in the composite Higgs model, however there we had expanded around a vev, i.e. we used the Goldstone matrix $\Sigma = \Sigma_0 U$, where $\Sigma_0 = (0, 0, 0, 0, 1)$ was the vev. In our case this vev simply corresponds to the IR boundary conditions, where the 1 indicates the direction along which the IR boundary conditions break the bulk gauge symmetry.

3.2.3 The holographic MCHM

Using the material of this section and the previous section, we will show now how to construct the MCHM in the holographic set-up. First of all, we require a bulk $SO(5) \times U(1)_X$ gauge symmetry, which is broken in the IR to $SO(4) \times U(1)_X$. Then on the UV there should be mass terms breaking $SU(2)_R \times U(1)_X$ to $U(1)_Y$ such that $Y = T_R^3 + X$. The first step is to assign Dirichlet boundary conditions on the IR brane to the generators in the $SO(5)/SO(4)$ coset. This is equivalent to the step in section 3.1.3 where we expand around the vacuum Σ_0. In the 5D model we will get 4 massless A_5 modes which must be gauged away using the procedure discussed in the previous section. These correspond to the Goldstone-Higgs degrees of freedom in the composite Higgs model.

The next thing we need to do is to match the 5D model to the 4D model. The simplest way to do this is to match the models in the limit that the Higgs fluctuations go to zero. In the 4D model this corresponds to $\Sigma = \Sigma_0$, eq. (3.1.17). In the 5D model it corresponds to the holographic action for the gauge fields with $U = \mathbb{1}$,

$$S = -\frac{1}{2}\int d^4x \left(P_T^{\mu\nu}\right)\left(\frac{1}{g_{5,X}^2} X_\mu \Pi_+(p^2) X_\nu + \frac{1}{g_5^2} A_\mu^a \Pi_+(p^2) A_\nu^a + \frac{1}{g_5^2} A_\mu^{\hat{a}} \Pi_-(p^2) A_\nu^{\hat{a}}\right). \tag{3.2.31}$$

Matching to eq. (3.1.17) (after taking out a factor of the gauge coupling), we find

$$\Pi_X = \Pi_+, \quad \Pi_a = \Pi_+, \quad \Pi_{\hat{a}} = \Pi_- \tag{3.2.32}$$

leading to,

$$\Pi_0 = \Pi_+, \quad \Pi_1 = 2\left(\Pi_- - \Pi_+\right). \tag{3.2.33}$$

When we apply the gauge fixing procedure outlined in section 3.2.2 the Higgs couplings arise via the UV boundary conditions and we obtain the same action as in section 3.1.3, thus we can simply take the work from that section and use the holographic form factors we have obtained here. Doing so gives us an explicit way to calculate observables in 4D in terms of 5D inputs. For example, we can write the 4D $SU(2)_L$ gauge coupling in terms of the 5D gauge coupling using,

$$\frac{\Pi_+'(p^2 = 0)}{g_5^2} = \frac{1}{g^2}, \quad \Rightarrow g_5^2 = g^2 R \ln(\Omega) \tag{3.2.34}$$

where $\Omega = R'/R$. We can also calculate the decay constant of the Goldstones using,

$$\Pi_{\hat{a}}(p^2 = 0) = \Pi_{-}(p^2 = 0) = \frac{f_\pi^2}{2}, \quad \Rightarrow f_\pi^2 = \frac{4M_{KK}^2}{g^2 \ln(\Omega)} \tag{3.2.35}$$

where $M_{KK} = 1/R'$. We refer to $\ln(\Omega)$ as the 5D volume, and it will play an important role in the calculations we do later. The crucial feature of our observations is that one can control the size of f_π by altering the 5D volume without the need to increase M_{KK}. Thus we can increase the decay constant without pushing up the masses of the KK modes.

When looking at contributions to the Higgs potential the hypercharge contributions will be small compared to the $SU(2)_L$ contributions, thus we will ignore it. The relevant effective action is then,

$$\mathcal{L} = (P_T)^{\mu\nu} \frac{1}{g_5^2} \left(\Pi_0 + \frac{s_h^2}{4} \Pi_1 \right) L_\mu^a L_\nu^a, \tag{3.2.36}$$

where the form factors are given in eq. (3.2.33) and eq. (3.2.22).

3.2.4 Intermediate scales and their holographic interpretation

At several points so far in this work we have mentioned the phrase 'intermediate scale' and given a short description of what we meant by that. In this section we will go into more detail on what we mean by an intermediate scale, and discuss how to overcome a particular theoretical issue encountered when they are present. In this section it is more intuitive to use notation familiar with that of the previous chapter than the current chapter, i.e. we work in the y basis, however the results can be translated easily.

In the warped extra dimensional models the UV scale is denoted by M_5, where the curvature constant k, having mass dimension 1, is assumed to be of this order. The length of the extra dimension having mass dimension -1 is assumed to be of the order $1/M_5$. The IR scale in the model is defined by the red-shifted mass scale at the IR brane[1],

$$M_{KK} = ke^{-kL}. \tag{3.2.37}$$

Let's suppose that the UV and IR scales are fixed and that we vary the length of the extra dimension ($L = k^{-1} \ln(k/M_{KK})$) to accommodate them. Regardless of what these scales are we expect that new physics related to a quantum theory of gravity will become apparent at $\sim 10^{18}$ GeV. Thus if we lower the UV scale in this model we refer to it as an intermediate scale. A key question is, what role does this UV scale play?

[1]Note that in the previous chapter we used a slightly different definition of M_{KK}, which was equal to the mass of the first KK vector boson.

An important role it plays is in defining the interaction strength of the massless graviton, which must come out to be that observed in our universe. Let us take the 5D gravity action [2]

$$S = \int d^4x \int_0^L dy \sqrt{|g|} M_5^3 \left(-\frac{\mathcal{R}_5}{2} + 6k^2 \right) + \sqrt{|g|} M_5^3 k_{0,L} \Big|_0^L \tag{3.2.38}$$

where $\mathcal{R}_5$ is the 5D Ricci scalar and the bulk and brane terms proportional to k and $k_{0,L}$ are the bulk cosmological constant and brane tensions responsible for the AdS warping in the bulk. These terms are chosen such that they give the metric of eq. (2.1.1) with $A(y) = ky$. Studying fluctuations around the metric in the above action gives equations of motion for the spin-2 degrees of freedom. These equations of motion permit a massless mode solution, and the interaction strength of this massless mode in the effective theory can be found by integrating over the extra dimension. This interaction strength is defined by an effective Planck mass, found to be

$$M_{Pl}^2 = \frac{M_5^3}{k} \left(1 - e^{-2kL} \right). \tag{3.2.39}$$

Now assuming that $M_5 \sim k$ and $kL \gg 1$, we have that $M_{Pl} \sim k$. We require that $M_{Pl} \sim 10^{18}$ GeV to correctly reproduce 4D gravity, thus lowering M_5 and k leads to a problem.

Another role played by the UV scale is in the relation between 4D and 5D gauge couplings. Take a 5D abelian gauge field in the Randall-Sundrum geometry,

$$S = -\frac{1}{4} \int d^4x \int_0^L dy \sqrt{|g|} \left(\frac{1}{g_5^2} + \tau_0 L \delta(y) + \tau_L \delta(y - L) L \right) F^{MN} F_{MN} \tag{3.2.40}$$

where the $\tau_{0,L}$ are brane localised kinetic terms (BKTs) for the gauge bosons. Performing a simple analysis along the lines of section 2.2.2 we can easily show that the spectrum of A_μ KK modes derived from this action in the presence of Neumann boundary conditions for the A_μ modes permit a massless mode with a flat wave function along the extra dimension. Integrating over the extra dimension we can express the effective 4D gauge coupling as

$$\frac{1}{g_4^2} = \tau_0 + \tau_L + \frac{L}{g_5^2} = \tau_0 + \tau_L + \frac{\ln(\Omega)}{k g_5^2} \tag{3.2.41}$$

where $\Omega = k/M_{KK}$ is the ratio of energy scales. The AdS/CFT correspondence [153] postulates that these weakly coupled 5D AdS models are dual to strongly coupled 4D CFTs, and the expression in eq. (3.2.41) bears a striking resemblance to a gauge coupling in 4D that has been run from some UV scale (k) to an IR scale (M_{KK}) with a renormalisation group equation

$$\mu \frac{d}{d\mu} \frac{1}{g_4^2(\mu)} = -b, \qquad b = \frac{1}{k g_5^2}. \tag{3.2.42}$$

[2] This is covered in slightly more detail in chapter 4 so we will not repeat all the details here.

This line of argument is followed in more detail in [154, 155], and for more general comments on holography and these 5D models we refer the reader to [156]. The logarithmic dependence on the scales in eq. (3.2.42) is a very interesting feature of the AdS models in particular, for example we do not see this behaviour in flat extra dimensions. In this analogy the BKT at the UV brane (τ_0) would be the bare coupling and the BKT at the IR brane (τ_{IR}) would be a threshold correction. On the CFT side with a large number of colours, denoted by N, this beta function coefficient is calculated to be $N/16\pi^2$. This simply arises as a colour factor in loop diagrams involving the CFT 'quarks'. Therefore equating both sides of the duality we find

$$N = \frac{16\pi^2}{kg_5^2} = (1 - \tau_0^2 g_4^2 - \tau_L g_4^2)\frac{16\pi^2}{g_4^2 \ln(\Omega)}. \tag{3.2.43}$$

Therefore when we introduce an intermediate scale in the 5D models, i.e. lower the UV scale, we are effectively varying the number of colours in the dual 4D CFT. In this sense it seems natural to treat kL as a free parameter in these models, rather than fixing it to ensure that $k \sim M_{Pl}$ and $M_{KK} \sim$ TeV.

To solve the problem of reproducing the correct effective Planck mass for the graviton zero mode we introduce a BKT for gravity on the UV brane, which is simply a UV localised contribution to the Ricci scalar [129]. Adding a $-r_0 M_5^3 \mathcal{R}_5 \delta(y)/k$ term to eq. (3.2.38) we find that the effective Planck mass is modified to

$$M_{Pl}^2 = \frac{M_5^3}{k}\left(r_0 + 1 - e^{-2kL}\right). \tag{3.2.44}$$

If we suppose that the dimensionless quantity r_0 can be extremely large in order to give the correct effective Planck mass, i.e. $r_0 \sim ((10^{18}\text{ GeV})/M_5)^3$, then we are able to have an intermediate scale while also reproducing the correct interaction strength for the zero mode graviton.

3.3 Holographic fermions and partial compositeness

In order to have a coupling between the fermions and the Goldstone of the broken global symmetry, we need to have fermion interactions which break the global symmetry. A popular way to do this is known as partial compositeness [157], and not only does it generate the Yukawa couplings, but it can also provide a natural framework in which the Yukawa couplings are hierarchical. The couplings that break the global symmetry are of the form,

$$\mathcal{L} = Y_{5D}\left(\bar{q}\mathcal{O} + h.c.\right) \tag{3.3.1}$$

where q is a light SM fermion and $\mathcal{O}$ is an operator of the strong sector, i.e. it transforms in a full rep of the global symmetry. Since the SM fields will not transform in full reps of the global symmetry, this coupling is not invariant under the full global symmetry and thus generates the Yukawa couplings between the fermions and the Goldstones. Results calculated in the large-N limit of $SU(N)$ gauge theories show that quark masses are exponentially sensitive to the anomalous dimension of the quark, thus one can naturally get large suppressions or enhancements in the masses. An in depth discussion of this is beyond the scope of this thesis, as we will focus on the holographic calculations of the effective action.

The operator $\mathcal{O}$ in eq. (3.3.2) can be thought of as a tower of fermionic states, such that the above coupling can be written as a mass mixing term,

$$\mathcal{L} = \sum_n \delta m_n \left(\bar{q}\Psi_n + h.c.\right) \tag{3.3.2}$$

where Ψ_n are heavy fermionic states. This picture of partial compositeness can easily be understood from the work we have done in previous sections. That is, the holographic dual of partial compositeness is simply a mass mixing between a KK tower with a zero mode, and a KK tower without a zero mode. The 5D fields will transform in complete reps of the global symmetry, and since this global symmetry is exact in the bulk, the mass mixings which violate this must only be present on the IR brane. These interactions not only induce a mass mixing, but they can project out some of the zero modes in the 5D multiplet, meaning that at the massless level the zero modes may not transform in compete reps of the global symmetry.

3.3.1 Holography for fermions

Let us take two Dirac fermions in the 5D Randall-Sundrum model with a mass mixing on the IR brane,

$$\begin{aligned} S = \int d^5x\sqrt{|g|}\sum_{a=1,2}\left(\frac{i}{2}\bar{\psi}_a\gamma^M\partial_M\psi_a - \frac{i}{2}\left(\partial_M\bar{\psi}_a\right)\gamma^M\psi_a - m_a\bar{\psi}_a\psi_a\right) \\ - \int d^4x\sqrt{|g|}\tilde{m}\left(\bar{\psi}_{1L}\psi_{2R} + \bar{\psi}_{2R}\psi_{1L} + h.c.\right)\Big|_{R'}. \end{aligned} \tag{3.3.3}$$

As we discussed in section 2.1.3, since the bulk equations for the fermions are first order, and we require two boundary conditions for each chirality, once we fix the boundary conditions for one chirality, the others are automatically determined. However, in the holographic procedure we define our degrees of freedom via the boundary conditions on the UV brane, so this is a little more complicated in the fermion case than for bosons. We

need to choose which chirality we want as the holographic source field on the UV brane, and then fix it such that the variation of this field on the brane is zero and the other chirality is allowed to vary freely. For our case here we will choose a left-handed source for ψ_1 and a right handed source for ψ_2,

$$\begin{aligned}\psi_{1L}(p,R) &= \tilde{\psi}_{1L}(p)\\ \psi_{2R}(p,R) &= \tilde{\psi}_{2R}(p)\end{aligned} \tag{3.3.4}$$

such that, $\delta\psi_{1L} = \delta\psi_{2R} = 0$ and $\delta\psi_{1R} = \delta\psi_{2L} \neq 0$. When we vary the action to find the equations of motion in the bulk we find the following terms arising on the branes,

$$\begin{aligned}\delta S_{branes} = \frac{1}{2}\int d^4x\sqrt{|g|}\sum_{a=1,2}\left(\bar{\psi}_{aL}\delta\psi_{aR} - \bar{\psi}_{aR}\delta\psi_{aL} + h.c.\right)\Big|_R^{R'}\\ - \int d^4x\sqrt{|g|}\tilde{m}\left(\bar{\psi}_{1L}\delta\psi_{2R} + \delta\bar{\psi}_{1L}\psi_{2R} + h.c.\right)\Big|_{R'}.\end{aligned} \tag{3.3.5}$$

Due to the holographic UV boundary condition and the mixing terms on the IR brane, these do not vanish automatically. Note that if we had no IR mixing terms, we would simply have Neumann and Dirichlet boundary conditions in the IR and the IR terms would indeed vanish. To make this variation vanish we need to add the following terms to the UV and IR branes,

$$\begin{aligned}S_{UV} &= \frac{1}{2}\int d^4x\sqrt{|g|}\left(\bar{\psi}_{1L}\psi_{1R} - \bar{\psi}_{2L}\psi_{2R} + h.c.\right)\Big|_R\\ S_{IR} &= \mp\frac{1}{2}\int d^4x\sqrt{|g|}\left(\bar{\psi}_{1L}\psi_{1R} - \bar{\psi}_{2L}\psi_{2R} + h.c.\right)\Big|_{R'}.\end{aligned} \tag{3.3.6}$$

Note the difference in the sign of the required additional terms for ψ_1 and ψ_2, this is due to the fact that we have chosen different chiralities for their holographic source fields. For the IR boundary condition we have two cases;

(i) $S_{IR} = -\int d^4x(\ldots)$

(ii) $S_{IR} = +\int d^4x(\ldots)$.

In case (i) the IR variation vanishes for,

$$\begin{aligned}\psi_{1R}(R') &= -\tilde{m}\psi_{2R}(R')\\ \psi_{2L}(R') &= \tilde{m}\psi_{1L}(R'),\end{aligned} \tag{3.3.7}$$

and in case (ii) it vanishes for,

$$\begin{aligned}\psi_{1R}(R') &= -\frac{1}{\tilde{m}}\psi_{2R}(R')\\ \psi_{2L}(R') &= \frac{1}{\tilde{m}}\psi_{1L}(R').\end{aligned} \tag{3.3.8}$$

For now we will stick with case (i), but we can see that cases (i) and (ii) are simply related by $\tilde{m} \to 1/\tilde{m}$. We will see later why having these two cases is useful. The bulk equations of motion derived from the above action using the same methods as used in 2.1.3 are,

$$\left(\partial_y \pm \frac{c_f}{R}\right) \psi_{fL,fR} = \pm \not{p} \psi_{fR,fL} \tag{3.3.9}$$

where we have rescaled $\psi \to \frac{r^2}{R^2}\psi$ and set $m_f = c_f/R$. The solutions obeying the above boundary conditions can be constructed from the following functions,

$$\begin{aligned} G_p^+(r,c) &= \sqrt{r}\left(Y_{c-1/2}(pR')J_{c+1/2}(pr) - J_{c-1/2}(pR')Y_{c+1/2}(pr)\right) \\ G_p^-(r,c) &= \sqrt{r}\left(Y_{c-1/2}(pR')J_{c-1/2}(pr) - J_{c-1/2}(pR')Y_{c-1/2}(pr)\right) \end{aligned} \tag{3.3.10}$$

where $G_p^-(R') = 0$, $\left(\partial_y \pm \frac{c}{r}\right) G_p^\pm(r,c) = \pm G_p^\mp(r,c)$, and $G_p^+(R',a) = G_p^+(R',b)$ for any 5D masses a and b. The most general solutions to the equations of motion are,

$$\begin{aligned} \psi_{1L}(p,r) &= \left(A_1 G_p^+(r,c_1) + B_1 G_p^-(r,-c_1)\right)\tilde{\psi}_{1L} \\ \psi_{1R}(p,r) &= \left(A_1 G_p^-(r,c_1) - B_1 G_p^+(r,-c_1)\right)\frac{\not{p}}{p}\tilde{\psi}_{1L} \\ \psi_{2R}(p,r) &= \left(A_2 G_p^+(r,-c_2) + B_2 G_p^-(r,c_2)\right)\tilde{\psi}_{2R} \\ \psi_{2L}(p,r) &= \left(-A_2 G_p^-(r,-c_2) + B_2 G_p^+(r,c_2)\right)\frac{\not{p}}{p}\tilde{\psi}_{2R}, \end{aligned} \tag{3.3.11}$$

where the A_f and B_f coefficients need to be fixed by the boundary conditions. The required algebra is basic, although lengthy. Making use of the fact that $G^-(R',c) = 0$ and $G^+(R',a) = G^+(R',b)$ for any 5D masses a and b, we find that,

$$\begin{aligned} \psi_{1L}(p,r) =& \frac{1}{N}\left(G^+(r,c_1)G^+(-c_2) - \tilde{m}^2 G^-(r,-c_1)G^-(c_2)\right)\tilde{\psi}_{1L} \\ &- \frac{m}{N}\frac{\not{p}}{p}\left(G^+(r,c_1)G^-(-c_1) - G^-(r,-c_1)G^+(c_1)\right)\tilde{\psi}_{2R} \\ \psi_{1R}(p,r) =& \frac{1}{N}\frac{\not{p}}{p}\left(G^+(-c_2)G^-(r,c_1) + \tilde{m}^2 G^-(c_2)G^+(r,-c_1)\right)\tilde{\psi}_{1L} \\ &- \frac{m}{N}\left(G^+(c_1)G^+(r,-c_1) + G^-(-c_1)G^-(r,c_1)\right)\tilde{\psi}_{2R} \\ \psi_{2R}(p,r) =& \frac{m}{N}\frac{\not{p}}{p}\left(G^+(-c_2)G^-(r,c_2) - G^-(c_2)G^+(r,-c_2)\right)\tilde{\psi}_{1L} \\ &+ \frac{1}{N}\left(G^+(c_1)G^+(r,-c_2) - \tilde{m}^2 G^-(-c_1)G^-(r,c_2)\right)\tilde{\psi}_{2R} \\ \psi_{2L}(p,r) =& \frac{m}{N}\left(G^+(-c_2)G^+(r,c_2) + G^-(c_2)G^-(r,-c_2)\right)\tilde{\psi}_{1L} \\ &- \frac{1}{N}\frac{\not{p}}{p}\left(G^+(c_1)G^-(r,-c_2) + \tilde{m}^2 G^-(-c_1)G^+(r,c_2)\right)\tilde{\psi}_{2R} \end{aligned} \tag{3.3.12}$$

where $G(c) \equiv G(R,c)$ and $N = G^+(c_1)G^+(-c_2) - \tilde{m}^2 G^-(-c_1)G^-(c_2)$. Note that there are no terms dependent on R' here as they have all cancelled out. Taking the brane mass to zero decouples the two Dirac fermions, and if we used the case (ii) boundary conditions

this would correspond to taking the brane mass to be very large. Plugging back into the action we find that only those terms that we added to the UV brane survive,

$$\begin{aligned}\mathcal{L} &= \frac{1}{2}\left(\bar{\psi}_{1L}\psi_{1R} - \bar{\psi}_{2R}\psi_{2L} + h.c.\right) \\ &= \bar{\tilde{\psi}}_{1L}\Pi_1^f(p)\not{p}\tilde{\psi}_{1L} + \bar{\tilde{\psi}}_{2R}\Pi_2^f(p)\not{p}\tilde{\psi}_{2R} - \bar{\tilde{\psi}}_{1L}M^f(p)\tilde{\psi}_{2R} + h.c.\end{aligned} \tag{3.3.13}$$

where,

$$\begin{aligned}\Pi_1^f &= \frac{1}{p}\frac{G_p^+(-c_2)G_p^-(c_1) + \tilde{m}^2 G_p^-(c_2)G_p^+(-c_1)}{G_p^+(c_1)G_p^+(-c_2) - \tilde{m}^2 G_p^-(-c_1)G_p^-(c_2)}, \\ \Pi_2^f &= \frac{1}{p}\frac{G_p^-(-c_2)G_p^+(c_1) + \tilde{m}^2 G_p^+(c_2)G_p^-(-c_1)}{G_p^+(c_1)G_p^+(-c_2) - \tilde{m}^2 G_p^-(-c_1)G_p^-(c_2)}, \\ M^f &= \frac{m}{2}\frac{G^+(-c_2)G^+(c_2) + G^-(-c_2)G^-(c_2) + G^+(-c_1)G^+(c_1) + G^-(-c_1)G^-(c_1)}{G_p^+(c_1)G_p^+(-c_2) - \tilde{m}^2 G_p^-(-c_1)G_p^-(c_2)}.\end{aligned} \tag{3.3.14}$$

Using the boundary conditions for case (ii) we find a similar action,

$$\begin{aligned}\mathcal{L} &= \frac{1}{2}\left(\bar{\psi}_{1L}\psi_{1R} - \bar{\psi}_{2R}\psi_{2L} + h.c.\right) \\ &= \bar{\tilde{\psi}}_{1L}\hat{\Pi}_1^f(p)\not{p}\tilde{\psi}_{1L} + \bar{\tilde{\psi}}_{2R}\hat{\Pi}_2^f(p)\not{p}\tilde{\psi}_{2R} - \bar{\tilde{\psi}}_{1L}\hat{M}^f(p)\tilde{\psi}_{2R} - \bar{\tilde{\psi}}_{2R}\hat{M}^f(p)\tilde{\psi}_{1L}\end{aligned} \tag{3.3.15}$$

where,

$$\begin{aligned}\hat{\Pi}_1^f &= \Pi_1^f\left(\tilde{m} \to 1/\tilde{m}\right) \\ \hat{\Pi}_2^f &= \Pi_2^f\left(\tilde{m} \to 1/\tilde{m}\right) \\ \hat{M}^f &= M^f\left(\tilde{m} \to 1/\tilde{m}\right).\end{aligned} \tag{3.3.16}$$

In the limit where the mass terms are zero the KK masses are simply given by,

$$\begin{aligned}m_{1,n} &= \text{zeros}\left(\Pi_1^f\right) \\ m_{2,n} &= \text{zeros}\left(\Pi_2^f\right).\end{aligned} \tag{3.3.17}$$

However when the mass terms are non-zero we can see from the equations of motion that the KK masses are given by,

$$m_n = \text{zeros}\left(p^2\Pi_1^f\Pi_2^f - \left(M^f\right)^2\right). \tag{3.3.18}$$

It may be the case that we want to give a Dirichlet boundary condition to a holographic source field. In previous sections we did something similar with gauge fields and scalar fields, where we dynamically imposed the Dirichlet boundary condition by adding a large UV brane mass. In the fermion case we do something different, because the boundary

conditions of one chirality are linked to the other chirality. Say we have a left-handed holographic source field ψ and we wish to give it a Dirichlet boundary condition on the UV, i.e. switch the source field to the right-handed chirality. We can add an additional term on the UV brane, a coupling to some right-handed field λ,

$$\mathcal{L} = \bar{\psi}\frac{\not{p}}{p}\Pi\psi + \bar{\lambda}\psi + \bar{\psi}\lambda. \tag{3.3.19}$$

Now solving for λ gives the equation of motion, $\psi = 0$, thus generating the Dirichlet boundary condition. We then allow λ to play the role of the right-handed degrees of freedom. We do this by solving for ψ, giving, $\psi = -\lambda\left(\Pi\frac{\not{p}}{p}\right)^{-1}$, and plugging back into the action to find

$$\mathcal{L} = -\bar{\lambda}\left(\Pi\frac{\not{p}}{p}\right)^{-1}\lambda. \tag{3.3.20}$$

So the mass spectrum of this field is given by the poles rather than the zeros of the form factor, just as in the bosonic case.

3.3.2 Fermions in the MCHM$_5$

There are many ways one could embed the SM fermions in the global $SO(5)$ symmetry, however for our analysis we choose to focus on the case in which the SM fermions are embedded in fundamentals of the global $SO(5)$ symmetry. One can embed the up and down type quarks into four $SO(5)$ multiplets, here will use the third generation as an example,

$$\begin{aligned}
\xi_{q1} =& \frac{1}{\sqrt{2}}\begin{pmatrix} b_L \\ -ib_L \\ t_L \\ it_L \\ 0 \end{pmatrix}_{\frac{2}{3}}, \quad \xi_u = \begin{pmatrix} 0 \\ 0 \\ 0 \\ 0 \\ t_R \end{pmatrix}_{\frac{2}{3}}, \\
\xi_{q2} =& \frac{1}{\sqrt{2}}\begin{pmatrix} ib_L \\ b_L \\ -it_L \\ t_L \\ 0 \end{pmatrix}_{-\frac{1}{3}}, \quad \xi_d = \begin{pmatrix} 0 \\ 0 \\ 0 \\ 0 \\ b_R \end{pmatrix}_{-\frac{1}{3}}.
\end{aligned} \tag{3.3.21}$$

where the subscripts refer to the $U(1)_X$ charges, and $Y = T_R^3 + X$. In $\xi_{q1,q2}$ the top and bottom quarks transform as $SU(2)_L$ doublets and the right-handed quarks are singlets under the custodial symmetry. These multiplets are incomplete, however by including

the full multiplets we find that there are exotic states with hypercharge $Y = 7/6$ and $Y = -5/6$ which will correspond to heavy top partners in the model. Notice that we have two $SU(2)_L$ doublets, say q_{1L} and q_{2L}, these are required to give both the top and bottom quarks mass. We can make one linear combination of the doublets massive by introducing a mass mixing between that linear combination and a heavy fermion. The massless doublet is then identified with the orthogonal combination, say $q_L = q_{1L} + q_{2L}$. We expect that the top quark is much more composite than the bottom quark, following the arguments in [84] this leads to $q_L \simeq q_{1L}$ being a valid approximation. Also, ξ_{q1} and ξ_u will contribute much more to the Higgs potential than any other field in the SM, thus from now on we will only deal with these fields.

As we did for the gauge sector, we write down the most general $SO(5)$ invariant action. This turns out to be,

$$\begin{aligned}\mathcal{L} &= \bar{\xi}^i_{q1} \not{p} \left(\delta^{ij}\Pi^{q1}_0 + \Sigma^i\Sigma^j\Pi^{q1}_1\right)\xi^j_{q1} + \bar{\xi}^i_u \not{p}\left(\delta^{ij}\Pi^u_0 + \Sigma^i\Sigma^j\Pi^u_1\right)\xi^j_u + \bar{\xi}^i_{q1}\left(\delta^{ij}M^{q1}_0 + \Sigma^i\Sigma^j M^{q1}_1\right)\xi^j_u + h.c. \\ &= \bar{q}_L \not{p}\left(\Pi^{q1}_0 + \frac{s_h^2}{2}\hat{H}\hat{H}^\dagger\Pi^{q1}_1\right)q_L + \bar{u}_R\not{p}\left(\Pi^u_0 + \frac{s_h^2}{2}\Pi^u_1\right)u_R + \frac{s_h c_h}{\sqrt{2}}M^u_1\bar{q}_L\hat{H}u_R + h.c..\end{aligned} \tag{3.3.22}$$

where $\Sigma = \frac{s_h}{h}\left(h_1, h_2, h_3, h_4, h\cot(h/f_\pi)\right)$. In the limit where the Higgs fluctuations go to zero, this reduces to,

$$\mathcal{L} = \bar{q}_L \not{p}\Pi^{q1}_0 q_L + \bar{u}_R\not{p}\Pi^u_0 u_R. \tag{3.3.23}$$

Now we turn to the 5D implementation where we are forced to add complete Dirac multiplets into the bulk in order to preserve 5D Lorentz invariance. Thus when we embed the SM fields into these 5D multiplets, we must use boundary conditions to 'project out' non-SM zero modes. Because of this, the 5D realisation automatically completes the 5D multiplets of eq. (3.3.21) with vector-like quarks. Just looking at ξ_{q1} and ξ_u we have,

$$\xi_{q1} = \begin{bmatrix}\psi'_{q1}(-+)\\ \psi_{q1}(++)\\ \eta_{q1}(--)\end{bmatrix}_{\frac{2}{3}}, \quad \xi_u = \begin{bmatrix}\psi'_u(+-)\\ \psi_u(+-)\\ \eta_u(-+)\end{bmatrix}_{\frac{2}{3}}, \tag{3.3.24}$$

where $\psi_{q,u}$ are bi-doublets of the $SU(2)\times SU(2)_R$ global symmetry, and the $(\pm,\pm)$ indicate the boundary conditions on the UV and IR branes of the left-handed chiral components, respectively, in the limit of no IR brane mixings. It follows that fermion fields with $(++)$ will have a massless left-handed component, while those with $(--)$ have a massless right-handed component, and fields with $(+-)$ or $(-+)$ have no massless components. In addition to this, the linear combination $(\psi_{q1,L} - \psi_{q2,L})$ should be given a mass on the UV

brane so that only $(\psi_{q1,L} + \psi_{q2,L})$ has a massless component. We then identify the SM left-handed doublet as $\psi_q = (\psi_{q1,L} + \psi_{q2,L})$. As mentioned previously, we can make the approximation $\psi_q \simeq \psi_{q1,L}$. The 5D masses of the above multiplets are denoted as c_q/R and c_u/R, respectively, where c_q and c_u are dimensionless.

For the $q1$ fields we will use the left-handed chiralities as the source fields and for the u fields we will use the right handed chirality,

$$\xi_{q1,L}(r = R) = \chi_L, \quad \xi_{u,R}(r = R) = \chi_R. \tag{3.3.25}$$

We also have some mass mixings on the IR brane such that the $SO(4)$ symmetry is preserved,

$$\mathcal{L}_{IR} = \sqrt{|g|}\left(m_u \bar{q}_{1L}^{(2,2)} u_R^{(2,2)} + M_u \bar{q}_{1R}^{(1,1)} u_L^{(1,1)} + h.c.\right)\Big|_{R'}, \tag{3.3.26}$$

where the $(2,2)$ and $(1,1)$ superscripts indicate the bi-doublet and singlet components of the fermion multiplets. We would like the boundary conditions in eq. (3.3.24) to be obtained in the limit where $m_u, M_u \to 0$, thus we will use case (i) and case (ii) for the $(2,2)$ and $(1,1)$ components, respectively. This leads to the following boundary conditions,

$$\begin{aligned} q_{1L}^{(2,2)} &= \frac{1}{m_u} u_L^{(2,2)}\Big|_{R'} \qquad & u_R^{(2,2)} &= -\frac{1}{m_u} q_{1R}^{(2,2)}\Big|_{R'} \\ q_{1L}^{(1,1)} &= M_u u_L^{(1,1)}\Big|_{R'} \qquad & u_R^{(1,1)} &= -M_u q_{1R}^{(1,1)}\Big|_{R'}. \end{aligned} \tag{3.3.27}$$

We can see from these expressions that we do indeed arrive at the boundary conditions in eq. (3.3.24) for vanishing brane masses, and also that for very large brane masses we effectively flip the IR boundary conditions in eq. (3.3.24). Writing the source fields in the $SO(5)$ notation after turning off fields with Dirichlet boundary conditions on the UV brane, we have,

$$\chi_L = \frac{1}{\sqrt{2}} \begin{pmatrix} b_L \\ -ib_L \\ t_L \\ it_L \\ 0 \end{pmatrix}, \quad \chi_R = \begin{pmatrix} 0 \\ 0 \\ 0 \\ 0 \\ t_R \end{pmatrix}, \tag{3.3.28}$$

which is equivalent to eq. (3.3.21) once we take $\psi_q \simeq \psi_{q1,L}$ and drop the right-handed bottom quark. These quark multiplets are charged under the $SO(5)$ symmetry, thus after we implement the gauge fixing procedure to remove the A_5 degrees of freedom these multiplets will couple to the Higgs via the UV boundary conditions. In the limit where the Higgs fluctuation is zero the holographic action for the top quark is

$$\mathcal{L}_{hol} = \bar{\chi}_L \not{p} \Pi_b^q \chi_L + \bar{\chi}_R \not{p} \Pi_s^u \chi_R \tag{3.3.29}$$

where,

$$\Pi_b^q = \Pi_1^f \left(c_1 = c_q, c_2 = c_u, \tilde{m} = m_u\right)$$
$$\Pi_s^u = \hat{\Pi}_2^f \left(c_1 = c_q, c_2 = c_u, \tilde{m} = 1/M_u\right), \tag{3.3.30}$$

where c_q and c_u are the 5D masses for the ξ_{q1} and ξ_u multiplets, respectively. Matching the 5D theory to the 4D theory is more complicated in this case than it is in the gauge case, so we will address it separately in the next section.

3.3.3 Matching 5D to 4D for quarks in the MCHM$_5$

Just as in the gauge case, to match the 5D and 4D theories one must look at the interactions of the the full $SO(5)$ multiplets. Let us start with the most general action for two $SO(5)$ multiplets in 4D,

$$\psi_{1L} = \begin{pmatrix} \psi_1^b \\ \psi_1^s \end{pmatrix}, \quad \psi_{2R} = \begin{pmatrix} \psi_2^b \\ \psi_2^s \end{pmatrix} \tag{3.3.31}$$

where the b and s superscripts correspond to bi-doublet and singlet components, respectively. The most general action we can write down is again,

$$\begin{aligned}\mathcal{L} =& \bar{\psi}_{1L}^i \not{p} \left(\delta^{ij}\Pi_0^{1L} + \Sigma^i\Sigma^j\Pi_1^{1L}\right)\psi_{1L}^j + \bar{\psi}_{2R}^i \not{p} \left(\delta^{ij}\Pi_0^{2R} + \Sigma^i\Sigma^j\Pi_1^{2R}\right)\psi_{2R}^j \\ &+ \bar{\psi}_{1L}^i \left(\delta^{ij}M_0 + \Sigma^i\Sigma^j M_1\right)\psi_{2R}^j + h.c..\end{aligned} \tag{3.3.32}$$

Expanding this we find

$$\begin{aligned}\bar{\psi}^i\Sigma^i\Sigma^j\psi^j =& \frac{s_h^2}{h^2}h_ih_j\bar{\psi}^{bi}\psi^{bj} + \bar{\psi}^{bi}\frac{s_hc_h}{h}h^i\psi^s + \bar{\psi}^s\frac{s_hc_h}{h}h_i\psi^{bi} + c_h^2\bar{\psi}^s\psi^s \\ \bar{\psi}_{1L}^i\Sigma^i\Sigma^j\psi_{2R}^j =& \frac{s_h^2}{h^2}h_ih_j\bar{\psi}_{1L}^{bi}\psi_{2R}^{bj} + \bar{\psi}_{2L}^{bi}\frac{s_hc_h}{h}h^{bi}\psi_{2R}^s + \bar{\psi}_{1L}^s\frac{s_hc_h}{h}h_i\psi_{2R}^{bi} + c_h^2\bar{\psi}_{1L}^s\psi_{2R}^s.\end{aligned} \tag{3.3.33}$$

where $h_i = (h_1, h_2, h_3, h_4)$. Now going to the zero fluctuation limit we have,

$$\begin{aligned}\mathcal{L} =& \bar{\psi}_{1L}^b\Pi_0^{1L}\psi_{1L}^b + \bar{\psi}_{1L}^s\left(\Pi_0^{1L} + \Pi_1^{1L}\right)\psi_{1L}^s + \bar{\psi}_{2R}^b\Pi_0^{2R}\psi_{2R} + \bar{\psi}_{2R}^s\left(\Pi_0^{2R} + \Pi_1^{2R}\right)\psi_{2R}^s \\ &+ \bar{\psi}_{1L}^bM_0\psi_{2R}^b + \bar{\psi}_{1L}^s\left(M_0 + M_1\right)\psi_{2R}^s.\end{aligned} \tag{3.3.34}$$

Keeping the full $SO(5)$ multiplets means that all the form factors survive in the zero fluctuation limit, making the matching possible. In the 5D model, keeping the full multiplets and going to the zero fluctuation limit (i.e. $U = \mathbb{1}$ in the UV boundary conditions), we arrive at,

$$\begin{aligned}\mathcal{L} =& \bar{\psi}_{1L}^b\Pi_b^q\psi_{1L}^b + \bar{\psi}_{1L}^s\Pi_s^q\psi_{1L}^s + \bar{\psi}_{2R}^b\Pi_b^u\psi_{2R}^b + \bar{\psi}_{2R}^s\Pi_s^u\psi_{2R}^s \\ &+ \bar{\psi}_{1L}^bM_b\psi_{2R}^b + \bar{\psi}_{1L}^sM_s\psi_{2R}^s,\end{aligned} \tag{3.3.35}$$

where the expressions for the form factors are calculated using methods outlined in previous sections,

$$\begin{aligned}
\Pi_b^q &= \Pi_1^f(c_1 = c_q, c_2 = c_u, \tilde{m} = m_u),\\
\Pi_s^q &= \hat{\Pi}_1^f(c_1 = c_q, c_2 = c_u, \tilde{m} = M_u),\\
\Pi_b^u &= \Pi_2^f(c_1 = c_q, c_2 = c_u, \tilde{m} = m_u),\\
\Pi_s^u &= \hat{\Pi}_2^f(c_1 = c_q, c_2 = c_u, \tilde{m} = M_u),\\
M_b &= M^f(c_1 = c_q, c_2 = c_u, \tilde{m} = m_u),\\
M_s &= \hat{M}^f(c_1 = c_q, c_2 = c_u, \tilde{m} = M_u).
\end{aligned} \tag{3.3.36}$$

Then matching to the 4D action we have,

$$\begin{aligned}
\Pi_0^{1L} = \Pi_b^q, \quad \Pi_1^{1L} =& \Pi_s^q - \Pi_b^q, \quad \Pi_0^{2R} = \Pi_b^u\\
\Pi_1^{2R} = \Pi_s^u - \Pi_b^u, \quad M_0 =& - M_b, \quad M_1 = M_b - M_s.
\end{aligned} \tag{3.3.37}$$

Expanding some of the terms in the 4D action, we find

$$\begin{aligned}
h_i\psi^{bi} =& \frac{1}{\sqrt{2}}\begin{pmatrix} h_1 - ih_2 \\ h_3 + ih_4 \end{pmatrix}\begin{pmatrix} b_L \\ t_L \end{pmatrix} = \frac{1}{\sqrt{2}} H q_L\\
h\bar{\psi}^b\psi^b h =& \frac{1}{2}\bar{q}_L H^\dagger H q_L
\end{aligned} \tag{3.3.38}$$

where we use the definitions in eq. (3.3.28). After a little manipulation, and applying the UV boundary conditions, we then arrive at eq. (3.3.22),

$$\mathcal{L} = \bar{q}_L \not{p}\left(\Pi_0^{q1} + \frac{s_h^2}{2}\hat{H}\hat{H}^\dagger\Pi_1^{q1}\right) q_L + \bar{u}_R \not{p}\left(\Pi_0^u + \frac{s_h^2}{2}\Pi_1^u\right) u_R + \frac{s_h c_h}{\sqrt{2}} M_1^u \bar{q}_L \hat{H} u_R + h.c., \tag{3.3.39}$$

and can identify,

$$\begin{aligned}
\Pi_0^{q1} &= \Pi_b^q,\\
\Pi_1^{q1} &= \Pi_s^q - \Pi_b^q,\\
\Pi_0^u &= \Pi_s^u,\\
\Pi_1^u &= 2(\Pi_b^u - \Pi_s^u),\\
M_1^u &= M_b - M_s.
\end{aligned} \tag{3.3.40}$$

We can read off the mass spectrum for the $Y = 2/3$ and $Y = 1/6$ top partners in the limit of $M_1^u = 0$ as

$$\begin{aligned}
m_{2/3} &= \text{zeros}(\not{p}\Pi_0^{q1}),\\
m_{1/6} &= \text{zeros}(\not{p}\Pi_0^u),
\end{aligned} \tag{3.3.41}$$

We can obtain the mass spectrum of the 7/6 fermion by looking at the mass spectrum of the ψ'_{uR} fields appearing in eq. (3.3.24). These have right handed source fields with the right handed components having Dirichlet boundary conditions in the UV. The relevant form factor is $\Pi_0^{2R} = \Pi_b^u = \Pi_0^u + \frac{1}{2}\Pi_1^u$. Following the steps in section 3.3.1, we find

$$m_{7/6} = \text{poles}\left(\not{p}\left(\Pi_0^u + \frac{1}{2}\Pi_1^u\right)\right). \tag{3.3.42}$$

After EWSB the 2/3 and 1/6 states mix giving a mass spectrum of the form,

$$\text{zeros}\left(p^2\left(\Pi_0^q + \frac{s_h^2}{2}\Pi_1^q\right)\left(\Pi_0^u + \frac{s_h^2}{2}\Pi_1^u\right) - \frac{s_h c_h}{\sqrt{2}h}M_1^u\right), \tag{3.3.43}$$

which will contain the top partner mass as its first zero. We have discussed previously that the $SO(5)$ symmetry is restored in the $m_u \to 1/M_u$ limit. This is seen from the fact that the form factors multiplying s_h or c_h terms in the fermion action go to zero in this limit. But there is also another special limit, one can easily check that in the limit where $m_u \to -1/M_u$ the Π_1 form factors vanish, whereas the M_1^u form factor survives.

3.4 Higgs potential and EWSB in the MCHM$_5$

In the previous sections we have demonstrated how to construct an explicit formulation of form factors in a low energy Minimal Composite Higgs Model using holographic techniques in a warped extra dimension. This low energy effective theory contains, at tree level, all the SM fields coupled to a Higgs doublet, which, due to its Goldstone nature has no potential at tree-level. We now need examine the one-loop contributions to the Higgs potential from the SM fields. In doing so we will neglect contributions from hypercharge and light fermions, thus the effective action we work with can be written as

$$\begin{aligned}\mathcal{L} = (P_T)^{\mu\nu}\frac{1}{g_5^2}\left(\Pi_0 + \frac{s_h^2}{4}\Pi_1\right)L_\mu^a L_\nu^a + \bar{q}_L\not{p}\left(\Pi_0^{q1} + \frac{s_h^2}{2}\hat{H}\hat{H}^\dagger\Pi_1^{q1}\right)q_L \\ + \bar{u}_R\not{p}\left(\Pi_0^u + \frac{s_h^2}{2}\Pi_1^u\right)u_R + \frac{s_h c_h}{\sqrt{2}}M_1^u\bar{q}_L\hat{H}u_R + h.c.,\end{aligned} \tag{3.4.1}$$

where the form factors have been calculated holographically in previous sections. We intend to study the features of EWSB in this model, i.e. how the Higgs mass and top partner masses are correlated with each other and with parameters in the 5D model. It is generally found that when one or both of the multiplets has a large composite mixing, there will be relatively light fermionic states in the model. This large compositeness also generally implies a large gap in the masses of the lightest (1/6), (2/3) and (7/6) top partners. By varying the 5D parameters of the model we want to investigate how we can

alter the spectrum of top partners we expect to observe. And just to summarise, from the 5D description of the model we have six parameters,

$$M_{KK} \quad \ln\Omega \quad c_q \quad c_u \quad m_u \quad M_u. \tag{3.4.2}$$

We can use three observables to fit to v, m_h and m_t, leaving us with three free parameters. Here we will demonstrate the freedom that these parameters give in the top sector. In particular, there are three aspects we wish to study,

- How the 5D parameters are related to the top partner masses;
- How the top partner masses are related to s_h, and;
- How much 5D contributions alter the top Yukawa deviation expected from 4D composite Higgs models.

3.4.1 The Higgs potential

From the effective action for the gauge fields and the top quark it is a simple exercise to write down the Coleman-Weinberg expression for the one-loop Higgs potential. After a Wick rotation we arrive at the following field-dependent potential,

$$V(h) = \int \frac{d^4p_E}{(2\pi)^4}\left(\frac{3}{2}\ln\left[1+\frac{3}{2}\frac{\Pi_1}{\Pi_0}\right] - 6\ln\left[\left(1+\frac{s_h^2}{2}\frac{\Pi_1^q}{\Pi_0^q}\right)\left(1+\frac{s_h^2}{2}\frac{\Pi_1^u}{\Pi_0^u}\right)+\frac{s_h^2c_h^2}{2}\frac{(M_1^u)^2}{p_E^2\Pi_0^q\Pi_0^u}\right]\right). \tag{3.4.3}$$

Expanding these logs, it is found that the potential has the following form,

$$V(h) \simeq (\alpha_G+\alpha_F)s_h^2 - \beta_F s_h^2 c_h^2 \tag{3.4.4}$$

where the F and G subscripts refer to gauge and fermion contributions. Notice that without the fermion contribution one cannot achieve EWSB at all. Minimising this we find that the Higgs potential has a non-trivial ground state when $\beta_F > 0$ and $\beta_F > |\alpha_F + \alpha_G|$, situated at

$$s_h^2 = \frac{1}{2} - \frac{\alpha_G+\alpha_F}{2\beta_F}. \tag{3.4.5}$$

Taking the second derivative of $V(h)$ we find

$$m_H^2 = \frac{8\beta_F}{f_\pi^2}s_h^2c_h^2. \tag{3.4.6}$$

After EWSB it is found that the mass of the top is given by,

$$m_t^2 \simeq \frac{s_h^2c_h^2}{2}\left.\frac{(M_1^u)^2}{(\Pi_0^q+\frac{s_h^2}{2}\Pi_1^q)(\Pi_0^u+\frac{s_h^2}{2}\Pi_1^u)}\right|_{p^2=(174\text{GeV})^2}. \tag{3.4.7}$$

Since the top quark gives by far the most dominant contribution to the potential, we should expect a lot of correlation between the top partner spectrum and the Higgs mass. Approximating the form factors by their limiting expressions for vanishing momentum, we can write this in terms of the 5D parameters as

$$m_t^2 \simeq \frac{M_u v \sqrt{(\tilde{c}_q-2)\tilde{c}_q(\tilde{c}_u-2)\tilde{c}_u}\sqrt{1-\frac{v^2}{f_\pi^2}}(1-m_u M_u)}{f_\pi L_1 \sqrt{-(\tilde{c}_q-2)M_u^2+\frac{\tilde{c}_u v^2(m_u^2M_u^2-1)}{f_\pi^2}+\tilde{c}_u}\sqrt{M_u^2\left(\tilde{c}_q m_u^2\left(2-\frac{v^2}{f_\pi^2}\right)-2\tilde{c}_u+4\right)+\frac{\tilde{c}_q v^2}{f_\pi^2}}}, \tag{3.4.8}$$

where we have defined

$$c_u = \frac{\tilde{c}_u - 1}{2} \quad \text{and} \quad c_q = \frac{1-\tilde{c}_q}{2}, \tag{3.4.9}$$

such that $0 \leq \tilde{c}_q$, and $\tilde{c}_u \leq 2$, and the profiles are flat ($c_{q,u} = \pm 1/2$) for $\tilde{c}_{q,u} = 0$.

3.4.2 Yukawa couplings in the holographic MCHM$_5$

From the discussion above it is seen that the Yukawa coupling of the top quark in MCHM$_5$ deviates from its Standard Model value. Following the definition of the effective Yukawa coupling by [112],

$$y_\psi^{(0)} \simeq \frac{dm_\psi^{(0)}}{dv}, \tag{3.4.10}$$

we will be interested in the quantity

$$\kappa_t = \frac{y_t^{(0)}}{y_{t,SM}^{(0)}} = \frac{y_t^{(0)} v}{m_t^{(0)}}. \tag{3.4.11}$$

The current LHC ATLAS bounds are $\kappa_t = 0.94 \pm 0.21$ at 2σ [158]. This bound is expected to be strengthened to the ten percent level after the current run.

From (3.4.7) we may calculate κ_t in terms of the 5D form factors. To quartic order in $s_h = v/f_\pi$, we have

$$\kappa_t = 1 - \frac{s_h^2}{c_h^2} - s_h^2\left(\frac{\Pi_1^q}{2\Pi_0^q}+\frac{\Pi_1^u}{2\Pi_0^u}\right) + s_h^4\left(\frac{(\Pi_1^q)^2}{4(\Pi_0^q)^2}+\frac{(\Pi_1^u)^2}{4(\Pi_0^u)^2}\right) + O\left(s_h^5\right). \tag{3.4.12}$$

As by definition, the Standard Model result ($\kappa_t = 1$) is recovered in the limit $s_h \to 0$. Also, as we have noted above, if the IR brane masses are related as $M_u = -1/m_u$, the fermion form factors vanish ($\Pi_1^q = \Pi_1^u = 0$). In this case the BSM Yukawa corrections are universal and equal to $-s_h^2/c_h^2$ (to all orders in s_h). From (3.4.8), in terms of the fermion profiles we have,

$$\frac{y_\psi^{(0)} v}{m_\psi^{(0)}} = 1 - \frac{s_h^2}{c_h^2} - s_h^2\left(\frac{\left(m_u^2M_u^2-1\right)\left(M_u^2\left(\tilde{c}_q\left((2-\tilde{c}_q)-2\tilde{c}_u m_u^2\right)-2(2-\tilde{c}_u)\tilde{c}_u\right)+\tilde{c}_q\tilde{c}_u\right)}{2M_u^2\left(-\tilde{c}_q m_u^2-(2-\tilde{c}_u)\right)\left((2-\tilde{c}_q)M_u^2+\tilde{c}_u\right)}\right) + O\left(s_h^4\right). \tag{3.4.13}$$

In section 3.5.2 we will study how these additional contributions proportional to $\left(m_u^2 M_u^2 - 1\right)$ can play a role in alleviating tensions with bounds from the LHC.

3.5 Top sector in the holographic MCHM$_5$

In the previous sections we described the set-up of the holographic MCHM$_5$ in some detail, now we make use of this work and look at two different aspects of the top sector physics in the model. First, we look at the top partners spectrums predicted by the model once we require that it gives the correct Higgs mass, top mass, and Higgs vev. We then move on to look at corrections to the top Yukawa coupling in this model and specifically look at the effects the IR mixing parameters have on this quantity.

3.5.1 Top partners and a low UV scale

Taking the values of s_h and c_h at the minimum of $V(h)$, we can re-write the Higgs mass term from eq. (3.4.6) as

$$m_H^2 = \frac{2}{f_\pi^2}\frac{\beta^2 - \alpha^2}{\beta}. \tag{3.5.1}$$

The α and β terms are of dimension four and we can expect them to be $\sim M_{KK}^4$. Thus to obtain a light Higgs we require a degree of cancellation among the terms in the Higgs potential. A similar cancellation is also required to obtain a light vacuum expectation value. Due to the required cancellation among these terms, the precise value of s_h alone is only a crude estimate of the fine-tuning of the model.

It has been shown that if $M_{KK} \sim 1$ TeV, and $f_\pi \sim 500$ GeV, one requires the ξ_u multiplet to have a large composite mixing in order to get the correct degree of cancellation in α and β, and thus obtain the correct values of m_H, $m_{t,pole}$ and v [84]. This implies that light top partners are expected in models with a large mass gap among the different charged states. Similar results have been observed in the 4D realisations, however in these cases there is more freedom with the model and light top partners can be avoided more easily. Currently, the prediction of light top partners from holographic models is in tension with observations at the LHC.

The obvious way to avoid these constraints is to push up M_{KK}, but in doing one severely increases the fine-tuning of the model and it becomes "un-natural". There have been several attempts at alleviating the need for light top partners without increasing the fine-tuning, in both the purely 4D and the holographic picture. An example of the former is [66, 127], in which the authors show that by embedding the third generation in

different representations of SO(5), the structure of the Higgs mass term can be altered. For particular cases a light Higgs could be obtained with top partners ~ 1 TeV in this way. The authors point out that to achieve a light Higgs with moderate fine-tuning, it is preferred to have $m_T/f_\pi \sim 1$, where m_T is the scale of the top partner masses. To highlight an example of a holographic approach, in [124] the realisation of the model includes leptonic contributions to the Higgs potential, which allow the authors to show that a light Higgs can be achieved while having top partners ~ 1 TeV, with only moderate fine-tuning.

In this work we wish to investigate an alternative method of reducing the need for light top partners in the holographic realisation of the model. Moving the top zero mode wave functions away from the IR brane increases the mass of the top partners, but simultaneously results in an increase in the Higgs mass. However, by lowering the UV scale (i.e. lowering $\ln(\Omega)$) we increase f_π and suppress the Higgs mass. Using this mechanism we can push the top zero mode wave functions further from the IR, pushing up the top partner masses, while keeping the Higgs mass at the observed value. As discussed in section 3.2.4, in the 4D dual lowering the UV scale corresponds to an increase in the number of colours "N" of the strongly coupled gauge theory [59, 84].

To illustrate this idea we perform a scan in which we fix $M_{KK} = 1.1$ TeV and vary the other parameters in the ranges $0.2 < c_q < 0.4$, $-0.4 < c_u < 0.4$, $-2 < m_u M_u < -0.5$ and $20 < \ln(\Omega) < 50$. For $c_q = 0.5$ ($c_u = -0.5$) the 5D profile of the left-handed (right-handed) zero mode will be flat. So the choices of fermion localisations ensure that the composite mixing for q_L is small, whereas the mixing of the t_R state is allowed to be large or small. We find two distinct cases in the results, $|m_u| < 1.4$ and $|m_u| > 1.4$. In figures 3.1 and 3.2 below we show how c_u and $\ln(\Omega)$ are correlated after we fix $m_{t,pole}$, m_H, and v to their observed values.

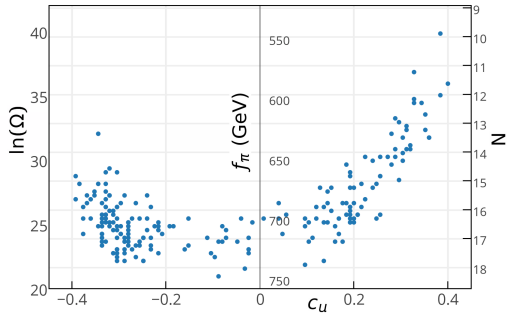

Figure 3.1: Correlation between c_u and $\ln(\Omega)$ when $|m_u| < 1.4$.

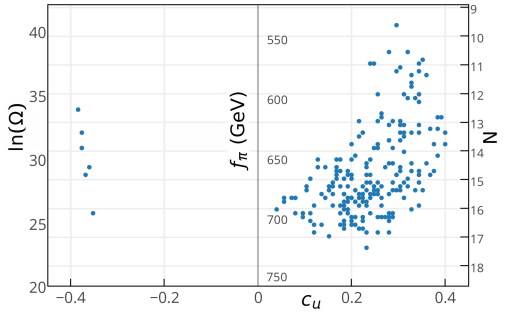

Figure 3.2: Correlation between c_u and $\ln(\Omega)$ when $|m_u| > 1.4$.

From these plots it is clear that for a large value of $\ln(\Omega)$ ($\gtrsim 35$), a light Higgs requires the spurious multiplet to have large positive values of c_u. However by allowing for smaller values of $\ln(\Omega)$ we can have significantly different values for this c_u parameter. The effects of this on the top partner spectrum are shown below in figures 3.3 and 3.4.

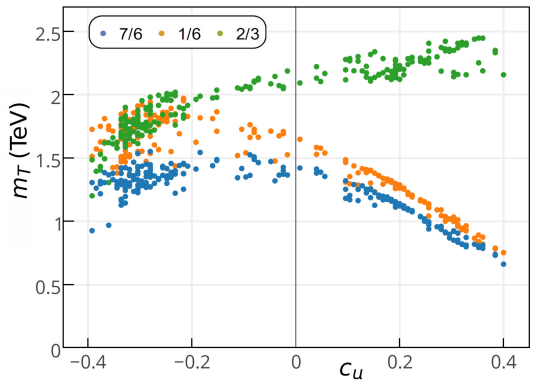

Figure 3.3: Correlation between c_u and the top partner masses when $|m_u| < 1.4$. Here the green points correspond to the top partner with hypercharge (2/3), the orange with (1/6), and the blue with (7/6).

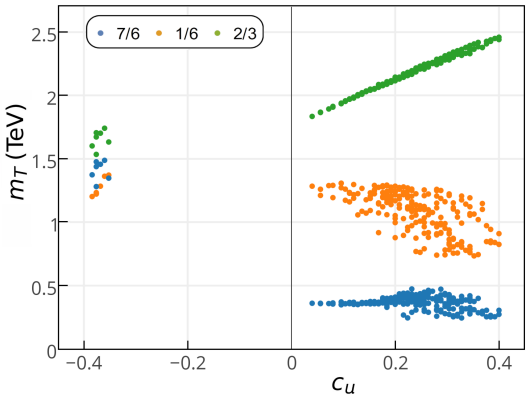

Figure 3.4: Correlation between c_u and the top partner masses when $|m_u| > 1.4$. As in the left panel, the different coloured points correspond to top partners with different hypercharge.

If we were to fix $\ln(\Omega)$ to be > 35, we would be forced to have $c_u \gtrsim 0.3$. This results in a distinct top partner spectrum in which the left-handed top partner and exotic top partners are $\lesssim 1$ TeV while the right-handed top partner is ~ 2 TeV. However, by lowering the value of $\ln(\Omega)$ we can move c_u to regions with less composite mixing in which the top partner spectrum is remarkably different. We can easily have scenarios where all the top partners have masses $\gtrsim 1$ TeV, and where the mass gap among the different charged states is very small. Note that, in the 4D picture, having $\ln(\Omega) \sim 37$ means having the number of colours at ~ 10. Lowering $\ln(\Omega)$ to ~ 25 means that $N \sim 15$. In the case of figure 3.3, we can say that the mass gap between the top partners is strongly related to their degree of compositeness.

Since we fix $M_{KK} = 1.1$ TeV and fix the vev, varying $\ln(\Omega)$ is analogous to varying s_h. In figures 3.5 and 3.6 we see the correlation between top partner masses and s_h explicitly.

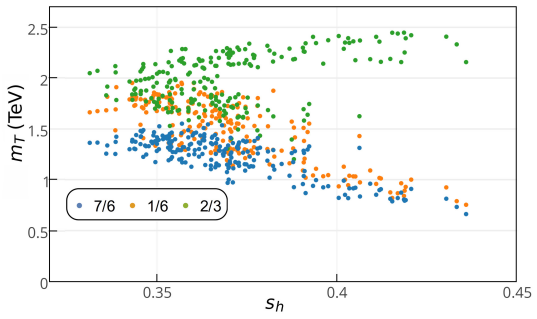

Figure 3.5: Correlation between s_h and the top partner masses when $|m_u| < 1.4$. As above, the different coloured points correspond to top partners with different hypercharge.

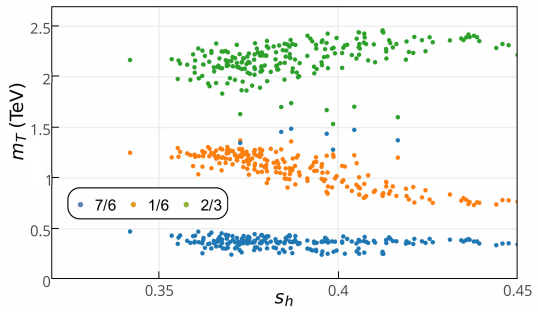

Figure 3.6: Correlation between s_h and the top partner masses when $|m_u| > 1.4$.

From figure 3.5 it appears that reducing the mass gap between the top partners is strongly correlated with a reduction in s_h. However we do not see this behaviour in figure 3.6. Thus from the above figures we can conclude that, when $|m_u| \lesssim 1.4$ we can have less composite mixing and a smaller s_h is correlated with a smaller mass gap among the top partners, and an increase in the mass of the lightest top partner. Whereas for $|m_u| \gtrsim 1.4$, we are forced to have a larger composite mixing, and lowering s_h does not alter the top partner spectrum very much.

Taking the case where $|m_u| < 1.4$, it is useful to plot the masses of the 7/6 partners against the masses of the 2/3 partners and to look at how s_h varies here. From figure 3.7 we see that lower values of s_h are not necessarily correlated with a smaller mass gap, but with heavier 7/6 partners.

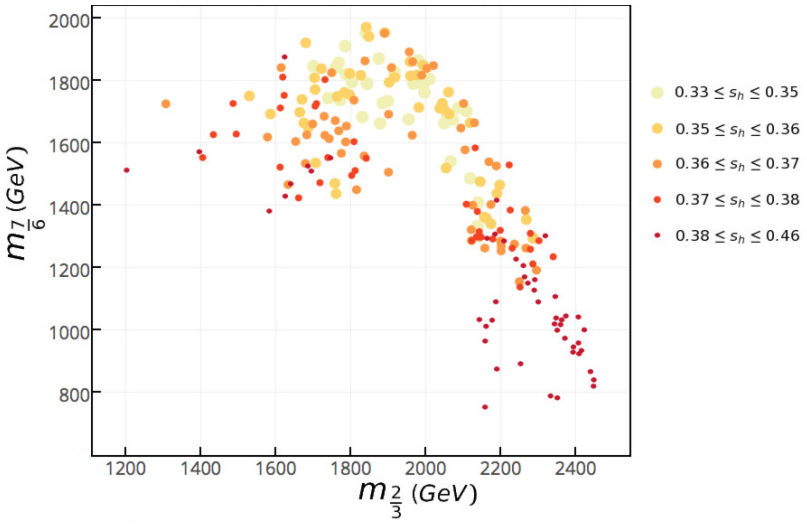

Figure 3.7: Here we plot the masses of the hypercharge 7/6 multiplet against the hypercharge 2/3 singlet and show how the value of s_h depends on these masses.

In figures 3.8 and 3.9 we perform similar scans, except we allow M_{KK} to vary. In one case, we have a very light top partner with a large mass gap, and in the other we have no light top partners and a small mass gap.

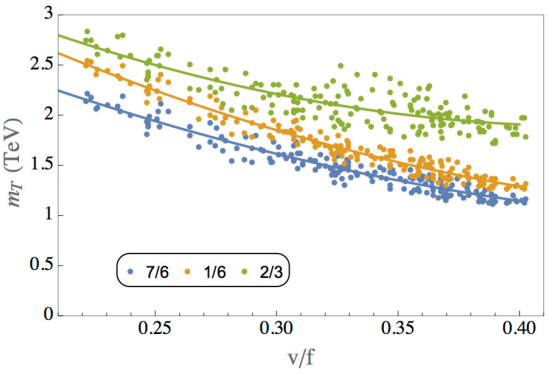

Figure 3.8: $c_q = 0.4$, $0 \leq -c_u \leq 0.4$, $1 \leq M_{KK}(\text{TeV}) \leq 2$ TeV, $20 \lesssim \ln(\Omega) \lesssim 30$ and $m_u = -1/M_u$. As above, the different coloured points correspond to top partners with different hypercharge.

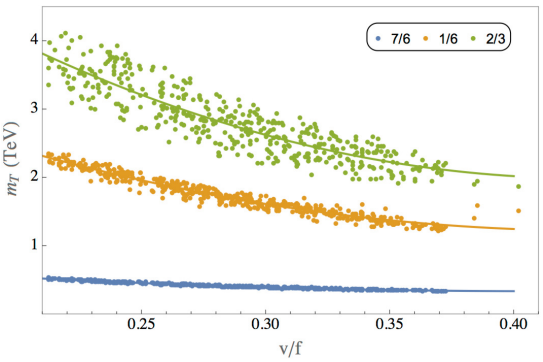

Figure 3.9: $c_q = 0.2$, $0 \leq c_u \leq 0.4$, $1 \leq M_{KK}(\text{TeV}) \leq 2$ TeV, $20 \lesssim \ln(\Omega) \lesssim 30$ and $m_u = -1/M_u$.

One would naturally expect that by reducing s_h, the mass of the top partners increase. What we show here is that this is only true in the case that $0 \leq -c_u \leq 0.4$, i.e. when there is less composite mixing for ξ_u. When $0 \leq c_u \leq 0.4$, i.e. large composite mixing, we clearly show that lowering s_h does not result in an increase in the mass of the lightest

state. This is hinted at in figure 3.6, and re-enforced by the data in figure 3.9.

In studying composite Higgs models in 4D it is found that one expects the following approximate relation to hold,

$$m_H^2 \sim \frac{3}{16\pi^2}\left(\frac{v}{f_\pi}\right)^2 m_T^2 \tag{3.5.2}$$

where m_T is the mass of the top partners. Since we fix v to its SM value, this implies a linear relation between the Higgs mass and both the top partner masses and the ratio v/f. In the figures 3.10 and 3.11 test we test the latter relation, finding that this relation receives O(1) corrections in the dual model.

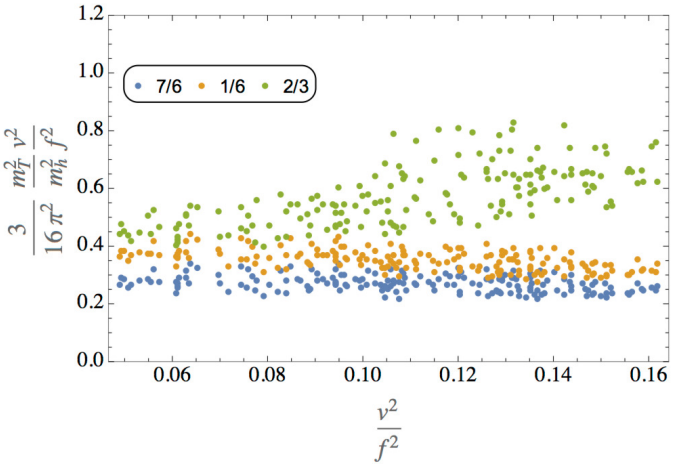

Figure 3.10: $c_q = 0.4$, $0 \leq c_u \leq 0.4$, $1 \leq M_{KK}(\text{TeV}) \leq 2$ TeV, $20 \lesssim \ln(\Omega) \lesssim 30$ and $m_u = -1/M_u$. As above, the different coloured points correspond to top partners with different hypercharge.

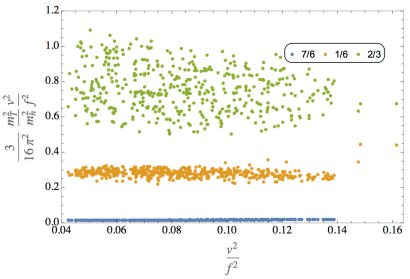

Figure 3.11: $c_q = 0.2$, $0 \leq -c_u \leq 0.4$, $1 \leq M_{KK}(\text{TeV}) \leq 2$ TeV, $20 \lesssim \ln(\Omega) \lesssim 30$ and $m_u = -1/M_u$.

It is useful at this point to compare our results to those obtained in explicit 4D realisations. Although varying $\ln(\Omega)$ produces results which differ from what is usually expected in the holographic models, it appears that doing this allows for a better comparison to the 4D models. In fact, the results we have obtained here, with the mass gap among the top partners varying, agree quite well with the explicit 4D realisations in [64,69]. In these works they show that $m_H^2 \sim \ln(m_{7/6}/m_{2/3})$, implying that a smaller mass gap results in a lighter Higgs, which is exactly what we find here.

In [85] it was shown that increasing the scale M_{KK} in this 5D realisation leads to heavier top partners and lower values of s_h, but also a larger fine-tuning. It is now interesting to ask what effect lowering $\ln(\Omega)$ has on the fine-tuning in this model, since it also leads to heavier top partners and lower values of s_h, one might expect an increase in

the fine-tuning. To quantify the fine-tuning in our model, in accordance with what was done in [85], we use the Barbieri-Giudice parameterisation [159],

$$\Delta_{BG} = \sqrt{\sum_i \left(\frac{\partial \log s_h^2}{\partial \log k_i} \right)} \tag{3.5.3}$$

where k_i are the input parameters M_{KK}, c_u, c_q, m_u, M_u, and $\ln(\Omega)$. The Δ_{BG} parameter measures the sensitivity of s_h^2 to changes in the input parameters. In figure 3.12 we plot the values of this parameter for the data we have with $|m_u| < 1.4$ as a function of the 5D localisation c_u and $\ln(\Omega)$. On the same plots we include the values of $1/s_h^2$ for each point to show how s_h and Δ_{BG} are correlated. Other observables for these data points have been shown in figures 3.1, 3.3, 3.5, and 3.7.

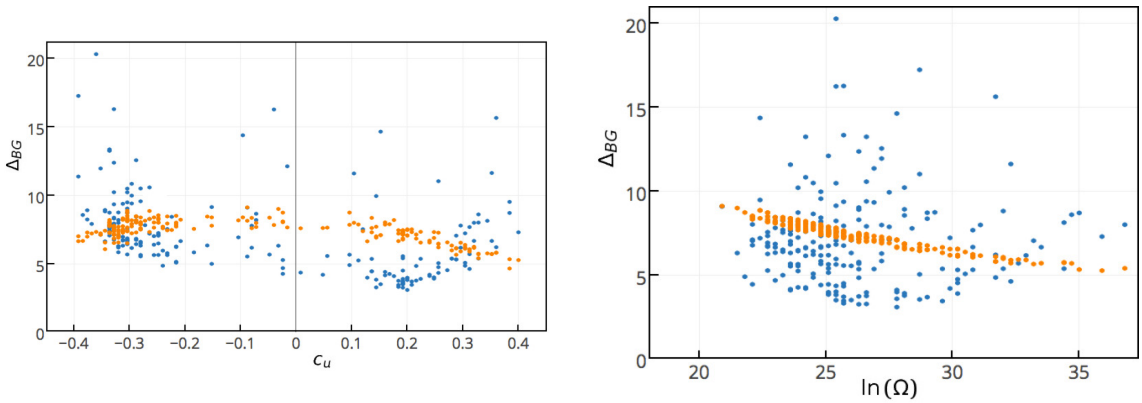

Figure 3.12: The blue points are the values of Δ_{BG} calculated from eq. (3.5.3), while the orange points are the values of $1/s_h^2$ for each point.

These plots show us something very interesting, that is, lowering $\ln(\Omega)$ allows for a reduced fine-tuning in the Higgs potential and heavier top partners. This result should not be too surprising since varying $\ln(\Omega)$ in the 5D models results in changes to the effective couplings between KK states and the Higgs in the effective theory, and it has been shown using an explicit 4D realisation in [127] that the fine-tuning in composite Higgs models depends strongly on these couplings. We can see from the plots that the fine-tuning is minimised for $c_u \sim 0.2$ and $25 < \ln(\Omega) < 30$, which is slightly IR localised, and corresponds to the lightest top partner being just above 1 TeV (7/6 partner), with the next top partner laying just above 2 TeV (2/3 partner).

3.5.2 The top Yukawa coupling

In this section we study deviations to the top Yukawa coupling and possible future measurements of the Higgs in association with a hard object (vector boson, jet) as a probe for

the Higgs-top-antitop form factor. First of all, we look at the top Yukawa coupling. We expect an inverse scaling between M_u and (the negative of) m_u. We will take a mildly more general relation

$$M_u = -\frac{a_1}{m_u} \tag{3.5.4}$$

with a_1 a real constant. In this case the expression simplifies to

$$\frac{y_\psi^{(0)} v}{m_\psi^{(0)}} = 1 - \frac{s_h^2}{c_h^2} - s_h^2 \left(a_1^2 - 1\right) \left(\frac{\tilde{c}_q}{2a_1^2 \tilde{c}_q + 2(2 - \tilde{c}_u) M_u^2} - \frac{\tilde{c}_u}{(2 - \tilde{c}_q) M_u^2 + \tilde{c}_u} \right) + O\left(s_h^4\right) \tag{3.5.5}$$

It is now obvious that the additional Yukawa correction due to 5D effects vanishes for either $a_1 = \pm 1$, and for flat profiles. It is also seen that the contribution switches sign for $a_1^2 = 1$ and for

$$a_1^2 = \frac{1}{2} + \frac{M_u^2 \left((2 - \tilde{c}_q)\tilde{c}_q - 2(2 - \tilde{c}_u)\tilde{c}_u\right)}{2\tilde{c}_q \tilde{c}_u}$$

In other words, in the region

$$\frac{1}{2} + \frac{M_u^2 \left((2 - \tilde{c}_q)\tilde{c}_q - 2(2 - \tilde{c}_u)\tilde{c}_u\right)}{2\tilde{c}_q \tilde{c}_u} < a_1^2 < 1$$

there can be an effective cancelation between the universal contribution and the Yukawa contribution. We can see this explicitly for two benchmark scenarios, $a_1 = 0.8$ and $a_1 =$

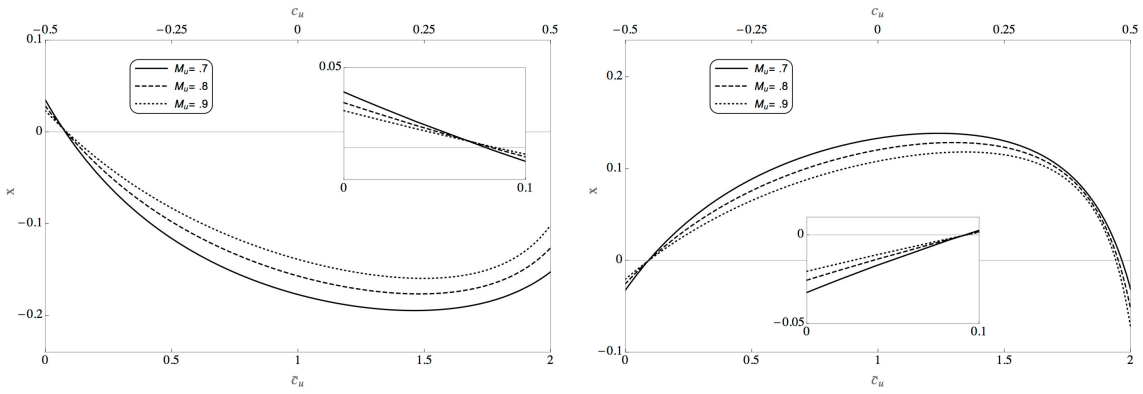

(a) $c_q = 0.4$ ($\tilde{c}_q = 0.2$) and $a_1 = 1.2$ (b) $c_q = 0.4$ ($\tilde{c}_q = 0.2$) and $a_1 = 0.8$

Figure 3.13: Profile contribution to the Yukawa coupling: It is seen that the contribution is larger for IR localised fermions, and that the sign is dependent on the sign of $(a_1 - 1)$. The values of M_u are chosen such that the scan results will map between the curves.

1.2. Writing

$$\frac{y_\psi^{(0)} v}{m_\psi^{(0)}} = 1 - s_h^2 \left(\frac{1}{c_h^2} - x \right) + O\left(s_h^4\right) \tag{3.5.6}$$

where x is the Yukawa correction (modulo s_h^{-2}),

$$x = \left(1 - a_1^2\right)\left(\frac{\tilde{c}_q}{2a_1^2\tilde{c}_q + 2(2-\tilde{c}_u)M_u^2} - \frac{\tilde{c}_u}{(2-\tilde{c}_q)M_u^2 + \tilde{c}_u}\right).$$

We plot this isolated mode contribution for the benchmarks in figure 3.13. Here we see indeed that the sign of the correction is dependent on the sign of $a_1 - 1$, that is, on the relation between the brane masses M_u and m_u. It is also seen that the correction is expected to be out of experimental reach for a small departure of $a_1 = 1$. However, the contribution can be made more sizeable values of a_1. For instance, in the case in which $a_1 = 1.5$, one finds a maximum of $x = 0.6$ for $\tilde{c}_u \approx 1.7$. We use this large case to plot the range of imaginable contributions in the $\kappa_V - \kappa_t$ plane in figure 3.14.

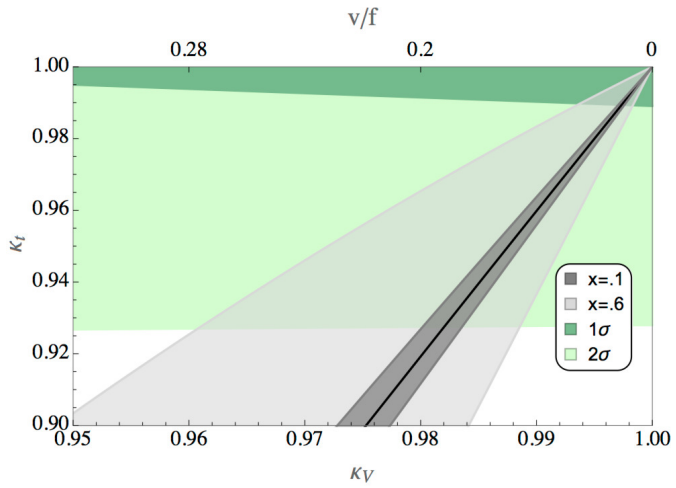

Figure 3.14: Profile contribution to the Yukawa coupling: in terms of the experimental variables κ_t and κ_V. In light and dark green the ATLAS 1σ and 2σ limits from [160].

Chapter 4

A little KK graviton at 750 GeV?

In December 2015 at the beginning of Run 2 at the LHC there were some exciting hints of new physics beyond the Standard Model as an excess in the diphoton channel at $m_{\gamma\gamma} \sim 750$ GeV was observed with a cross-section of a few fb above the background [6,7]. The analysis of further data has revealed that this excess was nothing but a statistical fluctuation, thus the excess has gone away [8]. Despite this, the work done in attempting to identify the source of the resonance prompted many interesting investigations into the kinds of new physics that could give rise to this relatively low mass excess while evading constraints in other channels. This excess was interpreted as a resonance with $\sigma_{prod}(pp \to X) \times \mathrm{Br}(X \to \gamma\gamma) \simeq 5$ fb [161–166]. In this chapter we will discuss a model which can reproduce this signal while remaining within all other stringent constraints set by the data analysed during the first run of the LHC.

We suppose that this resonance was produced by a composite spin-2 state of a strongly coupled gauge theory confining at the TeV scale, just like those described in previous chapters. Again, one can try to describe this scenario using five-dimensional (5D) holographic models, which are proposed to be dual to classes of strongly coupled gauge theories in 4D. These models naturally give rise to two candidate particles which could have described the observed diphoton excess, one is the radion (spin-0), and the other is a KK graviton (spin-2). The radion is related to fluctuations in the size of the extra dimension, i.e. the distance between the UV and IR branes, while the KK gravitons are heavier excitations of the fluctuations of the Minkowski components of the metric.

Irrespective of the spin, in RS the resonance is linked to the origin of electroweak symmetry breaking, and hence the Higgs sector. There has been a fair amount of work exploring this relation, and the scenario which stands out as most natural is the holographic composite Higgs. This has been presented in detail in the previous chapter.

In the current chapter, the final sub-project comprising this thesis, we wish to explore whether the composite Higgs idea would have been compatible with a spin-2 resonance with the characteristics of the excess observed diphoton signal. Despite the revelation that the excess was no more than a statistical fluctuation, the ideas explored here are interesting in their own right as the question of a light KK graviton in a holographic composite Higgs scenario has not yet been thoroughly explored in other works. We find that successful models point to a scenario with a low UV scale in the 5D model, several orders of magnitude below the Planck scale. In the previous chapter we discussed these intermediate scales and showed that they also allow for heavier top-partners and reduced fine-tuning in the Higgs potentials of these holographic composite Higgs scenarios. Note that while performing this analysis we assume that the radion is heavy enough such that it does not significantly affect the phenomenology of the KK graviton.

In the section 4.1 we will review some of the work on KK gravitons and how the first graviton KK mode can be made lighter than the KK spin-1 states. In the section 4.2 we will discuss the specifics of the model, giving explicit expressions for the couplings of the KK graviton, the branching fractions to SM particles, and the experimental bounds that our model must remain within. And finally in section 4.3 we will discuss the phenomenology of the KK graviton, detailing the parameters in the model and how we can fix a subset of them to reproduce the diphoton cross-section and the KK graviton mass at 750 GeV. We show how the branching fractions of the KK graviton to the SM fields change as we lower the UV scale of the model.

4.1 Warped KK gravitons

Let us start by describing the general properties of warped gravitons in RS. In deriving the couplings and 5D properties of the KK gravitons we closely follow the work in [167–170]. To begin, let us consider the following 5D action,

$$S_5 = \int d^4x \int_0^L dy\ \sqrt{|g|} M_5^3 \left(-\frac{\mathcal{R}_5}{2} + 6k^2 \right) + \left(\sqrt{|g|} M_5^3 (k_B \pm \frac{1}{2k} r_{0,L} \mathcal{R}_4) \right) \Big|_0^L \quad (4.1.1)$$

where the RS metric and its fluctuations can be described by,

$$ds^2 = e^{-2ky} \left(\eta_{\mu\nu} + h_{\mu\nu}(x,y) \right) dx^\mu dx^\nu - dy^2. \quad (4.1.2)$$

The co-ordinate y labels the position along the extra dimension, which is bounded by two 3-branes at $y = 0$ (UV) and $y = L$ (IR). The above action is simply the 5D Einstein-Hilbert action with a 5D cosmological constant, and on the branes we have additional Ricci-scalar

terms with localised cosmological constants which we refer to as brane tensions. The bulk cosmological constant and the brane tensions must be precisely chosen so that the background metric is that of the RS model.

The quantity k is known as the curvature constant and parametrises the warping in the bulk of the extra dimension, and M_5 is the UV mass scale in the 5D theory. The $h_{\mu\nu}(x, y)$ fluctuation would correspond to the bulk graviton field. Note that we have neglected fluctuations along the y direction, which would represent the radion dynamics. The radion is a scalar field which arises as fluctuations along the fifth component of the extra dimension. In an exact AdS space this radion is exactly massless, a feature related to the freedom in choosing a length for the extra dimension. If one makes the choice of size for this extra dimension dynamical, in that it is determined by the minima of some potential which perturbs the AdS background, then the radion acquires a mass which is proportional to this perturbation from AdS. The most popular example of this is the Goldberger-Wise mechanism [10].

One can perform a KK decomposition on the field $h_{\mu\nu}(x, y) = \sum_n f_n^g(y) h_{\mu\nu}^n(x)$, where each Kaluza-Klein mode $h_{\mu\nu}^n(x)$ represents a 4D massive graviton of mass m_n with a 5D profile f_n^g obeying the following eigenvalue equation in the bulk,

$$\partial_y^2 f_n^g - 4k\partial_y f_n^g + m_n^2 e^{2ky} f_n^g = 0, \tag{4.1.3}$$

where the mass m_n of the n^{th} KK mode is of the order $M_{KK} \equiv ke^{-kL}$.

Turning to the boundary terms in eq. (4.1.1), k_B is a brane tension, whose effect is to compensate the negative bulk cosmological constant k. The Ricci scalar terms on the branes proportional to $r_{0,L}$ imply brane kinetic terms (BKTs) for the graviton modes (and the radion's). These BKTs result in modifications to the boundary conditions of the 5D profiles of on-shell 4D graviton modes,

$$\left(k\partial_y f_n^g + r_0 m_n^2 f_n^g\right)\Big|_0 = 0 \tag{4.1.4}$$

$$\left(e^{-2kL} k\partial_y f_n^g - r_L m_n^2 f_n^g\right)\Big|_L = 0. \tag{4.1.5}$$

The boundary conditions along with the eigenvalue equation permit a flat massless graviton zero mode. However, when we lower the UV scale of the model to below the Planck scale the interaction strength of this graviton will become larger than is observed in our universe. Thus 4D gravity will not be correctly reproduced by the model. If one imposes a Dirichlet boundary condition $\left(f_n^g(y)\Big|_{brane} = 0\right)$ for the profiles on either brane, the graviton zero mode would not be present, leading to an effective theory with no dynamical 4D gravity. Another option, as discussed in section 3.2.4, is to allow the UV

BKT for the gravitons to be very large [129]. This will suppress the interaction strength of the zero mode graviton such that it correctly reproduces 4D gravity, while acting like a boundary mass term for the KK gravitons. The phenomenology of the KK gravitons discussed in this chapter is independent of whether we use a Dirichlet UV boundary condition or have a large UV BKT.

The general solution to eq. (4.1.3) is

$$f_n^g = \frac{e^{2ky}}{N_n^{1/2}} \left(J_2 \left(z_n e^{k(y-L)} \right) + \alpha_n Y_2 \left(z_n e^{k(y-L)} \right) \right) \tag{4.1.6}$$

where $z_n = \frac{m_n}{M_{KK}}$. The value of α_n and m_n is fixed by the boundary conditions and N_n by the normalisation condition. In this work we will consider two cases,

(i) Mixed boundary conditions on the UV and IR branes (Eqs. 4.1.4). Applying the UV boundary conditions we find

$$\alpha_n^{(i)} = -\frac{J_1(z_n') + r_0 z_n' J_2(z_n')}{Y_1(z_n') + r_0 z_n' Y_2(z_n')} \tag{4.1.7}$$

where $z_n' = m_n/k = e^{-kL} z_n$.

(ii) Dirichlet boundary condition on the UV brane, and a mixed boundary condition on the IR brane. The UV boundary conditions lead to

$$\alpha_n^{(ii)} = -\frac{J_2(z_n')}{Y_2(z_n')} \tag{4.1.8}$$

Case (i) exhibits a massless graviton, whereas case (ii) does not. Also note that when $m_n \neq 0$, one can map solutions of case (i) and (ii) by taking the limit of $r_0 \to \infty$ as a Dirichlet boundary condition is just a limiting case of mixed boundary conditions. Therefore, when the 4D modes are on-shell, a large BKT has a similar effect as a localised mass term for the KK modes.

The values of the masses, m_n, are fixed by applying the IR boundary condition. Since we consider the same IR boundary conditions for both cases, the masses of the lowest lying modes are approximately the same in both cases. The condition imposed on the IR boundary is as follows,

$$J_1(z_n) - r_L z_n J_2(z_n) = -\alpha_n^{(i)} \left(Y_1(z_n) - r_L z_n Y_2(z_n) \right) \ , \tag{4.1.9}$$

where in case (ii) we would set $r_0 = 0$, and there would be additional terms suppressed by m_n/k which one can neglect.

The $Y_a(x)$ function diverges at $x \to 0$ hence the terms $\sim Y_1(z_n')$ dominate. With no IR BKT, the masses of the lowest lying modes are then approximately given by the zeroes

of $J_1(z_n)$, namely 3.8, 7, 10.2, 13.3 in units of M_{KK}. In contrast, the KK masses of bulk spin-1 fields are given by the zeroes of $J_0(z_n)$, i.e. 2.4, 5.5, 8.7 and so on. This pattern can be altered with non-zero BKTs for either the graviton or the spin-1 fields, but here for simplicity we only consider the BKT for the graviton.

For large values of r_L, one can expand the Bessel functions in the IR boundary condition and obtain the following approximate solution for the lightest massive mode,

$$m_g \simeq \frac{2M_{KK}}{\sqrt{r_L}}. \tag{4.1.10}$$

Thus for increasing values of r_L, one can suppress the lightest spin-2 mode and make it lighter than the spin-1 modes.

To completely fix the integration constants in the 5D profile we impose the normalisation of the graviton kinetic terms,

$$\frac{M_5^3}{k}\int_0^L dy\; e^{-2ky} f_n^g f_m^g \left(k + r_0\delta(y) + r_L\delta(y-L)\right) = 4\delta_{mn}. \tag{4.1.11}$$

We find that in case (i) the normalised zero mode solution is $f_0 = 2/M_P$ where,

$$M_{Pl}^2 = \frac{M_5^3}{k}\left(1 - e^{-2kL} + r_0 + e^{-2kL} r_L\right) \tag{4.1.12}$$

is the effective 4D Planck mass and determines the scale of the 4D gravity. Remember that in case (ii), there is no graviton zero mode, hence no meaning of a scale of gravity in the effective theory.

Before continuing, it is worth discussing a possible issue which arises in this scenario. Having such a large BKT on the IR brane for the graviton induces a negative kinetic term for the radion, revealing an instability in the model. This has also been discussed in [170]. However, as recently pointed out in [171], this feature can be avoided if one allows for a particular form of gravity BKT which breaks 5D Lorentz invariance while preserving the 4D symmetry. In our work we will assume such a mechanism is in place to prevent the appearance of the ghost-like radion state.

In the following sections we will study the phenomenology of a light KK graviton in the Little Randall-Sundrum model, with the focus of incorporating this resonance within the composite Higgs scenario without violating experimental constraints arising from LHC searches or electroweak precision measurements. In the holographic interpretation of such a scenario one would expect a 4D strongly interacting gauge theory which confines at the TeV scale, producing the Higgs and a 750 GeV spin-2 state as composites.

4.2 Production and decay of the little graviton

In the following, we consider an extra-dimensional set-up with all the SM fields propagating in the bulk, along with an enlarged bulk custodial gauge symmetry $SU(2)_L \times SU(2)_R \times U(1)_X$. The SM gauge fields exhibit flat zero mode profiles, whereas any non-SM gauge fields are given Dirichlet boundary conditions on the UV brane and thus do not have zero modes. On the other hand, massless (before electroweak symmetry breaking) SM fermions and Higgs can be localised anywhere in the 5D bulk using 5D mass parameters. The profiles of these fields can be written as

$$f_a = \sqrt{\frac{2ak}{1 - e^{-2akL}}} e^{-aky} \tag{4.2.1}$$

where the kinetic terms of these fields are normalised to 1, i.e. $\int_0^L dy\ f_a^2 = 1$, and $a = (a_h, a_q, a_{tr}, a_{br})$ are the 5D mass/localisation parameters for the Higgs and the third generation quarks. We assume that the lighter fermions are localised in the UV and for the bulk gauge fields we simply take $a = 0$.

A special case is given by $a_h = -1$, i.e. the couplings describe those of a holographic composite Higgs model. In this class of models, one requires an IR localised right-handed top quark in order to trigger EWSB, corresponding to $a_{tr} < 0$. Note that when the Higgs and the top are localised in the IR, there are bounds from EWPOs and the direct detection of spin-1 KK modes that we must take into account [3,25,86,172,173]. To avoid these constraints we assume that $M_{KK} \geq 1$ TeV, implying that the lightest spin-1 states will be $\gtrsim 2.5$ TeV. Then, fixing the lightest KK graviton mass to 750 GeV, implies that $r_L \geq 64/9 \simeq 7.1$.

The graviton interactions to SM particles are given by dimension-five operators which we will normalize to the electroweak scale v for convenience. The specific expressions of these operators can be found elsewhere in the literature, e.g. [174]. One can then compute the partial decay widths of the graviton, which we will denote by $X_{\mu\nu}$, to the

SM fields [170, 174],

$$\begin{aligned}
\Gamma(X \to gg) =& \frac{c_g^2 m_X^3}{10\pi v^2} \ , \ \Gamma(X \to \gamma\gamma) = \frac{c_{\gamma\gamma}^2 m_X^3}{80\pi v^2} \\
\Gamma(X \to hh) =& \frac{c_h^2 m_X^3}{960\pi v^2}(1-4r_h)^{5/2} \\
\Gamma(X \to f\bar{f}) =& \frac{N_c(c_{fl}^2 + c_{fr}^2) m_X^3}{320\pi v^2}(1-4r_f)^{3/2}(1+8r_f/3) \\
\Gamma(X \to ZZ) =& \frac{m_X^3}{80\pi v^2}\sqrt{1-4r_Z}\left(c_{ZZ}^2 + \frac{c_h^2}{12} + \frac{r_Z}{3}\left(3c_h^2 - 20c_h c_{ZZ} - 9c_{ZZ}^2\right)\right. \\
& \left. +2\frac{r_Z^2}{3}\left(7c_h^2 + 10c_h c_{ZZ} + 9c_{ZZ}^2\right)\right) \\
\Gamma(X \to WW) =& \frac{m_X^3}{40\pi v^2}\sqrt{1-4r_W}\left(c_W^2 + \frac{c_h^2}{12} + \frac{r_W}{3}\left(3c_h^2 - 20c_h c_W - 9c_W^2\right)\right. \\
& \left. +2\frac{r_W^2}{3}\left(7c_h^2 + 10c_h c_W + 9c_W^2\right)\right) \\
\Gamma(X \to Z\gamma) =& \frac{c_{Z\gamma}^2 m_X^3}{40\pi v^2}(1-r_Z)^3\left(1 + \frac{r_Z}{2} + \frac{r_Z^2}{6}\right)
\end{aligned} \tag{4.2.2}$$

where $c_{\gamma\gamma} = s_\theta^2 c_W + c_\theta^2 c_B$, $c_{ZZ} = c_\theta^2 c_W + s_\theta^2 c_B$, $c_{Z\gamma} = s_\theta c_\theta (c_W - c_B)$, $r_i = (m_i/m_X)^2$, and $m_X = 750$ GeV is the lightest KK graviton mass. The precise values of the Wilson coefficients, c_i, depend on the particular model, i.e. they depend on k, M_5, M_{KK}, the localisation of the bulk field, and on the graviton BKTs. To be precise, they are given by the overlap integral of the KK graviton profile and the profile of the particular SM field,

$$c_a = \frac{v}{2}\int_0^L f_a^2 f_1^g dy. \tag{4.2.3}$$

The value of these constants are approximately independent of whether one imposes a Neumann or Dirichlet boundary condition on the UV brane for the graviton. The value of c_a for massless gauge fields is a special case, for flat 5D profiles the integral in eq. (4.2.3) approaches a limit where $c_a \sim \frac{1}{kL}$. Therefore, varying kL could significantly alter the production of the KK graviton via gluon fusion and its decay in the diphoton channel.

Assuming that gluon fusion is the dominant production mechanism, we can approximate the production cross-section of the KK graviton with the expression [170, 175–178],

$$\sigma_{prod}(gg \to X) \simeq (1.2 \times 10^4) c_g^2 \text{ pb}. \tag{4.2.4}$$

In order to get a cross-section of $\tilde{x}$ fb for the $X \to \gamma\gamma$ final state, one would require,

$$c_g^2 c_{\gamma\gamma}^2 \frac{m_X}{\Gamma_{tot}} \simeq (2.25 \times 10^{-7})\tilde{x}, \tag{4.2.5}$$

where Γ_{tot} is the total width of the KK graviton. In this scenario one only needs to look at $\Gamma(X \to ff)/\Gamma(X \to \gamma\gamma)$ (with ff some final state) to determine whether or not these

predictions are in contradiction with existing bounds from Run 1 and 2 LHC data. The current upper bounds on these ratios are [179–184],

	ZZ	WW	$Z\gamma$	hh	$t\bar{t}$
$R_{ff} = \frac{\Gamma(X\to ff)}{\Gamma(X\to\gamma\gamma)}$	10	40	6	40	400

Table 4.1

Since the transverse components of the gauge fields are flat, one automatically obtains that, $c_g = c_{\gamma\gamma} = c_W = c_B$. This can only be altered if we include BKTs for the gauge fields [170], however one must be careful as these can alter the tree-level corrections to the electroweak precision observables.

4.3 A little graviton and a composite Higgs

We are primarily interested in the scenarios in which the Higgs arises as the fifth component of a 5D gauge field. In the holographic interpretation of this the Higgs would be a composite pseudo Goldstone boson of a strongly interacting gauge sector, the same sector which gives rise to a spin-2 composite state with a mass of 750 GeV. In this case the Higgs localisation is fixed to $a_h = -1$, and an IR localised right-handed top is required in order to achieve electroweak symmetry breaking [1]. In [170] it was shown that with $k \sim 10^{16}$ GeV, this scenario could not be realized with only the graviton field experiencing BKTs. Here we investigate lowering the UV scale, without introducing any additional brane terms which could lead to issues with EWPOs.

To ensure we have the lightest KK graviton at 750 GeV, we trade the IR BKT for the resonance mass and the scale M_{KK}

$$r_L = \left(\frac{2M_{KK}}{m_X}\right)^2. \tag{4.3.1}$$

We can then approximate expression for c_a for the flat 5D profiles as

$$c_{flat} \simeq \left(\frac{k}{M_5}\right)^{3/2} \frac{m_X v}{M_{KK}^2} \frac{1}{8kL}, \tag{4.3.2}$$

which shows how lowering the KK scale or the ratio k/M_5 leads to a global increase in the couplings, whereas lowering kL only significantly affects couplings to flat profiles such as the photon and the gluon.

[1] Although one could consider non-minimal composite Higgs scenarios where electroweak symmetry breaking does not rely primarily on the top, e.g. see-saw composite Higgs [126, 185].

The model parameters are therefore the 5D localisations, M_{KK}, r_L, $\Omega = e^{kL}$, and k/M_5, such that $M_5\Omega^{-1} \sim k\Omega^{-1} \sim \mathcal{O}$ (TeV). We fix $M_{KK} = 1.2$ TeV which leads to a safe value for the spin-1 resonance mass ($m_{KK}^{W',Z'} \sim 2.9$ TeV). As mentioned before, we use r_L to set the lightest KK graviton mass. The value of k/M_5 modulates the signal strength $\sigma(pp \to X \to \gamma\gamma)$, as the diphoton cross-section is $\sim 1/\Gamma_{tot} \sim (M_5/k)^3$.

At the end of the day, we only have Ω and the 5D localisations to fit to the data. In each scenario we will fix the 5D localisations, vary Ω incrementally, and correct k/M_5 each time in order to keep the diphoton cross-section constant, which we will set to a value of 5 fb as a ballpark figure. We describe some of the different scenarios below.

- *Composite Higgs scenario with IR top* ($a_h = -1$, $a_{ql} = 0$, $a_{tr} = -0.3$)
  With a large UV scale the model is ruled out in the $t\bar{t}$, hh, WW and ZZ channels. However at $k \sim 10^8$ TeV the $t\bar{t}$ channel is within current constraints, whereas the hh cross-section is still too large until $\sim 10^8$ TeV. The most problematic are the WW and ZZ channels, which are not within current constraints until $k \sim M_5 \sim 10^4$ and 10^3 TeV, respectively. Thus the composite Higgs models are consistent with this scenario when the UV scale is at ~ 1000 TeV.

- *Flat Higgs and top* ($a_h = 0$, $a_{ql} = 0$, $a_{tr} = 0$)
  This scenario is within constraints at $k \sim M_{Pl}$, and the branching ratios do not change substantially as one lowers the UV scale, while keeping the diphoton rate fixed. Thus this scenario is a consistent model able to incorporate 4D gravity, however it is not a composite Higgs scenario since the Higgs profile is flat.

- *Composite Higgs scenario with very IR top* ($a_h = -1$, $a_{ql} = 0$, $a_{tr} = -3$)
  This time the $t\bar{t}$ channel is only within constraints when $k \sim 10^4$ TeV, however the WW and ZZ channels are still the most constraining. This scenario is still within the experimental constraints at $k \sim M_5 \sim 1000$ TeV. The very IR localised top is not excluded by direct searches due to the large $t\bar{t}$ background in this mass region. One consequence of a top further in the IR is that one can obtain a larger total width than in the previous cases.

The results for the first scenario are presented in figure 4.1, and the numerical results from the composite Higgs scenarios can be seen explicitly in tables 4.2 and 4.3. Note that R_{WW}, R_{ZZ} and R_{hh} do not change between the two tables, since their 5D localisations are kept constant. It is also important to note that the limiting factor, or the reason for requiring $k \sim 1000$ TeV, is solely due to the Higgs localisation. Not only does an

IR Higgs increase the coupling to the Higgs, but it also increases the couplings to the longitudinal gauge bosons, and these channels are tightly constrained by experimental data. When one lowers the UV scale, the couplings of the KK graviton to the transverse components increases, reducing the size of the WW and ZZ branching ratios relative to the $\gamma\gamma$ branching ratio. Although we have kept M_{KK} fixed in these tables, we checked that varying this parameter does not change the ratios R_{ff}, as all the decay widths are equally suppressed by $1/M_{KK}^2$. Once we fix k/M_5 to reproduce the diphoton cross-section, a shift in M_{KK} has no effect on the total width or the production cross-section either. From the data, we can also see that when the UV scale is low the model not only produces acceptable decay rates in all channels, but it also has an acceptable value for the ratio k/M_5. This ratio is constrained by the assumption that higher derivative gravity terms in the bulk can be neglected, and an acceptable bound is taken to be $k/M_5 \lesssim 2$ [168]. In [170] where a BKT for the hypercharge field was used instead of a low UV scale, much larger values of k/M_5 were required. The reason for this is that as we lower the UV scale, we increase the coupling to photons and gluons, thus we also increase the production cross-section. With a hypercharge BKT one can increase the photon coupling but additional gluon BKTs would be required to increase the production cross-section, and in the absence of these additional gluon BKTs one requires a large value of k/M_5.

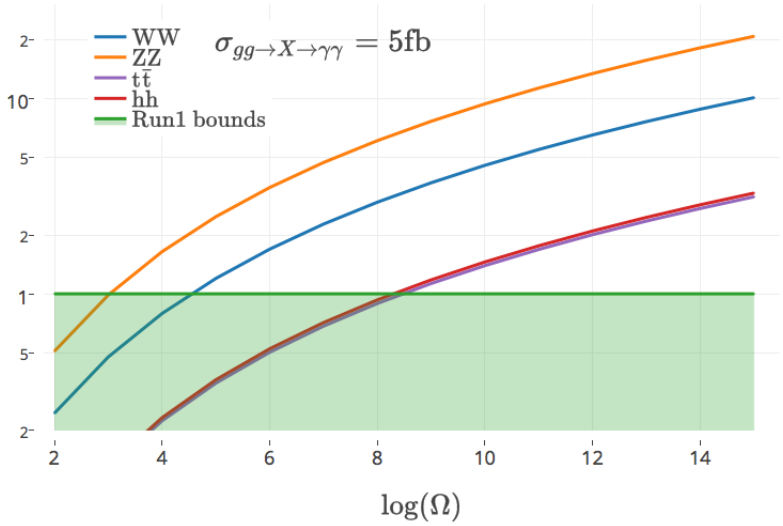

Figure 4.1: In this plot we show the ratio of different decay rates of the 750 GeV KK graviton vs the bound on this rate from table 4.1. The 5D parameters are those from the 'Composite Higgs scenario with IR top', thus corresponding to the data in table 4.2. The shaded region indicates areas of the parameter space in which decays into an individual channel are within the bounds.

Table 4.2: Composite Higgs scenario with IR top, ($a_h = -1$, $a_{ql} = 0$, $a_{tr} = -0.3$). The k/M_5 ratio is altered at each iteration to keep $\sigma(pp \to X \to \gamma\gamma) = 5$ fb.

$\log(\Omega)$	k/M_5	$\sigma_{prod}(pp \to X)$ [pb]	R_{WW}	R_{ZZ}	$R_{t\bar{t}}$	R_{hh}	Γ_{tot}
2	1.19	0.25	9.8	5.1	23	2.3	0.03
3	1.94	0.47	19	9.9	51	5.2	0.1
4	2.78	0.78	32	16	90	9.3	0.28
5	3.70	1.18	48	25	140	15	0.65
6	4.69	1.67	68	35	201	21	1.3
7	5.74	2.25	91	47	274	29	2.3
8	6.83	2.91	118	61	357	37	3.9
9	7.98	3.66	148	76	452	47	6.2
10	9.17	4.50	182	94	558	58	9.4
11	10.40	5.43	219	113	675	70	14
12	11.67	6.45	259	134	803	84	19
13	12.98	7.55	304	156	942	98	26
14	14.32	8.74	351	181	1092	114	35
15	15.69	10.02	403	207	1254	131	46

Table 4.3: Composite Higgs scenario with very IR top, ($a_h = -1$, $a_{ql} = 0$, $a_{tr} = -3$). The k/M_5 ratio is altered at each iteration to keep $\sigma(pp \to X \to \gamma\gamma) = 5$ fb.

$\log(\Omega)$	k/M_5	$\sigma_{prod}(pp \to X)$ [pb]	R_{WW}	R_{ZZ}	$R_{t\bar{t}}$	R_{hh}	Γ_{tot}
2	1.50	0.50	9.8	5.1	72	2.3	0.11
3	2.51	1.03	19	9.9	162	5.2	0.49
4	3.65	1.77	32	16	288	9.3	1.5
5	4.90	2.73	48	25	449	15	3.4
6	6.22	3.90	68	35	647	21	7.0
7	7.62	5.28	91	47	880	29	13
8	9.10	6.87	118	61	1149	37	22
9	10.64	8.68	148	76	1454	47	35
10	12.24	10.69	182	94	1795	58	53
11	13.89	12.92	219	113	2172	70	77
12	15.56	15.36	259	134	2585	84	109
13	17.34	18.01	304	156	3034	98	150
14	19.14	20.87	351	181	3519	114	201
15	20.98	23.95	403	207	4039	131	265

Chapter 5

Conclusions

In the first part of this thesis we have revisited the scenario of a bulk Higgs in warped extra dimensions, without assuming deviations from AdS space or imposing a custodial symmetry. Our aim was to investigate the robustness of bounds on the KK scale from electroweak observables and modifications of SM Yukawa couplings. We then discuss prospects for observing new physics at future collider experiments.

Performing a standard electroweak precision analysis, we confirm that a bulk Higgs rather than a brane Higgs brings down the limit on the KK scale, which in this chapter we take to be mass of the lightest vector resonance, from about 15 TeV to about 8 TeV. A bulk Higgs reduces mixing between KK gauge boson excitations and the SM particles after electroweak symmetry breaking. The Higgs, being a bulk field, also has KK excitiations which contribute to gauge boson masses etc., but their impact is unobservable for the foreseeable future. However, deviations from the SM values of the HZZ and HWW couplings at the sub-percent level will be induced by KK gauge boson mixing. These effects will be very difficult to see at ILC, but TLEP with a predicted sensitivity of better than 0.2% could detect them.

We then include into the analysis higher dimensional operators which parametrize unknown contributions from a UV completion of our setup. We find that a dimension-8 operator in 5D can have an non-negligible impact on the T parameter. The bound on the KK scale of 8 TeV, derived previously is therefore not robust. We therefore argue that this unknown contribution could bring the KK scale down to at least about 5 TeV. The LHC run at 13 TeV could then discover KK resonances in the simple scenario presented here.

Finally, we investigate whether additional bounds on the KK scale can be derived from deviations in fermion Yukawa couplings, in particular for the top quark. We find

that even with a KK scale of only 5 TeV, the enhancements in the top Yukawa coupling can be larger than 10%. However there are areas of parameter space where this enhancement can be much smaller and hence this will not generally lead to tension with observed Higgs production at current experiments. Such a tension would require large values of the associated 5D Yukawa coupling. In the future it will be interesting to look for Yukawa deviations for the top quark at the high-luminosity LHC. The enhancements in the bottom and tau Yukawa couplings can also be as large as a few percent, making this detectable at ILC and TLEP. Furthermore, top Yukawa coupling misalignment should be taken into account in models where top loops induce electroweak symmetry breaking, e.g. warped geometry realisations of composite Higgs models [16–18].

As is well known, models of the type presented here often generate large flavour and CP-violation from KK exchange. These may induce bounds on the KK scale which are much more stringent than the ones we have considered. However, one should bare in mind that these flavour bounds depend on how the fermion mass pattern is generated, and can be reduced or almost avoided by flavour symmetries.

So we conclude that, even without an enlarged gauge symmetry, a bulk Higgs in pure AdS space opens the possibility to discover KK resonances during run 2 of the LHC.

In the second part of the thesis we addressed the question of whether or not a light Higgs implies light top partners in the Minimal Composite Higgs Model (MCHM_5). The experimental constraints on the detection of top partners can be avoided by increasing the scale M_{KK}, but this is at the cost of a severe fine-tuning. Attempts at realising the MCHM_5 model without light top partners and large fine-tuning have been primarily focussed on the fermion sector: 4D approaches include a different embedding of the third generation of quarks in representations of SO(5); holographic realisations include leptonic contributions to the Higgs potential. Here we propose an alternative method to alleviate the tension: we show that if the degree of composite mixing in the multiplets is reduced, the mass of the lightest top parters can be increased, without increasing the compositeness scale M_{KK}. To maintain a light Higgs, the cutoff in the 5D model (measured by $\ln\Omega$) is reduced. Interestingly, we find that the Higgs mass is proportional to the mass gap between the 7/6 and 2/3 charged top partners, in agreement with what is found in 4D explicit models [64, 69].

Since heavier top partners might naively lead one to expect more fine-tuning, we calculated this and found that as we lower $\ln(\Omega)$ the minimum value of the Barbieri-Giudici parameter tends to decrease. This is particularly nice, since we now know that

increasing M_{KK} and lowering $\ln(\Omega)$ both allow for heavier top partners and lower values of s_h, however only lowering $\ln(\Omega)$ does not lead to an increased fine-tuning. This result also correlates well with the 4D explicit realisations, where the Higgs mass and the fine-tuning are proportional to the coupling between the top partners and the Higgs, a quantity which is controlled by $\ln(\Omega)$ in the holographic models. We find that, with spin-1 states at ~ 2.5 TeV and the left-handed top localised away from the IR, the fine-tuning is minimised when the lightest top partner is above 1 TeV.

With an eye to the next LHC run we discuss the phenomenology of this version of the MCHM$_5$. In anticipation of improved LHC constraints on the lightest top Yukawa coupling, we show that a deviation from the relation between IR brane masses $m_u = -1/M_u$ can reduce or enhance the composite Higgs prediction for y_t as derived from symmetry arguments alone. The deviation from the Standard Model is captured in the parameters κ_V and κ_T, which allow for a comparison with the ATLAS data. In particular, it is seen that relaxing the brane mass relation may relieve the tension slightly by increasing the predicted coupling.

We further discussed the expected phenomenology of the top partner states in future searches. Testing the relation between the Higgs and top partner masses as a function of s_h, we find that the masses scale approximately linearly, as expected, with a slight deviation for the (2/3) exotic state.

In the last part of this thesis we studied a possible explanation of the infamous 750 GeV diphoton resonance (now shown to be a statistical fluctuation) within the framework of composite Higgs models. We studied the possibility that this excess could have been produced by a composite spin-2 resonance, where the bound state arises from the same strong dynamics that produces the composite Higgs. To study this scenario we used the same 5D techniques developed in the previous chapters. We found that the most economical way to successfully explain this excess, i.e. keeping effects of vector resonances and their localized kinetic terms under control, is to lower the UV scale of the 5D theory. In this framework (Little RS, intermediate scales), we focused on the scenario in which the 5D model describes a composite Higgs setup in 4D, and showed that the UV scale is required to be $\sim \mathcal{O}(1000$ TeV) to explain why the resonance would show up in the diphoton channel before it did in the WW and ZZ channels. Ultimately, the reason for requiring such a low UV scale is the Higgs profile localisation near the IR, which increases the KK graviton couplings to the Higgs and to the longitudinal components of the gauge bosons. Lowering the UV scale leads to an increase in the graviton coupling to

the transverse components of the gauge fields. We would like to note that although we have only considered the KK graviton phenomenology in this work, similar effects should be present in the phenomenology of the radion in these set-ups [186]. In the end we have shown that the once significant diphoton excess is compatible with a model in which strong dynamics at the TeV scale gives rise to the Higgs and a 750 GeV spin-2 state as composites of the underlying gauge theory.

Lastly we would like to comment on the predictions made by this model. By counting free parameters we see that, at least in the composite Higgs scenario, we can only vary Ω, M_{KK}, and the top localisation. Ω is strongly constrained by the Run1 and 2 limits from searches of heavy resonances to WW and ZZ. The top localisation does not affect R_{WW}, R_{ZZ} or R_{hh}, and shifting M_{KK} does not affect any of the R_{ff} ratios. Thus these R_{ff} values are definite predictions of the model. Some ways that these predictions might be affected are if the bulk SM gauge fields have non-zero BKTs, or if there are deformations to the AdS background geometry such as in [78]. Despite the diminished significance of this excess after the analysis of more data, the model building work done here demonstrates that these 5D models can still produce light new physics which may have yet evaded searches at the LHC, while remaining within other constraints set by LEP.

Through the work in this thesis we have attempted to illuminate some interesting scenarios for models with warped extra dimensions and composite Higgs BSM sectors. The focus of these studies has been on electroweak precision observables in non-custodial warped models, corrections to the top Yukawa coupling in warped models and holographic composite Higgs models, and the effect of intermediate scales on holographic composite Higgs models, and KK graviton phenomenology. We believe that the most important results from this work are that holographic composite Higgs models with a lower UV cutoff can significantly alleviate tension with top partner bounds from the LHC, while at the same time reduce the couplings of light new physics to SM particles.

.1 $SO(5)$ generators

The basis of $SO(5)$ generators we use is shown below,

$$T_L^1 = -\frac{i}{2}\begin{pmatrix} 0 & 0 & 0 & 1 & 0 \\ 0 & 0 & 1 & 0 & 0 \\ 0 & -1 & 0 & 0 & 0 \\ -1 & 0 & 0 & 0 & 0 \\ 0 & 0 & 0 & 0 & 0 \end{pmatrix}, \quad T_L^2 = -\frac{i}{2}\begin{pmatrix} 0 & 0 & -1 & 0 & 0 \\ 0 & 0 & 0 & 1 & 0 \\ 1 & 0 & 0 & 0 & 0 \\ 0 & -1 & 0 & 0 & 0 \\ 0 & 0 & 0 & 0 & 0 \end{pmatrix},$$

$$T_L^3 = -\frac{i}{2}\begin{pmatrix} 0 & 1 & 0 & 0 & 0 \\ -1 & 0 & 0 & 0 & 0 \\ 0 & 0 & 0 & 1 & 0 \\ 0 & 0 & -1 & 0 & 0 \\ 0 & 0 & 0 & 0 & 0 \end{pmatrix}, \quad T_R^1 = -\frac{i}{2}\begin{pmatrix} 0 & 0 & 0 & -1 & 0 \\ 0 & 0 & 1 & 0 & 0 \\ 0 & -1 & 0 & 0 & 0 \\ 1 & 0 & 0 & 0 & 0 \\ 0 & 0 & 0 & 0 & 0 \end{pmatrix},$$

$$T_R^2 = -\frac{i}{2}\begin{pmatrix} 0 & 0 & -1 & 0 & 0 \\ 0 & 0 & 0 & -1 & 0 \\ 1 & 0 & 0 & 0 & 0 \\ 0 & 1 & 0 & 0 & 0 \\ 0 & 0 & 0 & 0 & 0 \end{pmatrix}, \quad T_R^3 = -\frac{i}{2}\begin{pmatrix} 0 & 1 & 0 & 0 & 0 \\ -1 & 0 & 0 & 0 & 0 \\ 0 & 0 & 0 & -1 & 0 \\ 0 & 0 & 1 & 0 & 0 \\ 0 & 0 & 0 & 0 & 0 \end{pmatrix}$$

$$T^{\hat{1}} = -\frac{i}{\sqrt{2}}\begin{pmatrix} 0 & 0 & 0 & 0 & 1 \\ 0 & 0 & 0 & 0 & 0 \\ 0 & 0 & 0 & 0 & 0 \\ 0 & 0 & 0 & 0 & 0 \\ -1 & 0 & 0 & 0 & 0 \end{pmatrix}, \quad T^{\hat{2}} = -\frac{i}{\sqrt{2}}\begin{pmatrix} 0 & 0 & 0 & 0 & 0 \\ 0 & 0 & 0 & 0 & 1 \\ 0 & 0 & 0 & 0 & 0 \\ 0 & 0 & 0 & 0 & 0 \\ 0 & -1 & 0 & 0 & 0 \end{pmatrix},$$

$$T^{\hat{3}} = -\frac{i}{\sqrt{2}}\begin{pmatrix} 0 & 0 & 0 & 0 & 0 \\ 0 & 0 & 0 & 0 & 0 \\ 0 & 0 & 0 & 0 & 1 \\ 0 & 0 & 0 & 0 & 0 \\ 0 & 0 & -1 & 0 & 0 \end{pmatrix}, \quad T^{\hat{4}} = -\frac{i}{\sqrt{2}}\begin{pmatrix} 0 & 0 & 0 & 0 & 0 \\ 0 & 0 & 0 & 0 & 0 \\ 0 & 0 & 0 & 0 & 0 \\ 0 & 0 & 0 & 0 & 1 \\ 0 & 0 & 0 & -1 & 0 \end{pmatrix}. \tag{.1.1}$$

Bibliography

[1] **ATLAS** Collaboration, G. Aad et al., *Observation of a new particle in the search for the Standard Model Higgs boson with the ATLAS detector at the LHC*, *Phys. Lett.* **B716** (2012) 1–29, [arXiv:1207.7214].

[2] **CMS** Collaboration, S. Chatrchyan et al., *Observation of a new boson at a mass of 125 GeV with the CMS experiment at the LHC*, *Phys. Lett.* **B716** (2012) 30–61, [arXiv:1207.7235].

[3] B. M. Dillon and S. J. Huber, *Non-Custodial Warped Extra Dimensions at the LHC?*, arXiv:1410.7345.

[4] D. Croon, B. M. Dillon, S. J. Huber, and V. Sanz, *Exploring holographic Composite Higgs models*, arXiv:1510.08482.

[5] B. M. Dillon and V. Sanz, *A Little KK Graviton at 750 GeV*, arXiv:1603.09550.

[6] T. A. collaboration, *Search for resonances decaying to photon pairs in 3.2 fb^{-1} of pp collisions at $\sqrt{s}$ = 13 TeV with the ATLAS detector*, *ATLAS-CONF-2015-081* (2015).

[7] **CMS** Collaboration, C. Collaboration, *Search for new physics in high mass diphoton events in proton-proton collisions at 13TeV*, *CMS-PAS-EXO-15-004* (2015).

[8] **CMS** Collaboration, C. Collaboration, *Search for resonant production of high mass photon pairs using* $12.9\,\mathrm{fb}^{-1}$ *of proton-proton collisions at* $\sqrt{s} = 13$ TeV *and combined interpretation of searches at 8 and 13 TeV*, .

[9] L. Randall and R. Sundrum, *A large mass hierarchy from a small extra dimension*, *Phys.Rev.Lett.* **83** (1999) 3370–3373, [hep-ph/9905221].

[10] W. D. Goldberger and M. B. Wise, *Modulus stabilization with bulk fields*, *Phys.Rev.Lett.* **83** (1999) 4922–4925, [hep-ph/9907447].

[11] N. Arkani-Hamed and M. Schmaltz, *Hierarchies without symmetries from extra dimensions*, *Phys.Rev.* **D61** (2000) 033005, [hep-ph/9903417].

[12] S. J. Huber and Q. Shafi, *Fermion masses, mixings and proton decay in a randall-sundrum model*, *Phys.Lett.* **B498** (2001) 256–262, [hep-ph/0010195].

[13] T. Gherghetta and A. Pomarol, *Bulk fields and supersymmetry in a slice of ads*, *Nucl.Phys.* **B586** (2000) 141–162, [hep-ph/0003129].

[14] M. A. Luty and R. Sundrum, *Radius stabilization and anomaly mediated supersymmetry breaking*, *Phys.Rev.* **D62** (2000) 035008, [hep-th/9910202].

[15] C. Burgess, P. G. Camara, S. de Alwis, S. Giddings, A. Maharana, et al., *Warped supersymmetry breaking*, *JHEP* **0804** (2008) 053, [hep-th/0610255].

[16] K. Agashe, R. Contino, and A. Pomarol, *The minimal composite higgs model*, *Nucl.Phys.* **B719** (2005) 165–187, [hep-ph/0412089].

[17] R. Contino, T. Kramer, M. Son, and R. Sundrum, *Warped/composite phenomenology simplified*, *JHEP* **0705** (2007) 074, [hep-ph/0612180].

[18] R. Contino, *The higgs as a composite nambu-goldstone boson*, hep-ph/1005.4269.

[19] H. Davoudiasl, J. Hewett, and T. Rizzo, *Bulk gauge fields in the randall-sundrum model*, *Phys.Lett.* **B473** (2000) 43–49, [hep-ph/9911262].

[20] S. J. Huber and Q. Shafi, *Higgs mechanism and bulk gauge boson masses in the randall-sundrum model*, *Phys.Rev.* **D63** (2001) 045010, [hep-ph/0005286].

[21] H. Davoudiasl, B. Lillie, and T. G. Rizzo, *Off-the-wall Higgs in the universal Randall-Sundrum model*, *JHEP* **0608** (2006) 042, [hep-ph/0508279].

[22] G. Cacciapaglia, C. Csaki, G. Marandella, and J. Terning, *The Gaugephobic Higgs*, *JHEP* **0702** (2007) 036, [hep-ph/0611358].

[23] S. Chang, J. Hisano, H. Nakano, N. Okada, and M. Yamaguchi, *Bulk standard model in the randall-sundrum background*, *Phys.Rev.* **D62** (2000) 084025, [hep-ph/9912498].

[24] M. E. Peskin and T. Takeuchi, *Estimation of oblique electroweak corrections*, *Phys.Rev.* **D46** (1992) 381–409.

[25] K. Agashe, A. Delgado, M. J. May, and R. Sundrum, *Rs1, custodial isospin and precision tests*, *JHEP* **0308** (2003) 050, [hep-ph/0308036].

[26] M. S. Carena, E. Ponton, J. Santiago, and C. Wagner, *Electroweak constraints on warped models with custodial symmetry*, *Phys.Rev.* **D76** (2007) 035006, [hep-ph/0701055].

[27] S. Casagrande, F. Goertz, U. Haisch, M. Neubert, and T. Pfoh, *The custodial randall-sundrum model: From precision tests to higgs physics*, *JHEP* **1009** (2010) 014, [hep-ph/1005.4315].

[28] A. Falkowski and M. Perez-Victoria, *Electroweak breaking on a soft wall*, *JHEP* **0812** (2008) 107, [arXiv:0806.1737].

[29] J. A. Cabrer, G. von Gersdorff, and M. Quiros, *Warped electroweak breaking without custodial symmetry*, *Phys.Lett.* **B697** (2011) 208–214, [hep-ph/1011.2205].

[30] J. A. Cabrer, G. von Gersdorff, and M. Quiros, *Suppressing electroweak precision observables in 5d warped models*, *JHEP* **1105** (2011) 083, [hep-ph/1103.1388].

[31] J. A. Cabrer, G. von Gersdorff, and M. Quiros, *Warped 5d standard model consistent with ewpt*, *Fortsch.Phys.* **59** (2011) 1135–1138, [hep-ph/1104.5253].

[32] A. Carmona, E. Ponton, and J. Santiago, *Phenomenology of non-custodial warped models*, *JHEP* **1110** (2011) 137, [hep-ph/1107.1500].

[33] M. S. Carena, E. Ponton, T. M. Tait, and C. Wagner, *Opaque branes in warped backgrounds*, *Phys.Rev.* **D67** (2003) 096006, [hep-ph/0212307].

[34] P. R. Archer and S. J. Huber, *Reducing constraints in a higher dimensional extension of the randall and sundrum model*, *JHEP* **1103** (2011) 018, [hep-ph/1010.3588].

[35] P. R. Archer and S. J. Huber, *Electroweak constraints on warped geometry in five dimensions and beyond*, *JHEP* **1010** (2010) 032, [hep-ph/1004.1159].

[36] M. E. Peskin, *Comparison of lhc and ilc capabilities for higgs boson coupling measurements*, hep-ph/1207.2516.

[37] D. Asner, T. Barklow, C. Calancha, K. Fujii, N. Graf, et al., *Ilc higgs white paper*, hep-ph/1310.0763.

[38] H. Baer, T. Barklow, K. Fujii, Y. Gao, A. Hoang, et al., *The international linear collider technical design report - volume 2: Physics*, hep-ph/1306.6352.

[39] L. Linssen, A. Miyamoto, M. Stanitzki, and H. Weerts, *Physics and detectors at clic: Clic conceptual design report*, arXiv:1202.5940.

[40] **CLIC Physics Working Group** Collaboration, E. Accomando et al., *Physics at the clic multi-tev linear collider*, hep-ph/0412251.

[41] **TLEP Design Study Working Group** Collaboration, M. Bicer et al., *First look at the physics case of tlep*, *JHEP* **1401** (2014) 164, [hep-ex/1308.6176].

[42] **CMS Collaboration** Collaboration, *Projected performance of an upgraded cms detector at the lhc and hl-lhc: Contribution to the snowmass process*, arXiv:1307.7135.

[43] *Physics at a High-Luminosity LHC with ATLAS*, *ATLAS Collaboration* (2013) [hep-ex/1307.7292].

[44] F. del Aguila and J. Santiago, *Large top mixing from extra dimensions*, hep-ph/0011143.

[45] G. Panico and A. Wulzer, *Effective action and holography in 5D gauge theories*, *JHEP* **05** (2007) 060, [hep-th/0703287].

[46] T. Gherghetta and A. Pomarol, *A warped supersymmetric standard model*, *Nucl.Phys.* **B602** (2001) 3–22, [hep-ph/0012378].

[47] S. J. Huber and Q. Shafi, *Cosmological constant, gauge hierarchy and warped geometry*, *Phys.Rev.* **D68** (2003) 023503, [hep-ph/0207232].

[48] P. Breitenlohner and D. Z. Freedman, *Positive Energy in anti-De Sitter Backgrounds and Gauged Extended Supergravity*, *Phys.Lett.* **B115** (1982) 197.

[49] A. Azatov, M. Toharia, and L. Zhu, *Higgs Mediated FCNC's in Warped Extra Dimensions*, *Phys.Rev.* **D80** (2009) 035016, [hep-ph/0906.1990].

[50] *Constraints on New Phenomena via Higgs Coupling Measurements with the ATLAS Detector*, *The ATLAS collaboration* (2014) [ATLAS-CONF-2014-010].

[51] A. Delgado and A. Falkowski, *Electroweak observables in a general 5d background*, *JHEP* **0705** (2007) 097, [hep-ph/0702234].

[52] C. Csaki, J. Hubisz, and P. Meade, *Tasi lectures on electroweak symmetry breaking from extra dimensions*, hep-ph/0510275.

[53] Y. Grossman and M. Neubert, *Neutrino masses and mixings in nonfactorizable geometry*, *Phys.Lett.* **B474** (2000) 361–371, [hep-ph/9912408].

[54] S. J. Huber, *Flavor violation and warped geometry*, *Nucl.Phys.* **B666** (2003) 269–288, [hep-ph/0303183].

[55] M. Baak, M. Goebel, J. Haller, A. Hoecker, D. Kennedy, et al., *The electroweak fit of the standard model after the discovery of a new boson at the lhc*, *Eur.Phys.J.* **C72** (2012) 2205, [hep-ph/1209.2716].

[56] S. Fichet and G. von Gersdorff, *Anomalous gauge couplings from composite Higgs and warped extra dimensions*, *JHEP* **1403** (2014) 102, [hep-ph/1311.6815].

[57] P. R. Archer, M. Carena, A. Carmona, and M. Neubert, *Higgs Production and Decay in Models of a Warped Extra Dimension with a Bulk Higgs*, hep-ph/1408.5406.

[58] R. Barbieri, A. Pomarol, R. Rattazzi, and A. Strumia, *Electroweak symmetry breaking after LEP-1 and LEP-2*, *Nucl.Phys.* **B703** (2004) 127–146, [hep-ph/0405040].

[59] H. Davoudiasl, G. Perez, and A. Soni, *The little randall-sundrum model at the large hadron collider*, *Phys.Lett.* **B665** (2008) 67–71, [arXiv:0802.0203].

[60] S. Casagrande, F. Goertz, U. Haisch, M. Neubert, and T. Pfoh, *Flavor Physics in the Randall-Sundrum Model: I. Theoretical Setup and Electroweak Precision Tests*, *JHEP* **0810** (2008) 094, [hep-ph/0807.4937].

[61] A. J. Buras, B. Duling, and S. Gori, *The Impact of Kaluza-Klein Fermions on Standard Model Fermion Couplings in a RS Model with Custodial Protection*, *JHEP* **0909** (2009) 076, [hep-ph/0905.2318].

[62] M. Beneke, P. Moch, and J. Rohrwild, *Muon anomalous magnetic moment and penguin loops in warped extra dimensions*, *Int.J.Mod.Phys.* **A29** (2014) 1444011, [hep-ph/1404.7157].

[63] S. De Curtis, M. Redi, and A. Tesi, *The 4D Composite Higgs*, *JHEP* **04** (2012) 042, [arXiv:1110.1613].

[64] O. Matsedonskyi, G. Panico, and A. Wulzer, *Light Top Partners for a Light Composite Higgs*, *JHEP* **01** (2013) 164, [arXiv:1204.6333].

[65] D. Marzocca, M. Serone, and J. Shu, *General Composite Higgs Models*, *JHEP* **08** (2012) 013, [arXiv:1205.0770].

[66] A. Pomarol and F. Riva, *The Composite Higgs and Light Resonance Connection*, *JHEP* **08** (2012) 135, [arXiv:1205.6434].

[67] G. F. Giudice, C. Grojean, A. Pomarol, and R. Rattazzi, *The Strongly-Interacting Light Higgs*, *JHEP* **06** (2007) 045, [hep-ph/0703164].

[68] C. Anastasiou, E. Furlan, and J. Santiago, *Realistic Composite Higgs Models*, *Phys. Rev.* **D79** (2009) 075003, [arXiv:0901.2117].

[69] G. Panico and A. Wulzer, *The discrete composite higgs model*, *JHEP* **1109** (2011) 135, [arXiv:1106.2719].

[70] A. Azatov and J. Galloway, *Light custodians and higgs physics in composite models*, *Phys.Rev.* **D85** (2012) 055013, [arXiv:1110.5646].

[71] R. Lewis, C. Pica, and F. Sannino, *Light Asymmetric Dark Matter on the Lattice: SU(2) Technicolor with Two Fundamental Flavors*, *Phys. Rev.* **D85** (2012) 014504, [arXiv:1109.3513].

[72] A. Hietanen, R. Lewis, C. Pica, and F. Sannino, *Composite Goldstone Dark Matter: Experimental Predictions from the Lattice*, *JHEP* **12** (2014) 130, [arXiv:1308.4130].

[73] A. Hietanen, R. Lewis, C. Pica, and F. Sannino, *Fundamental Composite Higgs Dynamics on the Lattice: SU(2) with Two Flavors*, *JHEP* **07** (2014) 116, [arXiv:1404.2794].

[74] D. T. Son and M. A. Stephanov, *QCD and dimensional deconstruction*, *Phys. Rev.* **D69** (2004) 065020, [hep-ph/0304182].

[75] J. Erlich, E. Katz, D. T. Son, and M. A. Stephanov, *QCD and a holographic model of hadrons*, *Phys. Rev. Lett.* **95** (2005) 261602, [hep-ph/0501128].

[76] L. Da Rold and A. Pomarol, *Chiral symmetry breaking from five dimensional spaces*, *Nucl. Phys.* **B721** (2005) 79–97, [hep-ph/0501218].

[77] J. Hirn and V. Sanz, *Interpolating between low and high energy QCD via a 5-D Yang-Mills model*, *JHEP* **12** (2005) 030, [hep-ph/0507049].

[78] J. Hirn, N. Rius, and V. Sanz, *Geometric approach to condensates in holographic QCD*, *Phys. Rev.* **D73** (2006) 085005, [hep-ph/0512240].

[79] C. Csaki, C. Grojean, L. Pilo, and J. Terning, *Towards a realistic model of Higgsless electroweak symmetry breaking*, *Phys. Rev. Lett.* **92** (2004) 101802, [hep-ph/0308038].

[80] G. Cacciapaglia, C. Csaki, C. Grojean, and J. Terning, *Oblique corrections from higgsless models in warped space*, *Phys.Rev.* **D70** (2004) 075014, [hep-ph/0401160].

[81] J. Hirn and V. Sanz, *A negative s parameter from holographic technicolor*, *Phys.Rev.Lett.* **97** (2006) 121803, [hep-ph/0606086].

[82] J. Hirn and V. Sanz, *The Fifth dimension as an analogue computer for strong interactions at the LHC*, *JHEP* **03** (2007) 100, [hep-ph/0612239].

[83] R. Contino, Y. Nomura, and A. Pomarol, *Higgs as a holographic pseudoGoldstone boson*, *Nucl. Phys.* **B671** (2003) 148–174, [hep-ph/0306259].

[84] R. Contino, L. Da Rold, and A. Pomarol, *Light custodians in natural composite higgs models*, *Phys.Rev.* **D75** (2007) 055014, [hep-ph/0612048].

[85] P. R. Archer, *Fine Tuning in the Holographic Minimal Composite Higgs Model*, arXiv:1403.8048.

[86] K. Agashe and R. Contino, *The minimal composite higgs model and electroweak precision tests*, *Nucl.Phys.* **B742** (2006) 59–85, [hep-ph/0510164].

[87] G. Panico and A. Wulzer, *The Composite Nambu-Goldstone Higgs*, arXiv:1506.01961.

[88] G. von Gersdorff, E. Pontn, and R. Rosenfeld, *The Dynamical Composite Higgs*, *JHEP* **06** (2015) 119, [arXiv:1502.07340].

[89] M. Low, A. Tesi, and L.-T. Wang, *Twin Higgs mechanism and a composite Higgs boson*, *Phys. Rev.* **D91** (2015) 095012, [arXiv:1501.07890].

[90] R. Barbieri, D. Greco, R. Rattazzi, and A. Wulzer, *The Composite Twin Higgs scenario*, *JHEP* **08** (2015) 161, [arXiv:1501.07803].

[91] H.-C. Cheng, B. A. Dobrescu, and J. Gu, *Higgs mass from compositeness at a multi-TeV scale*, *JHEP* **08** (2014) 095, [arXiv:1311.5928].

[92] J. Barnard, T. Gherghetta, T. S. Ray, and A. Spray, *The Unnatural Composite Higgs*, *JHEP* **01** (2015) 067, [arXiv:1409.7391].

[93] H.-C. Cheng and J. Gu, *Top seesaw with a custodial symmetry, and the 126 GeV Higgs*, *JHEP* **10** (2014) 002, [arXiv:1406.6689].

[94] G. Ferretti, *UV Completions of Partial Compositeness: The Case for a SU(4) Gauge Group*, *JHEP* **06** (2014) 142, [arXiv:1404.7137].

[95] S. De Curtis, M. Redi, and E. Vigiani, *Non Minimal Terms in Composite Higgs Models and in QCD*, *JHEP* **06** (2014) 071, [arXiv:1403.3116].

[96] A. Carmona and M. Chala, *Composite Dark Sectors*, *JHEP* **06** (2015) 105, [arXiv:1504.00332].

[97] **CMS** Collaboration, V. Khachatryan et al., *Search for Vector-Like Charge 2/3 T Quarks in Proton-Proton Collisions at* $\sqrt{s} = 8$ *TeV*, arXiv:1509.04177.

[98] **ATLAS** Collaboration, G. Aad et al., *Search for production of vector-like quark pairs and of four top quarks in the lepton-plus-jets final state in pp collisions at* $\sqrt{s} = 8$ *TeV with the ATLAS detector*, *JHEP* **08** (2015) 105, [arXiv:1505.04306].

[99] A. De Simone, O. Matsedonskyi, R. Rattazzi, and A. Wulzer, *A First Top Partner Hunter's Guide*, *JHEP* **04** (2013) 004, [arXiv:1211.5663].

[100] M. Backovic, T. Flacke, J. H. Kim, and S. J. Lee, *Search Strategies for TeV Scale Fermionic Top Partners with Charge 2/3*, arXiv:1507.06568.

[101] A. Buckley, C. Englert, J. Ferrando, D. J. Miller, L. Moore, M. Russell, and C. D. White, *A global fit of top quark effective theory to data*, arXiv:1506.08845.

[102] J. Serra, *Beyond the Minimal Top Partner Decay*, arXiv:1506.05110.

[103] S. Dawson and E. Furlan, *Yukawa Corrections to Higgs Production in Top Partner Models*, *Phys. Rev.* **D89** (2014), no. 1 015012, [arXiv:1310.7593].

[104] C. Grojean, O. Matsedonskyi, and G. Panico, *Light top partners and precision physics*, *JHEP* **10** (2013) 160, [arXiv:1306.4655].

[105] M. Backovi?, T. Flacke, J. H. Kim, and S. J. Lee, *Boosted Event Topologies from TeV Scale Light Quark Composite Partners*, *JHEP* **04** (2015) 082, [arXiv:1410.8131].

[106] E. Drueke, J. Nutter, R. Schwienhorst, N. Vignaroli, D. G. E. Walker, and J.-H. Yu, *Single Top Production as a Probe of Heavy Resonances*, *Phys. Rev.* **D91** (2015), no. 5 054020, [arXiv:1409.7607].

[107] J. Reuter and M. Tonini, *Top Partner Discovery in the $T \to tZ$ channel at the LHC*, *JHEP* **01** (2015) 088, [arXiv:1409.6962].

[108] O. Matsedonskyi, G. Panico, and A. Wulzer, *On the Interpretation of Top Partners Searches*, *JHEP* **12** (2014) 097, [arXiv:1409.0100].

[109] B. Gripaios, T. Müller, M. A. Parker, and D. Sutherland, *Search Strategies for Top Partners in Composite Higgs models*, *JHEP* **08** (2014) 171, [arXiv:1406.5957].

[110] C.-Y. Chen, S. Dawson, and I. M. Lewis, *Top Partners and Higgs Boson Production*, *Phys. Rev.* **D90** (2014), no. 3 035016, [arXiv:1406.3349].

[111] A. Banfi, A. Martin, and V. Sanz, *Probing top-partners in Higgs+jets*, *JHEP* **08** (2014) 053, [arXiv:1308.4771].

[112] M. Carena, L. Da Rold, and E. Pontn, *Minimal Composite Higgs Models at the LHC*, *JHEP* **06** (2014) 159, [arXiv:1402.2987].

[113] C. Niehoff, P. Stangl, and D. M. Straub, *Direct and indirect signals of natural composite Higgs models*, arXiv:1508.00569.

[114] J. Barnard and M. White, *Collider constraints on tuning in composite Higgs models*, arXiv:1507.02332.

[115] G. Cacciapaglia, H. Cai, A. Deandrea, T. Flacke, S. J. Lee, and A. Parolini, *Composite scalars at the LHC: the Higgs, the Sextet and the Octet*, arXiv:1507.02283.

[116] A. Thamm, R. Torre, and A. Wulzer, *Future tests of Higgs compositeness: direct vs indirect*, *JHEP* **07** (2015) 100, [arXiv:1502.01701].

[117] S. Kanemura, K. Kaneta, N. Machida, and T. Shindou, *New resonance scale and fingerprint identification in minimal composite Higgs models*, *Phys. Rev.* **D91** (2015) 115016, [arXiv:1410.8413].

[118] N. Vignaroli, *New W? signals at the LHC*, *Phys. Rev.* **D89** (2014), no. 9 095027, [arXiv:1404.5558].

[119] M. Redi, V. Sanz, M. de Vries, and A. Weiler, *Strong Signatures of Right-Handed Compositeness*, *JHEP* **08** (2013) 008, [arXiv:1305.3818].

[120] K. Agashe, A. Azatov, T. Han, Y. Li, Z.-G. Si, and L. Zhu, *LHC Signals for Coset Electroweak Gauge Bosons in Warped/Composite PGB Higgs Models*, *Phys. Rev.* **D81** (2010) 096002, [arXiv:0911.0059].

[121] A. Carmona, M. Chala, and J. Santiago, *New Higgs Production Mechanism in Composite Higgs Models*, *JHEP* **07** (2012) 049, [arXiv:1205.2378].

[122] M. Redi and A. Tesi, *Implications of a Light Higgs in Composite Models*, *JHEP* **10** (2012) 166, [arXiv:1205.0232].

[123] R. Contino, D. Marzocca, D. Pappadopulo, and R. Rattazzi, *On the effect of resonances in composite Higgs phenomenology*, *JHEP* **10** (2011) 081, [arXiv:1109.1570].

[124] A. Carmona and F. Goertz, *A naturally light Higgs without light Top Partners*, *JHEP* **05** (2015) 002, [arXiv:1410.8555].

[125] D. Pappadopulo, A. Thamm, and R. Torre, *A minimally tuned composite Higgs model from an extra dimension*, *JHEP* **07** (2013) 058, [arXiv:1303.3062].

[126] V. Sanz and J. Setford, *Composite Higgses with seesaw EWSB*, *JHEP* **12** (2015) 154, [arXiv:1508.06133].

[127] G. Panico, M. Redi, A. Tesi, and A. Wulzer, *On the Tuning and the Mass of the Composite Higgs*, *JHEP* **03** (2013) 051, [arXiv:1210.7114].

[128] M. Bauer, S. Casagrande, L. Grunder, U. Haisch, and M. Neubert, *Little randall-sundrum models: epsilon(k) strikes again*, *Phys.Rev.* **D79** (2009) 076001, [hep-ph/0811.3678].

[129] D. P. George and K. L. McDonald, *Gravity on a Little Warped Space*, *Phys. Rev.* **D84** (2011) 064007, [arXiv:1107.0755].

[130] M. A. Shifman, A. I. Vainshtein, and V. I. Zakharov, *QCD and Resonance Physics. Theoretical Foundations*, *Nucl. Phys.* **B147** (1979) 385–447.

[131] M. A. Shifman, A. I. Vainshtein, and V. I. Zakharov, *QCD and Resonance Physics: Applications*, *Nucl. Phys.* **B147** (1979) 448–518.

[132] M. Knecht and E. de Rafael, *Patterns of spontaneous chiral symmetry breaking in the large N(c) limit of QCD - like theories*, *Phys. Lett.* **B424** (1998) 335–342, [hep-ph/9712457].

[133] E. de Rafael, *An Introduction to sum rules in QCD: Course*, in *Probing the standard model of particle interactions. Proceedings, Summer School in Theoretical Physics, NATO Advanced Study Institute, 68th session, Les Houches, France, July 28-September 5, 1997. Pt. 1, 2*, pp. 1171–1218, 1997. hep-ph/9802448.

[134] S. Weinberg, *Implications of Dynamical Symmetry Breaking*, *Phys. Rev.* **D13** (1976) 974–996.

[135] C. T. Hill and E. H. Simmons, *Strong dynamics and electroweak symmetry breaking*, *Phys. Rept.* **381** (2003) 235–402, [hep-ph/0203079]. [Erratum: Phys. Rept.390,553(2004)].

[136] K. Lane, *Two lectures on technicolor*, hep-ph/0202255.

[137] R. S. Chivukula, *Lectures on technicolor and compositeness*, in *Flavor physics for the millennium. Proceedings, Theoretical Advanced Study Institute in elementary particle physics, TASI 2000, Boulder, USA, June 4-30, 2000*, pp. 731–772, 2000. hep-ph/0011264.

[138] G. 't Hooft, *A Planar Diagram Theory for Strong Interactions*, *Nucl. Phys.* **B72** (1974) 461.

[139] E. Witten, *Baryons in the 1/n Expansion*, *Nucl. Phys.* **B160** (1979) 57–115.

[140] H. Georgi, *Effective field theory and electroweak radiative corrections*, *Nucl. Phys.* **B363** (1991) 301–325.

[141] R. Barbieri, A. Pomarol, R. Rattazzi, and A. Strumia, *Electroweak symmetry breaking after LEP-1 and LEP-2*, *Nucl. Phys.* **B703** (2004) 127–146, [hep-ph/0405040].

[142] A. Manohar and H. Georgi, *Chiral Quarks and the Nonrelativistic Quark Model*, *Nucl. Phys.* **B234** (1984) 189–212.

[143] H. Georgi and L. Randall, *Flavor Conserving CP Violation in Invisible Axion Models*, *Nucl. Phys.* **B276** (1986) 241–252.

[144] S. Dimopoulos and L. Susskind, *Mass Without Scalars*, *Nucl. Phys.* **B155** (1979) 237–252. [2,930(1979)].

[145] E. Eichten and K. D. Lane, *Dynamical Breaking of Weak Interaction Symmetries*, *Phys. Lett.* **B90** (1980) 125–130.

[146] B. Holdom, *Raising the Sideways Scale*, *Phys. Rev.* **D24** (1981) 1441.

[147] K. Yamawaki, M. Bando, and K.-i. Matumoto, *Scale Invariant Technicolor Model and a Technidilaton*, *Phys. Rev. Lett.* **56** (1986) 1335.

[148] T. Akiba and T. Yanagida, *Hierarchic Chiral Condensate*, *Phys. Lett.* **B169** (1986) 432–435.

[149] T. W. Appelquist, D. Karabali, and L. C. R. Wijewardhana, *Chiral Hierarchies and the Flavor Changing Neutral Current Problem in Technicolor*, *Phys. Rev. Lett.* **57** (1986) 957.

[150] T. Appelquist and L. C. R. Wijewardhana, *Chiral Hierarchies and Chiral Perturbations in Technicolor*, *Phys. Rev.* **D35** (1987) 774.

[151] T. Appelquist and L. C. R. Wijewardhana, *Chiral Hierarchies from Slowly Running Couplings in Technicolor Theories*, *Phys. Rev.* **D36** (1987) 568.

[152] A. Falkowski, *About the holographic pseudo-goldstone boson*, *Phys.Rev.* **D75** (2007) 025017, [hep-ph/0610336].

[153] J. M. Maldacena, *The Large N limit of superconformal field theories and supergravity*, *Int. J. Theor. Phys.* **38** (1999) 1113–1133, [hep-th/9711200]. [Adv. Theor. Math. Phys.2,231(1998)].

[154] K. Agashe, A. Delgado, and R. Sundrum, *Gauge coupling renormalization in RS1*, *Nucl. Phys.* **B643** (2002) 172–186, [hep-ph/0206099].

[155] K. Agashe and A. Delgado, *A Note on CFT dual of RS model with gauge fields in bulk*, *Phys. Rev.* **D67** (2003) 046003, [hep-th/0209212].

[156] N. Arkani-Hamed, M. Porrati, and L. Randall, *Holography and phenomenology*, *JHEP* **08** (2001) 017, [hep-th/0012148].

[157] D. B. Kaplan, *Flavor at SSC energies: A New mechanism for dynamically generated fermion masses*, *Nucl. Phys.* **B365** (1991) 259–278.

[158] **ATLAS** Collaboration, G. Aad et al., *Measurements of the Higgs boson production and decay rates and coupling strengths using pp collision data at $\sqrt{s} = 7$ and 8 TeV in the ATLAS experiment*, arXiv:1507.04548.

[159] R. Barbieri and G. F. Giudice, *Upper Bounds on Supersymmetric Particle Masses*, *Nucl. Phys.* **B306** (1988) 63–76.

[160] **ATLAS** Collaboration, G. Aad et al., *Constraints on new phenomena via Higgs boson couplings and invisible decays with the ATLAS detector*, arXiv:1509.00672.

[161] R. Franceschini, G. F. Giudice, J. F. Kamenik, M. McCullough, A. Pomarol, R. Rattazzi, M. Redi, F. Riva, A. Strumia, and R. Torre, *What is the gamma gamma resonance at 750 GeV?*, arXiv:1512.04933.

[162] J. Ellis, S. A. R. Ellis, J. Quevillon, V. Sanz, and T. You, *On the Interpretation of a Possible ~ 750 GeV Particle Decaying into $\gamma\gamma$*, arXiv:1512.05327.

[163] S. Di Chiara, L. Marzola, and M. Raidal, *First interpretation of the 750 GeV di-photon resonance at the LHC*, arXiv:1512.04939.

[164] J. Chakrabortty, A. Choudhury, P. Ghosh, S. Mondal, and T. Srivastava, *Di-photon resonance around 750 GeV: shedding light on the theory underneath*, arXiv:1512.05767.

[165] R. S. Gupta, S. Jger, Y. Kats, G. Perez, and E. Stamou, *Interpreting a 750 GeV Diphoton Resonance*, arXiv:1512.05332.

[166] F. Staub et al., *Precision tools and models to narrow in on the 750 GeV diphoton resonance*, arXiv:1602.05581.

[167] H. Davoudiasl, J. Hewett, and T. Rizzo, *Phenomenology of the Randall-Sundrum Gauge Hierarchy Model*, *Phys.Rev.Lett.* **84** (2000) 2080, [hep-ph/9909255].

[168] K. Agashe, H. Davoudiasl, G. Perez, and A. Soni, *Warped gravitons at the lhc and beyond*, *Phys.Rev.* **D76** (2007) 036006, [hep-ph/0701186].

[169] A. L. Fitzpatrick, J. Kaplan, L. Randall, and L.-T. Wang, *Searching for the kaluza-klein graviton in bulk rs models*, *JHEP* **0709** (2007) 013, [hep-ph/0701150].

[170] A. Falkowski and J. F. Kamenik, *Di-photon portal to warped gravity*, arXiv:1603.06980.

[171] B. M. Dillon, D. P. George, and K. L. McDonald, *Regarding the Radion in Randall-Sundrum Models with Brane Curvature*, arXiv:1605.03087.

[172] **CMS** Collaboration, *Search for ttbar resonances in semileptonic final state*, *CMS-PAS-B2G-12-006* (2012).

[173] **ATLAS** Collaboration, T. A. collaboration, *A search for $t\bar{t}$ resonances in the lepton plus jets final state with ATLAS using 14 $fb^{?1}$ of pp collisions at $\sqrt{s} = 8$ TeV*, *ATLAS-CONF-2013-052* (2013).

[174] H. M. Lee, M. Park, and V. Sanz, *Gravity-mediated (or Composite) Dark Matter*, *Eur. Phys. J.* **C74** (2014) 2715, [arXiv:1306.4107].

[175] P. Mathews, V. Ravindran, and K. Sridhar, *NLO-QCD corrections to dilepton production in the Randall-Sundrum model*, *JHEP* **10** (2005) 031, [hep-ph/0506158].

[176] J. Gao, C. S. Li, B. H. Li, C. P. Yuan, and H. X. Zhu, *Next-to-leading order QCD corrections to the heavy resonance production and decay into top quark pair at the LHC*, *Phys. Rev.* **D82** (2010) 014020, [arXiv:1004.0876].

[177] **NNPDF** Collaboration, R. D. Ball et al., *Parton distributions for the LHC Run II*, *JHEP* **04** (2015) 040, [arXiv:1410.8849].

[178] C. Han, H. M. Lee, M. Park, and V. Sanz, *The diphoton resonance as a gravity mediator of dark matter*, *Phys. Lett.* **B755** (2016) 371–379, [arXiv:1512.06376].

[179] T. A. collaboration, *Search for new phenomena in the dilepton final state using proton-proton collisions at ? s = 13 TeV with the ATLAS detector*, *ATLAS-CONF-2015-070* (2015).

[180] **ATLAS** Collaboration, G. Aad et al., *Search for an additional, heavy Higgs boson in the $H \to ZZ$ decay channel at $\sqrt{s} = 8$ TeV in pp collision data with the ATLAS detector*, *Eur. Phys. J.* **C76** (2016), no. 1 45, [arXiv:1507.05930].

[181] **CMS** Collaboration, V. Khachatryan et al., *Search for a Higgs Boson in the Mass Range from 145 to 1000 GeV Decaying to a Pair of W or Z Bosons*, *JHEP* **10** (2015) 144, [arXiv:1504.00936].

[182] **ATLAS** Collaboration, T. A. collaboration, *A search for resonant Higgs-pair production in the $b\bar{b}b\bar{b}$ final state in pp collisions at $\sqrt{s} = 8$ TeV*, *ATLAS-CONF-2014-005* (2014).

[183] T. A. collaboration, *Search for heavy resonances decaying to a Z boson and a photon in pp collisions at $\sqrt{s} = 13$ TeV with the ATLAS detector*, *ATLAS-CONF-2016-010* (2016).

[184] **CMS** Collaboration, S. Chatrchyan et al., *Searches for new physics using the $t\bar{t}$ invariant mass distribution in pp collisions at $\sqrt{s}$=8??TeV*, *Phys. Rev. Lett.* **111** (2013), no. 21 211804, [arXiv:1309.2030]. [Erratum: Phys. Rev. Lett.112,no.11,119903(2014)].

[185] J. M. No, V. Sanz, and J. Setford, *See-Saw Composite Higgses at the LHC: Linking Naturalness to the* 750 *GeV Di-Photon Resonance*, arXiv:1512.05700.

[186] H. Davoudiasl and C. Zhang, *750 GeV messenger of dark conformal symmetry breaking*, *Phys. Rev.* **D93** (2016), no. 5 055006, [arXiv:1512.07672].